VARIATIONS IN THE SHAPE OF THE CHIN IN SOUTH AFRICANS USING CONE BEAM COMPUTED TOMOGRAPHY SCANS

by

Sandra Braun

Submitted in fulfilment of the requirements for the degree

Master of Science in Anatomy

in the

Department of Anatomy

Faculty of Health Sciences

UNIVERSITY OF PRETORIA

June 2020

SUMMARY

VARIATIONS IN THE SHAPE OF THE CHIN IN SOUTH AFRICANS USING CONE BEAM COMPUTED TOMOGRAPHY SCANS

by

Sandra Braun

Supervisor: *Prof. A.C. Oettlé*

Extraordinary Lecturer, Department of Anatomy, University of Pretoria and Associate Professor, Department of Anatomy and Histology, School of Medicine, Sefako Makgatho Health Sciences University, Pretoria

Co-supervisors: *Dr. Alison F. Ridel*

Department of Anatomy, University of Pretoria

Prof. Ericka N. L'Abbé

Professor Physical Anthropology, Director Forensic Anthropology Research Centre, Department of Anatomy, University of Pretoria

Department: Department of Anatomy

University: University of Pretoria

Degree: MSc in Anatomy

Keywords: forensic anthropology, sex estimation, Walker, chin shape, geometric morphometrics, micro-focus X-ray computed tomography

Department of Anatomy
University of Pretoria

Summary:

In order to support identification of crime victims in South Africa, new methods need to be sought. If victim identification involving fingerprints, DNA or dental records are not possible, facial approximation is often the only alternative. In order to gain necessary background data for the identification of unknown individuals, e.g. for facial approximations, facial features of modern South Africans need to be investigated and shape-influencing factors identified. New imaging technologies have opened the possibility of including living, dentate individuals, as specimens in skeletal collections are often edentulous. The aim of this dissertation was to assess chin shape variation and the factors influencing it, in black and white South Africans.

In the first part, the mental eminence was assessed by applying a morphoscopic sex estimation technique, to test its applicability to 105 dry mandibles from the Pretoria Bone Collection, and to the respective micro-focus X-ray computed tomography (micro-XCT) scans, obtained at the Nuclear Energy Corporation South Africa. Fleiss Kappa, Cohen's Kappa and Wilcoxon Signed-Rank tests were applied. Score frequencies and observer performance were analysed. In the second part, the chin shape was assessed by quantifying its morphology, applying geometric morphometric methods to 291 retrospectively collected CBCT scans. The scans were obtained for medical reasons from dental patients, at the Oral and Dental Hospital, University of Pretoria. The possible influences of ancestry, sex, age and allometry on the chin shape were tested, using MAN(C)OVA, 50-50 MANOVA, permutation tests and discriminant function analysis (DFA) on the x-, y- and z-coordinates of the anatomical landmarks.

The morphoscopic method to estimate sex on the mental eminence, originally applied to bone, was found to be applicable to micro-XCT scans as well, and observer performance did not vary greatly between the two modalities. However, an observer's personal affinity to assess 3D images, the level of experience and tendency to over- or underscore in one of the two modalities cannot be excluded and should be individually tested. The chins of black females and white males had the highest probabilities of correct sex estimation. Ancestry,

age and allometry were significant chin shape influencing factors in the complete sample. In addition, ancestry influenced the chin shape significantly within the sex groups, allometry within the ancestral groups. Sexual dimorphism significantly influenced chin shape in the complete sample on the bony menton and in the ancestral groups. Most results from both parts of the study concurred, except the influence of age.

With the increasing availability of imaging techniques in forensic anthropology, researchers are motivated to look for new, and validate existing, methods in 3D. By assessing the applicability of a morphoscopic sex estimation technique to micro-XCT scans, and by investigating the chin shape variation using CBCT scans, the present study contributed to the quantifiable biological profiling methods involving 3D imaging techniques in South Africa.

This study could encourage further research on all five traits of the morphoscopic method in bone and 3D surfaces, and of the soft-tissue shape of the chin in the same populations.

LIST OF ABBREVIATIONS

2D	Two-dimensional
3D	Three-dimensional
ANOVA	Analysis of variance
b	Bone
BF	Black female
BM	Black male
CBCT	Cone beam computed tomography
CS	Centroid size
DFA	Discriminant Function Analysis
FARC	Forensic Anthropology Research Centre
GMM	Geometric morphometric
GPA	Generalised Procrustes Analysis
HMH	Half Maximum Height
InterOE	Interobserver error
IntraOE	Intraobserver error
MANCOVA	Multivariate analysis of covariance
MANOVA	Multivariate analysis of variance
MED	Mean Euclidean Distance
Micro-XCT	Micro-focus X-ray computed tomography
MIXRAD	Micro-focus X-ray Radiography and Tomography facility
Necsa	Nuclear Energy Corporation South Africa
Obs.	Observer
PBC	Pretoria Bone Collection
PC	Principal Component
PCA	Principal Component Analysis
SAPS	South African Police Services
VIC	Victim Identification Centre
WF	White female
WM	White male

DECLARATION

I declare that the dissertation, which I hereby submit for the degree Master of Science in Anatomy at the University of Pretoria, is my own work and has not previously been submitted by me for a degree at this or any other tertiary institution.

ETHICS STATEMENT

The author, whose name appears on the title page of this dissertation, has obtained, for the research described in this work, the applicable research ethics approval (Reference number 147/2019).

The author declares that she has observed the ethical standards required in terms of the University of Pretoria's Code of Ethics for Researchers and the Policy guidelines for responsible research.

Sandra Braun
UP student number 22291360
April 2020

UNIVERSITEIT VAN PRETORIA
UNIVERSITY OF PRETORIA
YUNIBESITHI YA PRETORIA

Faculty of Health Sciences

The Research Ethics Committee, Faculty Health Sciences, University of Pretoria complies with ICH-GCP guidelines and has US Federal wide Assurance.

- FWA 00002567, Approved dd 22 May 2002 and Expires 03/20/2022.
- IRB 0000 2235 IORG0001762 Approved dd 22/04/2014 and Expires 03/14/2020.

26 April 2019

Approval Certificate
New Application

Ethics Reference No.: 147/2019
Title: Variations in the shape of the chin in South Africans using Cone Beam Computed Tomography scans

Dear Mrs S Braun

The **New Application** as supported by documents received between 2019-03-26 and 2019-04-24 for your research, was approved by the Faculty of Health Sciences Research Ethics Committee on its quorate meeting of 2019-04-24.

Please note the following about your ethics approval:

- Ethics Approval is valid for 1 year and needs to be renewed annually by 2020-04-26.
- Please remember to use your protocol number (147/2019) on any documents or correspondence with the Research Ethics Committee regarding your research.
- Please note that the Research Ethics Committee may ask further questions, seek additional information, require further modification, monitor the conduct of your research, or suspend or withdraw ethics approval.

Ethics approval is subject to the following:

- The ethics approval is conditional on the research being conducted as stipulated by the details of all documents submitted to the Committee. In the event that a further need arises to change who the investigators are, the methods or any other aspect, such changes must be submitted as an Amendment for approval by the Committee.

We wish you the best with your research.

Yours sincerely

Dr R Sommers
MBChB MMed (Int) MPharmMed PhD
Deputy Chairperson of the Faculty of Health Sciences Research Ethics Committee, University of Pretoria

The Faculty of Health Sciences Research Ethics Committee complies with the SA National Act 61 of 2003 as it pertains to health research and the United States Code of Federal Regulations Title 45 and 46. This committee abides by the ethical norms and principles for research, established by the Declaration of Helsinki, the South African Medical Research Council Guidelines as well as the Guidelines for Ethical Research: Principles Structures and Processes, Second Edition 2015 (Department of Health)

Research Ethics Committee
Room 4-60, Level 4, Tswelopele Building
University of Pretoria, Private Bag X323
Arcadia 0007, South Africa
Tel +27 (0)12 356 3084
Email deepeka.behari@up.ac.za
www.up.ac.za

Fakulteit Gesondheidswetenskappe
Lefapha la Disaense tša Maphelo

ACKNOWLEDGEMENTS

My thanks go to my supervisors Prof Anna C. Oettlé, Dr Alison F. Ridel and Prof Ericka N. L'Abbé, for their constant and helpful support, for their creativity, constructive input, motivation and – on our first meeting – very warm welcome.

Charlotte Theye has kindly consented to my using the micro-focus X-ray computed tomography images she collected for her PhD – thank you very much for this! My thanks go to Gabi C. Krüger and Okuhle Sapo from the Pretoria Bone Collection. They kindly granted access to the bone collection and helped with the transport of mandibles for the morphoscopic method part of this study. In addition, Ms Krüger kindly assisted with the statistical analysis of the morphoscopic method results and gave me permission to take photos of some of the bones in the collection. Thank you also to Mrs Franci Swanepoel who drafted the muscles on the mandible (Figure 2.4). Dr de Beer from Necsa and Dr Ridel kindly granted permission to reuse their figures in this dissertation, thank you very much! Dr Jean Dumoncel helped out with questions regarding R, and so did Edwin de Jager; thank you very much to both of you! My sincere thanks go to Mrs Elizabeth van Rooyen (South Africa) and Mr Paul Anthony Lavender (UK/Switzerland), for professional language editing of this dissertation!

I would also like to thank Charlotte, Okuhle, Maritza, Gabi, Marine and Clarisa for being there and for being friends!

Meine Eltern, Erwin und Herta Braun, haben mich aus meiner Heimat, dem wunderschönen Südtirol, über das gesamte Projekt hinweg begleitet, unterstützt und ermutigt, zumeist über Skype. Ihnen gilt mein innigster Dank!

Jan, mein Ehemann, bester Freund und Lebensbegleiter, Du bist mir in jeder Hinsicht eine Stütze, ein Fels in der Brandung. Dafür werde ich Dir immer dankbar sein!

TABLE OF CONTENTS

LIST OF FIGURES

Chapter 4 Results

LIST OF TABLES

Chapter 8 Appendix

Appendix A

CHAPTER 1 INTRODUCTION

Forensic anthropologists in South Africa have been assisting the South African Police Services (SAPS) with the identification of a large number of unidentified bodies each year for more than a decade. Over 1,100 bodies remained unidentified in Gauteng Province alone between April 2018 and March 2019; the majority of them (360 bodies) at the Johannesburg mortuary (Bloom 2019). The high number of unidentified bodies, especially in Gauteng Province, could be partly attributed to the migrant working situation in South Africa (L'Abbé et al. 2005). When migrant workers from a different South African province or non-South African citizens lacking identification documentation die, but are not reported as missing, personal identification is rendered difficult or even impossible (Bloom 2015).

Another factor contributing to the high number of unidentified bodies is the crime rate. South Africa has one of the highest homicide rates worldwide (Krüger et al. 2018). In the year 2000, nearly 60,000 deaths due to injury had been registered, resulting in a higher overall unnatural death rate (157.8 per 100,000 population) than that of the entire African continent (139.5). Moreover, South Africa's unnatural death rate is nearly double the global rate of 86.9 per 100,000 population (Seedat et al. 2009). In 2007 and 2008, the nationwide South African homicide rate amounted to 39 per 100,000 population as recorded by the SAPS (Seedat et al. 2009). The current annual number of homicides is reported as approximately 32,600 (Statistics of South Africa 2018/2019). Even in rural areas, homicide can be the most frequent cause of death in men after HIV-related deaths and the most frequent cause of death in women (Otieno et al. 2015). The homicide rate for women is six times the global average, with half the homicides committed by the women's intimate partners (Seedat et al. 2009). In addition to migrant labour and immigration, factors contributing to the high homicide rate in South Africa have been identified as the unique political history and economic inequalities of the country, as well as alcohol and substance abuse, unemployment, lack of education and male dominance (Otieno et al. 2015).

The high number of unidentified victims per year is expected to remain an issue in South Africa if priority is not given to victim identification (Bloom 2015; 2019). When victim identification is not possible due to progressed soft-tissue decomposition and the lack of dental records, DNA or fingerprint databases, there is often a need to fall back on facial approximation methods (Short et al. 2014). Facial approximation can be done in two or in three dimensions (2D, 3D) (Snow et al. 1970; Gerasimov 1971; Taylor 2000; Wilkinson 2004). The underlying principle is in the relationship between the hard- and the soft-tissue of the face (Allam et al. 2018). In the present study, the quantification of the scanned chin morphology should contribute to the understanding of shape influencing demographic parameters, in order to then allow to correlate the hard- and soft-tissue of the lower face in South Africans. In 3D, the face can be reconstructed either manually (Gerasimov 1971) or virtually (Vanezis et al. 1989), with 3D imaging software. While the manual methods are considered subjective by the scientific community, the computer-based models aim at objectivity (Stephan et al. 2003; Guyomarc'h et al. 2014). Representations of facial approximations are published to instigate recognition among the populace as family and/or friends of the victim spot the reconstructed face. Hence, research efforts at the Forensic Anthropology Research Centre (FARC), University of Pretoria, are being undertaken to alleviate the problematic issues of victim identification and to further the scientific foundation on which to build facial approximations. The study by Dorfling and colleagues verified the current facial approximation guidelines (Stephan and Davidson 2008) regarding the position of the eyeballs in the socket (Dorfling et al. 2018). This allows a more adequate approximation of the position of the eyes in facial approximation. Recently, Ridel (2019) studied the shape variation of the hard-tissue shape and predicted the soft-tissue shape of the nose and the mid-face in South African populations, using cone beam computed tomography (CBCT) surfaces.

The increasing use of scanned bones in forensic anthropology has been leading researchers to test and to develop new methods (Garvin and Stock 2016; Dereli et al. 2018).

The present study made use of 3D imaging techniques to test an existing method (Walker 2008), and to develop a new method for forensic anthropology in South Africa.

In the first part of the study, a widely used morphoscopic method (Walker 2008) to estimate sex was tested regarding its applicability to 3D surface scans in South African populations. The study involved 105 mandibles from the Pretoria Bone Collection (PBC), and the corresponding micro-focus X-ray computed tomography (micro-XCT) surfaces from South African blacks and whites, allowing direct comparison between the scoring of bone and 3D surfaces. The aim was to test the method's applicability to micro-XCT scans by comparing scores in the two modalities (bone and micro-XCT scans) and among observers.

The second part of the study entailed the analysis of the bony chin shape variation in black and white South Africans and the possible influence ancestry, sex, age and allometry could wield over it. The CBCT scans of 291 dental patients were studied, applying geometric morphometric (GMM) methods. The aim was to broaden the knowledge on the chin shape variation, possibly influenced by the factors ancestry, sex, age and allometry. The verification of the shape variation connected to these factors could lay the foundation for research dedicated to victim identification in forensic anthropology in South Africa.

Thus far, no study had been carried out on the quantification of the chin shape variation with ancestry, sex, age and allometry, in black and white South Africans, involving craniometric landmarks and GMM.

The specific objectives of this study were to

1. assess the shape of the chin by testing the applicability of the Walker (2008) method on 105 dry mandibles and micro-XCT surface scans, and compare the scores between these two modalities among observers and to known sex, and to
2. analyse the chin shape variation using CBCT hard-tissue surfaces of 291 dental patients with geometric morphometrics (GMM). Within this study part to
    a. test the accuracy of the manual versus automatic placement of the nine pre-defined craniometric landmarks, and to
    b. determine and describe the covariance of the hard-tissue chin shape with the variables ancestry, age, sex and size (allometry).

CHAPTER 2 LITERATURE REVIEW

In this chapter, a literature review is given, underlining the aims of this study. An anthropological description, including an account of the anatomy of the mandible, evolutionary aspects of the prominent chin, as well as the genetic (ancestry, sex, age) and biomechanical (mastication, tooth loss, subsistence and speech) factors thought to possibly influence the mandible, will be described. Micro-focus X-ray computed tomography (micro-XCT) and cone beam computed tomography (CBCT) technologies will be highlighted, followed by a section on why and how anatomical landmarks are used. This will be followed by an introduction to forensic anthropology, and a description of shape variation within this field of research, using morphoscopic methods and geometric morphometrics (GMM).

2.1 ANTHROPOLOGICAL DESCRIPTION

The anatomy of the mandible and, more specifically, the chin in the adult will be described in the following section. Possible evolutionary aspects of the prominent human chin will follow, as well as genetic and biomechanical factors influencing its development and expression. Among the genetic factors, which may influence the shape of the mandible and the chin, are ancestry, sex, and age. Along with the effects of ageing, ontogenesis, tooth eruption and changes during adulthood will be outlined. Among the biomechanical factors, mastication and tooth loss as the most obvious influencing parameters on the morphology of the mandible and the chin will be discussed. Furthermore, subsistence strategy connected to the shape of the mandible will be evaluated as well as speech and its possible connection to the shape of the mandible and chin.

2.1.1 Mandibular anatomy

The mandible is a robust bone of the human skeleton and forms part of the skull. The mandible consists of the ramus and the body, connected at the mandibular angle. The condyle forms the temporomandibular joint with the glenoid fossa in the temporal bone of the cranium. Anteriorly in the mandible, the chin or menton is shaped by the mental tubercles and the mental protuberance, the latter being located on the fused mental symphysis (Netter 2014). An equal expression of the mental tubercles and the protuberance contributes to a rounded chin shape (Figure 2.1a), whereas a square chin shape (Figure 2.1b) is caused by a more prominent expression of the mental tubercles and an explicit fossa mentalis.

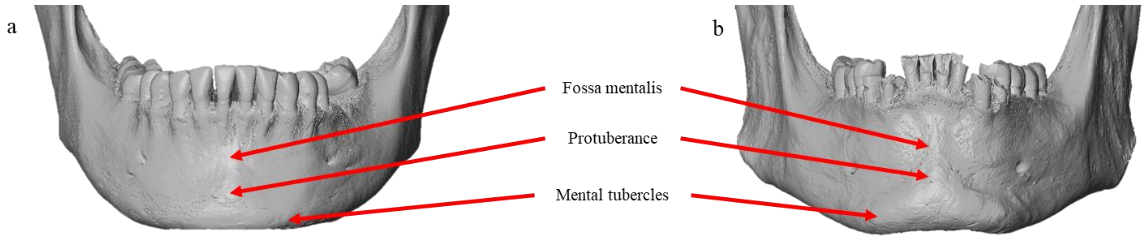

Figure 2.1 a) Round chin shape, b) square chin shape, depending on the morphology of the fossa mentalis, the protuberance and the mental tubercles (mandibles from the Pretoria Bone Collection).

If, however, the mental protuberance is markedly expressed, the chin shape is perceived as pointed (Loth and Henneberg 2001; Garvin and Ruff 2012).

In the alveolar part of the mandibular body, the teeth are anchored in deep sockets called alveoli (Figure 2.2).

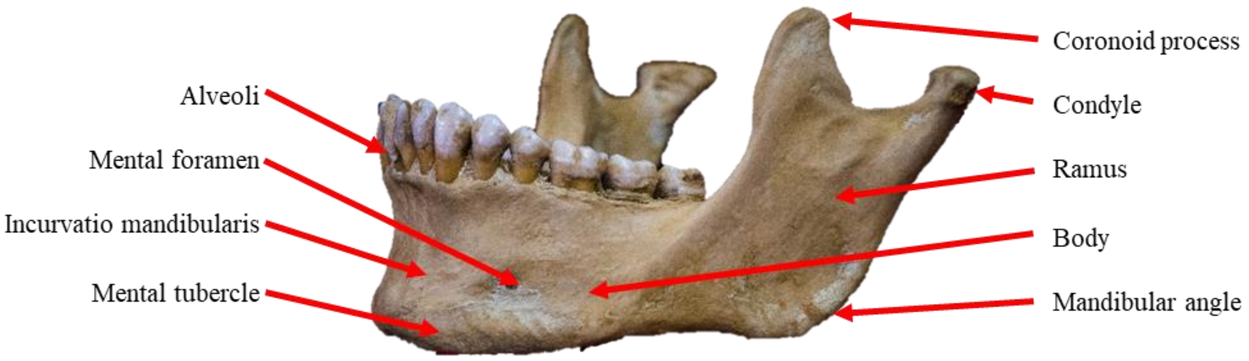

Figure 2.2 Bony features of the mandible, lateral view (photo taken by the author, courtesy curator of the Pretoria Bone Collection).

The incurvatio mandibularis or supramentale (Figure 2.3) is situated just above the mental protuberance. The incurvatio mandibularis deepens on either side into the fossa mentalis (Schwartz and Tattersall 2000) for the attachment of the mentalis muscle (Figure 2.4).

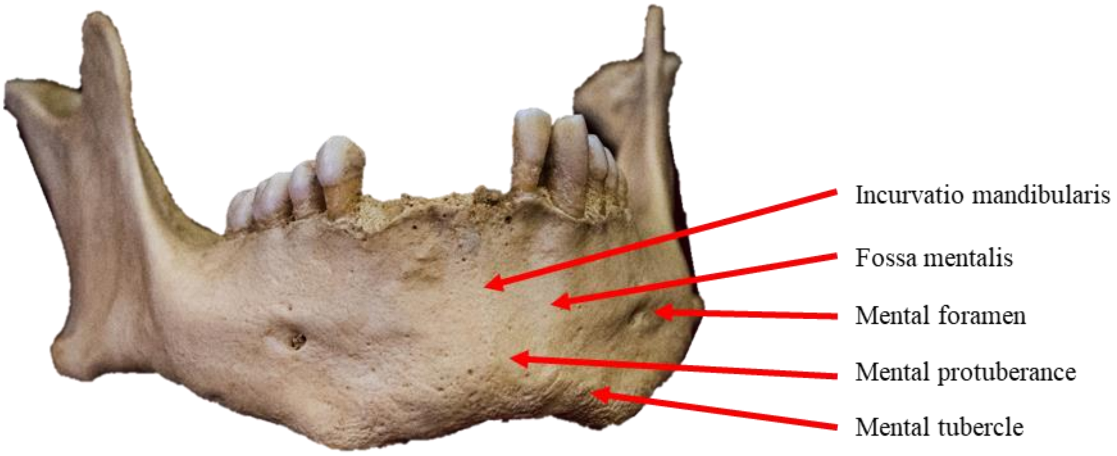

Figure 2.3 Bony features of the chin, frontal view (photo taken by the author, courtesy curator of the Pretoria Bone Collection).

Lateral to the mental tubercles originates the depressor anguli oris muscle, which draws the angle of the mouth downwards, and the depressor labii inferioris (Figure 2.4) moving the lower lip downwards (Standring 2008). Together with the masseter and the medial pterygoid muscles, the temporal muscle lifts the mandible into occlusal contact with the maxillary teeth (Potgieter et al. 1983). The depressor muscles of the mandible, in contrast, oppose this upward movement of the mandible while the digastric muscles pull the mandible down towards the hyoid bone, which in turn is braced by the infrahyoid muscles. The platysma, together with the effect of gravity, further increases the space between the maxilla and mandible. Bite force is dependent on the strength of the masseter, temporal and pterygoid muscles (Sella-Tunis et al. 2018).

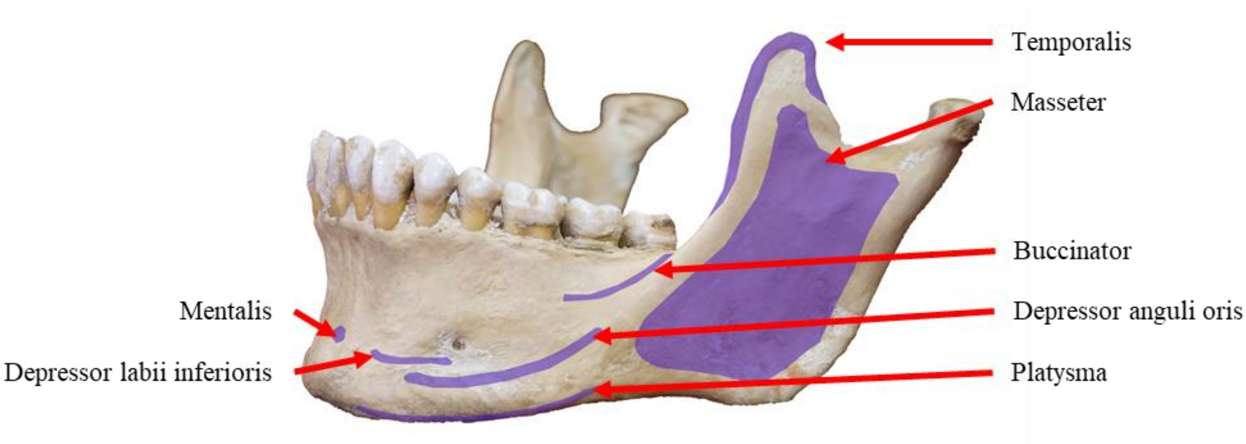

Figure 2.4 Muscle attachment sites on the lateral aspect of the mandible (photo taken by the author, courtesy curator of the Pretoria Bone Collection; muscle attachments drawn by Mrs Franci Swanepoel).

2.1.2 Possible evolutionary basis for chin shape variation

The prominent chin is a hallmark of modern human anatomy and numerous theories arose over the past 100 years, attempting to explain why the chin evolved in the first place (Hrdlička 1911). When the chin was studied in the human fossil record (Schwartz and Tattersall 2000), it was found that while some of the late Pleistocene specimens analysed exhibited a pronounced mental tuberosity, some of the juvenile Qafzeh fossils from the late Pleistocene (92,000 to 95,000 years), which are presumably anatomically modern *Homo sapiens*, did not. Neanderthals, on the other hand, lacked the expression of the trait completely (Schwartz and Tattersall 2000). The trait can thus not be used as a criterion for inclusion into, or exclusion of, the species *H. sapiens*.

A hypothesis for the evolution of the chin is sexual selection (Hershkovitz 1970). Further studies on this theory in the 1990s and early 2000s suggest the development of a prominent and square male chin due to a female preference, indicating social dominance, for a desirable trait in a potential mate (Grammer and Thornhill 1994; Thornhill and Gangestad 1999; Grammer et al. 2003; Borelli and Berneburg 2009). The perception of attractiveness in the female face in today’s central European region is based on childlike characteristics including, among other features, a small chin (Borelli and Berneburg 2009).

With the evolutionary reduction of the dental arch to a more vertical face, a connection between a protruding chin and space allotment in the oral cavity is suspected. The tongue can thus be accommodated anteriorly without obstructing the posterior space needed for breathing and swallowing (Coquerelle et al. 2013a; Coquerelle et al. 2013b). This theory would imply that a more prognathic facial shape has less necessity to develop a prominent chin as the available space for the tongue is provided by prognathism.

2.1.3 The influence of genetic and biomechanical factors on chin shape variation

The mandibular shape in humans is influenced by a variety of genetic factors (Fazekas and Kósa 1978), such as the appearance and expression of traits defined by geographical origin, or ancestry (İşcan and Steyn 2013), and the circulation of sex hormones (Roosenboom et al. 2018), thus expressing a certain degree of size and shape differences between the sexes (sexual dimorphism) (Thayer and Dobson 2010). The influence of ageing on the mandible, in contrast, is thought not to be discernible beyond youth (Windhager et al. 2019). Apart from the genetic influences, biomechanical factors may also contribute to mandibular shape, including mastication, tooth loss (Oettlé 2014; Bertl et al. 2016), subsistence and speech, which will be discussed in this section (Lieberman et al. 2001; Holton et al. 2015; Noback and Harvati 2015; Blasi et al. 2019).

2.1.3.1 Ancestry

Ancestral shape differences in the skeleton are based on human evolutionary geographic dispersion and genetic variation (İşcan and Steyn 2013; Spradley 2016). Ancestral shape variation in mandibular morphology is not only visible and measurable in the overall appearance of the mandible (breadth and width), it can also be ascertained in the shape of the ramus and the bony chin (Oettlé 2014). In South African and North American populations, ancestry is assessed morphoscopically (Spiros and Hefner 2019), and metrically (Spradley 2016) on the mandibular shape (L’Abbé et al. 2011; Hefner and Ousley 2014; Oettlé et al. 2017). The mandible of black South Africans is generally larger and presents with longer and broader rami than that of white South Africans (Tobias 1974), and it exhibits a lower degree of gonial eversion than that of whites (Oettlé et al. 2009a). Enhanced gonial eversion is thought to be directly linked to stronger muscle attachments of the masseter (Loth and Henneberg 2000). Despite the higher degree of gonial eversion and the more robust masseter attachment sites, mandibles of white South Africans are shorter and wider than in blacks (Parr 2005; Oettlé et al. 2009a). In addition to general mandibular shape and gonial eversion, the shape of the bony chin in black and white South Africans differs as well (Tobias

1974). While African groups exhibit a more pointed or rounded chin shape (Garvin and Ruff 2012), the chin in European groups tends to make a squarer impression (De Villiers 1968; Parr 2005; Oettlé 2014), constituting part of the ancestral shape variation.

2.1.3.2 Sexual dimorphism

Sex can be estimated either morphoscopically or metrically (Spradley 2016) and is based on the expression of sexual dimorphism, a term first described by Darwin (1871), referring to the size and shape differences between sexes in a species as well as the primary sex characteristics (Gilbert 2000). In modern humans, sexual dimorphism can involve up to 15% larger dimensions in males than in females (Larsen 2003). These so-called male-biased size differences as observed in humans may have evolved from enhanced male-male competition, resulting in better mating success (Barreto and Avise 2011).

Dimensions of the mandible in males are in general greater than in females: a greater general mandibular body height, especially at the mental symphysis, a greater degree of gonial eversion, a broader ramus, and also a flexure of the posterior margin of the ramus and a more acute gonial angle (Loth and Henneberg 1996; Loth and Henneberg 2000; Oettlé et al. 2009b; İşcan and Steyn 2013). Sexual dimorphism in the mandible is generally perceived as prominent, but ancestry-specific (Garvin and Ruff 2012). These researchers studied skulls from the 19th and 20th centuries in the United States and discovered that white American females displayed generally shorter chins than white males, and black females and males from the same region and period (Garvin and Ruff 2012). As corroborated by the study of Oettlé (2014), a more prominent or even square chin shape is associated with a male individual while a more rounded or even pointed chin shape (Byrnes et al. 2017) is associated with a female individual (İşcan and Steyn 2013).

While generally the chin can be and is used for sex estimation, a relatively great overlap of chin morphology between the sexes should be taken into account; Garvin and Ruff (2012) found that even when employing a new scanning method to quantify chin shape, the cross-validated results reached only 62.2% for correct sex estimation. While the chin has been used for sex estimation with morphoscopic methods, the lack of metrically founded results has been limiting repeatability of the estimation methods (Garvin and Ruff 2012).

Early childhood sex differences are expressed in the tooth eruption patterns, described in section 2.1.3.3 below, and in a shape dimorphism from birth to about three or four years of age (Coquerelle et al. 2011; Hutchinson et al. 2012). After that, until the age of 14 or 15 years, no sexual dimorphism is detectable (Franklin et al. 2007; Coquerelle et al. 2011). The early sexual dimorphism noted by Hutchinson (2010), but not by Franklin and colleagues (2007), could be related to the different materials used in the two studies (skeletonised versus cadaveric). Skeletonised material, as used by Franklin et al. (2007), might not fully represent the chin shape, as ossicles of the symphysis do not fuse with the mandibular bones until the first or second year of life (see section 2.1.3.3) (İşcan and Steyn 2013). Sexual dimorphism in early childhood includes a significantly greater mental angle (at the mental symphysis) in females as opposed to males.

2.1.3.3 Age

Like ancestry and sex, age is a demographic parameter estimated in forensic anthropology (Acsádi and Nemeskéri 1970). In this section, an overview will be given on the ontogenesis of the mandible and on the dental tooth eruption during childhood and early adulthood, followed by a description of morphological changes taking place during adulthood (İşcan and Steyn 2013; Guo et al. 2014).

Ontogenesis

The term ontogenesis refers to the development of an organism, from the fertilisation of the ovum to the adult stage (Gould 1977; Zetkin and Schaldach 1980). This section of the literature review focuses on the ontogenesis of the mandible and the chin.

The mandible ossifies in the middle of the third foetal month from membranous cartilage that disintegrates as soon as the shape of the mandible is final. Ossification of the mandible takes place at about the same time or slightly before that of the maxilla (Fazekas and Kósa 1978). In the foetus, the mandible consists of two halves, with the mental symphysis remaining unfused until sometime between the first and second year postpartum. Fusion of the mental symphysis starts from centres of ossification (ossicles) within the mesenchymal tissue in the symphysis. The ossicles fuse in the fifth or sixth month postpartum (Fazekas and Kósa 1978; Becker 1986; Reichs 1986), but do not fuse with the two mandibular bones until the first or second year of life (İşcan and Steyn 2013). The ossicles of the mental symphysis do not influence the shape of the mental protuberance (Fazekas and Kósa 1978), as their function is limited to the ossification of the mental symphysis. The prenatal growth of the mandibular arch is dedicated to the accommodation of the tongue and the developing deciduous dentition (Hutchinson et al. 2012).

The chin shape appears to be a developmental feature that does or does not form prominently during adolescence, from a vertical symphyseal shape as seen in profile during childhood. The degree of chin development can vary and produce an array of shapes (Schwartz and Tattersall 2000). In contrast to the other parts of the mandible, the variable ontogenetic allometry in the chin indicates the possibility that the allometry of the mental symphysis is not correlated with symphyseal stresses during mastication (Holton et al. 2015). Rather, the space arrangement for the tongue mass and the muscle attachments between the anteriorly limiting dental arch and the laryngopharynx posteriorly are more related to the ontogenetic expression of the mental region (DuBrul and Sicher 1954; Enlow 1990; Coquerelle et al. 2013a; Coquerelle et al. 2013b; Coquerelle et al. 2017).

Tooth eruption

The eruption sequence of teeth after birth is well studied and described, and defines the beginning and ending of the different stages of childhood and adolescence (Schaefer et al. 2009; Irish and Scott 2016). A difference in the tooth eruption patterns between females and males can be detected as early as two years of age (Hutchinson 2010). By definition, early childhood starts at around six months of age with the eruption of the first deciduous tooth, and ends with the eruption of the first permanent molar at about six years of age (Liversidge 2016). Likewise, childhood starts with the eruption of the first permanent tooth and ends when the permanent second premolar is erupted at between eleven and 13 years of age (Ubelaker 1984; İşcan and Steyn 2013). An individual is a young adult once the third molar has erupted and its roots are fully formed at approximately 18 to 21 years (İşcan and Steyn 2013; Guo et al. 2014). Hence, chronological age (see section 2.3) in individuals younger than 18 to 21 years can be estimated reasonably well, according to tooth development and eruption, among other skeletal developmental stages (İşcan and Steyn 2013). The expression of the mental eminence is fully developed well before the eruption of the third molar, namely between about 13 (females) and about 16 (males) years of age (Stock 2018).

Changes during adulthood

After the eruption of teeth, the mandible, and the skeleton on the whole, is not generally useful to estimate chronological age (İşcan and Steyn 2013). The difficulty is that due to the individual biological ageing factors, tooth loss associated with advanced age does not follow determinate patterns and is thus not a valuable age estimation method (Oettlé 2014). After the conclusion of dental eruption, the shape of the mandible and, more specifically, the chin is known to change slightly in the adult stage. When the influence of ageing on the hard- and soft-tissue in a modern Croatian sample was studied, the authors concluded that the female face changes at approximately the age of 50, especially in early menopause when hormonally-induced bone resorption in the mandible is reported to take place (Windhager et al. 2019). However, the mandibular shape changes were not statistically significant. The present study took South African populations into account and investigated any possible influence of ageing on the chin shape.

2.1.3.4 Biomechanical factors

In this section, the roles of mastication, tooth loss as well as subsistence will be discussed. It will become apparent how intertwined the three topics are as they all involve mastication and the relevant muscles. In tooth loss, the latter are reduced, thus influencing the ability to masticate and, in the process, the mandible is remodelled (Figure 2.5). Subsistence strategy is the determining factor for the masticatory stress in a population and thus influences mandibular morphology. Speech, in contrast, plays a different role, depending on the researchers’ perspectives and how the cause-effect relationship is viewed.

Mastication

Mandibular morphology has been found to be strongly influenced by the functional forces of mastication. Especially the masseter and temporalis muscles impact the shape of the mandible with their attachments on the ramus and the coronoid process, respectively. The cross-sectional areas of the masseter and temporalis muscles, representing muscle force, are found to covary with mandibular shape (Sella-Tunis et al. 2018); with increased muscle force, the ramus is wider and more trapezoidal, the coronoid process is stronger, the mandibular body shape is more rectangular, and the basal arch is more curved (Sella-Tunis et al. 2018), with the basal arch referring to the base of the mandibular body (Ronay et al. 2008). The mentioned covariance of masticatory muscle force and mandibular morphology is independent of sex. In contrast, a taller and narrower ramus, a more pointed coronoid process, a more triangular body shape and a more triangular basal arch were found to correspond to a lower cross-sectional area of the masseter and temporalis muscles (Sella-Tunis et al. 2018). However, as the direct correlation between these morphological observations and diet had not been part of the study by Sella-Tunis and colleagues (2018), a connection between muscle force and mandibular shape had to be sought by linking both phenomena to dental attrition and subsistence strategy (see below). Indeed, a connection between dental attrition and mandibular shape has been reported in a variety of studies, pointing to a covariance of diet, masseter and temporalis muscle force, dental attrition and mandibular morphology (Krogstad and Dahl 1985; Varrela 1990; Luther 1993). Thus, diet is thought to be connected to mandibular shape. Animal studies have shown the same effect: in pigs, a softer diet requiring lower bite force leads to different jaw and dental arch dimensions as compared to individuals with a normal diet (Ciochon et al. 1997).

The development of the prominent human chin in connection with mastication has been discussed, but was shown to be rather unlikely (Ichim et al. 2007; Fukase and Suwa 2008; Coquerelle et al. 2017). It was suggested that the masticatory stress on the mental symphysis stemmed from the opposing forces of dorsoventral shear versus lateral-transverse bending (‘wishboning’) (Hylander 1985). However, no correlation was found between chin prominence and the vertical bending and ‘wishboning’ resistance (Holton et al. 2015). Thus, the prominent human chin is thought not to have evolved in connection with mastication.

Tooth loss

The loss of teeth is expected to modify mandibular morphology as mastication is ensured by muscles and teeth. In tooth loss, the bite force is diminished, which impacts the shape of the mandible (Oettlé 2014). Parallel to the decreased bite force, the muscles of mastication reduce their size and the expression of their attachments on the bones (Oettlé 2014). As a result, resorption takes place in areas with decreased strain and the mandible is remodelled (Wolff 1986; Kingsmill 1999; Martinez-Maza et al. 2013; Patriquin 2013; Chou et al. 2015). Tooth loss over time can have considerable effects on mandibular morphology (Enlow et al. 1976; Kingsmill 1999; Martinez-Maza et al. 2013) (Figure 2.5): the chin appears more prominent through alveolar resorption and recession (Parr 2005) and the gonial angles become more obtuse in edentulous individuals (Parr et al. 2017). The changes in the morphology of the chin may in part also be mediated by the change in biomechanical forces in the edentulous mandible, with or without denture wearing over time. More specifically, the muscles attaching to the chin area, including the mentalis, could increase their activity with denture wearing (Tallgren and Tryde 1992; Tallgren 2003; KuĆ et al. 2015), and displace their attachments as the alveolar process is absorbed (Shannon 1972). Lingually, the genial tubercles are noted to enlarge (Jindal 2015) along with the volume of the genioglossus (Morelli et al. 2011) in the presence of macroglossia (Bucca et al. 2006) associated with tooth loss.

Figure 2.5 Reduced mandibular body height and increased mandibular angle following tooth loss (photo taken by the author, courtesy curator of the Pretoria Bone Collection).

Subsistence

The focus of this section centres on whether apart from the previously mentioned genetic factors, the subsistence strategy of a population could have a greater influence on the mandibular shape than diet and mastication in an individual. While diet refers to the nutrition of an individual or a population, subsistence is a nutritional strategy in a broader context, consisting of either hunting-gathering or agriculture (von Cramon-Taubadel 2011; Noback and Harvati 2015; Marklein et al. 2019). Mandibular traits of overall robusticity such as mandibular body breadth, bending rigidity and strength may be influenced by masticatory demands caused by different diets. Thus, a demanding diet in a hunter-gatherer subsistence based on dried meats and fish and unprocessed foods in general, representing a heavy masticatory load, can lead to increased overall mandibular robusticity and thus increased bite force. A relatively less demanding diet consisting of processed plant and animal foods of an agricultural subsistence strategy, resulting in a lower masticatory load, does not promote an increase in mandibular body breadth (Holmes and Ruff 2011). Diet thus influences mandibular morphology, but not beyond the developmental stages in adolescence (Holmes and Ruff 2011), apart from tooth loss and the subsequent mandibular modifications. Dietary influence could be explained by the difference in measurements and a possibly greater impact of subsistence strategies between the populations studied by Holmes and Ruff (2011), consuming varying diets. The results obtained by Holmes and Ruff (2011) can be generalised into forms of subsistence and the covarying mandibular morphologies. Hunter-gatherer populations are found to have generally longer and narrower mandibles than agricultural societies (von Cramon-Taubadel 2011; Toro-Ibacache et al. 2019), when confounding factors like climate, a possible shared history and geography are eliminated. The reduction in mandibular length in agricultural societies is continued in post-industrialisation, explaining the often-observed mismatch between mandibular size and dental crowding as well as malocclusion (von Cramon-Taubadel 2011). Contrary to the shape of the neurocranium, which generally is not linked with diet and subsistence, mandibular morphology and the characteristic size of the temporalis muscle are affected (Noback and Harvati 2015). No reports regarding the influence of diet and subsistence on the human chin shape could be found in the literature researched. However, as mentioned in the section on mastication above, the study by Holton and colleagues (2015) found no correlation between the human chin shape and mastication. If this finding is extrapolated to diet and subsistence, given the proximate connection between diet and mastication, it could be suspected that human chin shape, unlike mandibular shape, is not influenced by subsistence.

Speech

A theory connecting the shapes of the mandible and the chin to speech (Ichim et al. 2007) remains as yet unproven (Coquerelle et al. 2017). The theory proposed by Ichim and colleagues (2007) suggests that the number of mandibular muscular movements involved in speech is greater than that connected with mastication. Thus, it is argued that speech could have influenced the evolution of oral structures, even if the cause-effect relationship is difficult to establish (Bermejo-Fenoll et al. 2019). Further, the theory claims that muscles involved in speech execute stress on the mandibular symphysis, thus developing a prominent chin, which, however, has also not been proven. Although speech requires the coordination of a variety of orofacial muscles, mainly those of the tongue and the hyoid (Hiiemae and Palmer 2003), the cause-effect relationship could be explained differently. Speech appears not to have influenced the shapes of the mandible and chin. Alternatively, speech could have been influenced by maxillomandibular positioning, which, in turn, was influenced by subsistence strategies (Blasi et al. 2019). With the reduction of the pre-Neolithic edge-to-edge bite and the development of the overbite in agricultural societies consuming less demanding processed diets, more speech sounds, the so-called labiodentals, became possible. Labiodentals are produced by positioning the lower lip against the upper teeth (“f” or “v”) and require much less muscular involvement in an overbite than in an edge-to-edge bite (Blasi et al. 2019). The authors of the study argue that in today’s hunter-gatherer societies with an edge-to-edge bite, labiodentals are not as wide-spread as in populations with an agricultural subsistence strategy (Blasi et al. 2019).

A connection between speech and chin shape could possibly be seen in the specific ratio of pharyngeal height to oral cavity length, which is assumed to be determinant for speech (Lieberman et al. 2001). This ratio decreases from 1.5 to 1.0 between birth and six to eight years, after which it remains stable. Sexual dimorphism in this ratio does not play a role until puberty, when a slight descent of the larynx occurs. The postnatal descent of the larynx and hyoid is unique in humans (Lieberman et al. 2001) and could serve as an explanation for the human ability to speak. Hence, the prominent chin could have developed as part of this ratio, allowing for the necessary space in the oral cavity.

2.2 THREE-DIMENSIONAL ANATOMICAL EXTRACTIONS

Three-dimensional techniques for anatomical extractions, such as CBCT and micro-XCT scans, have been used in research since the early years of the new millennium (Scarfe et al. 2017). Within this time frame, the application of CBCT scans in forensic anthropology could have been in even wider use, were it not limited by factors such as access to devices and high costs of licensing three-dimensional (3D) imaging software (Garvin and Stock 2016). The advantage of this relatively new techniques is a non-invasive and non-destructive virtual visualisation of external and internal structures of an object (Pernter et al. 2007; Grabherr et al. 2009; Ramsthaler et al. 2010; Franklin et al. 2013; Ekizoglu et al. 2014; Garvin and Stock 2016; Seiler et al. 2019). Cone beam computed tomography and micro-XCT scans are described in the sections below. Anatomical landmarks, traditionally used for shape quantification in forensic anthropology, are discussed thereafter.

2.2.1 Cone beam computed tomography

Cone beam computed tomography is an imaging technique traditionally used for dental and medical diagnostic purposes (Scarfe et al. 2006; De Vos et al. 2009). During the scanning procedure, a patient is positioned so that the patient's head is stabilised (Figure 2.6a). The source of the cone-shaped X-ray beam and the reciprocating detector revolve 360° around the region of interest on the patient's head, depicting the pre-set field of view in one arc, and taking images at intervals (Figure 2.6b) with a resolution of 0.4 mm up to 0.125 mm (Scarfe et al. 2006).

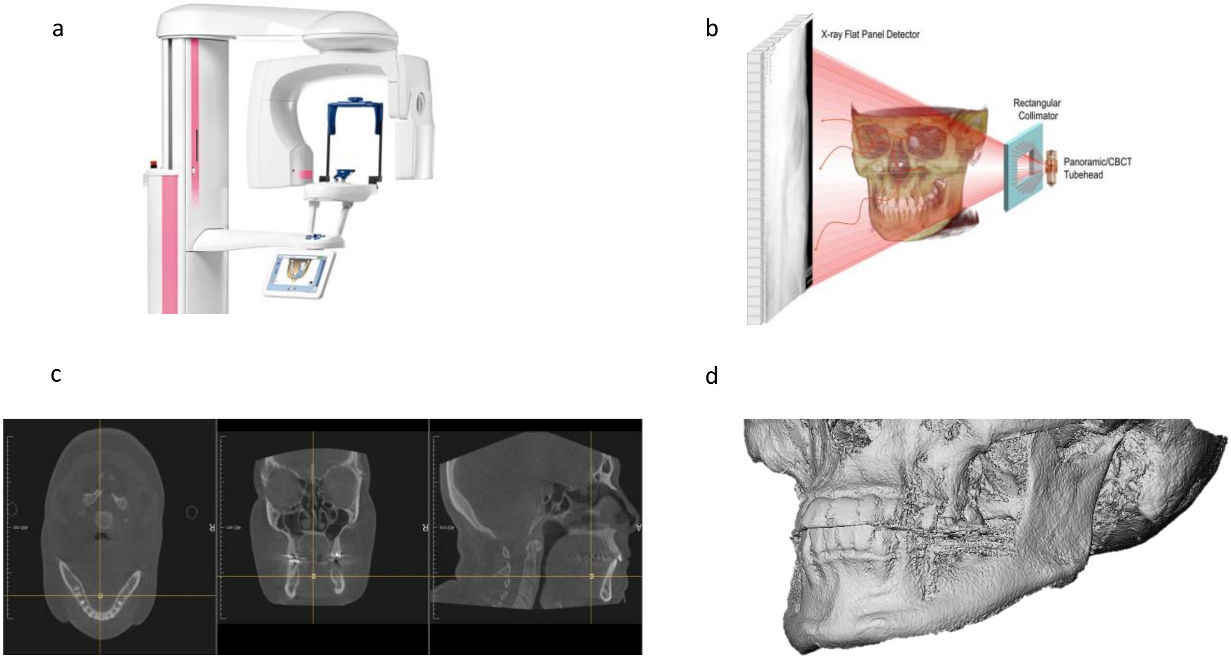

Figure 2.6 a) Planmeca ProMax ® 3D device (source: https://www.planmeca.com/imaging/3d-imaging/compare-our-units/), b) Geometric configuration of X-ray beam projection and sensor for CBCT imaging (source: Aust Dent J, Scarfe et al. 2017;62(1):33-50. With kind permission by Wiley), c) CBCT slice in 2D, axial (left), coronal (centre) and sagittal (right) view of the region of interest, d) CBCT surface in 3D.

Voxel size (pixel in the third dimension) in CBCT technology is isotropic, meaning it is equal in all three dimensions; in the Planmeca ProMax ® 3D device, the voxel size can be as low as 75 µm. So-called 'basis' or raw images are taken at specific degree intervals within the 360° with a radiation dosage up to 15 times lower than in conventional CT scanners (Scarfe et al. 2006). When combining the raw images, so-called 'projection data' is obtained. Suitable software programs with sophisticated algorithms combine the projection data into a 3D volumetric data set, which in turn is used for primary reconstruction of images (Scarfe et al. 2006; Scarfe et al. 2017). Images can be viewed in the different planes (Figure 2.6c) or in 3D (Figure 2.6d). The great advantage of CBCT scans applied to forensic anthropological research is the scanning process in the patients' upright position, thus avoiding distortion of soft-tissue in a supine position (Munn and Stephan 2018).

2.2.2 Micro-focus X-ray computed tomography

Micro-focus X-ray computed tomography is an imaging technique used to observe a variety of non-living materials with a resolution of between 1 and 100 µm (Sharma et al. 2014). The device from the Micro-focus X-ray Radiography and Tomography facility (MIXRAD) at the Nuclear Energy Corporation South Africa (Necsa) distinguishes itself by a 0.001 to 0.003 mm spot size and a voxel size of 0.0087 mm^3 (Hoffman and De Beer 2012) (Figure 2.7a). The scanning process is done by fixing the object to ensure no movement occurs during scanning (Figure 2.7b and 2.7c). Sample rotation takes place in the scanning cabinet in a vacuum (Hoffman and De Beer 2012). The rotation movement of the radiation source can move at intervals of up to 1/1000th of a degree and thus produces an enormous number of projections around 360° (Hoffman and De Beer 2012). The resulting 3D extraction from a micro-XCT scanning progress is a high-resolution image (Figure 2.7d).

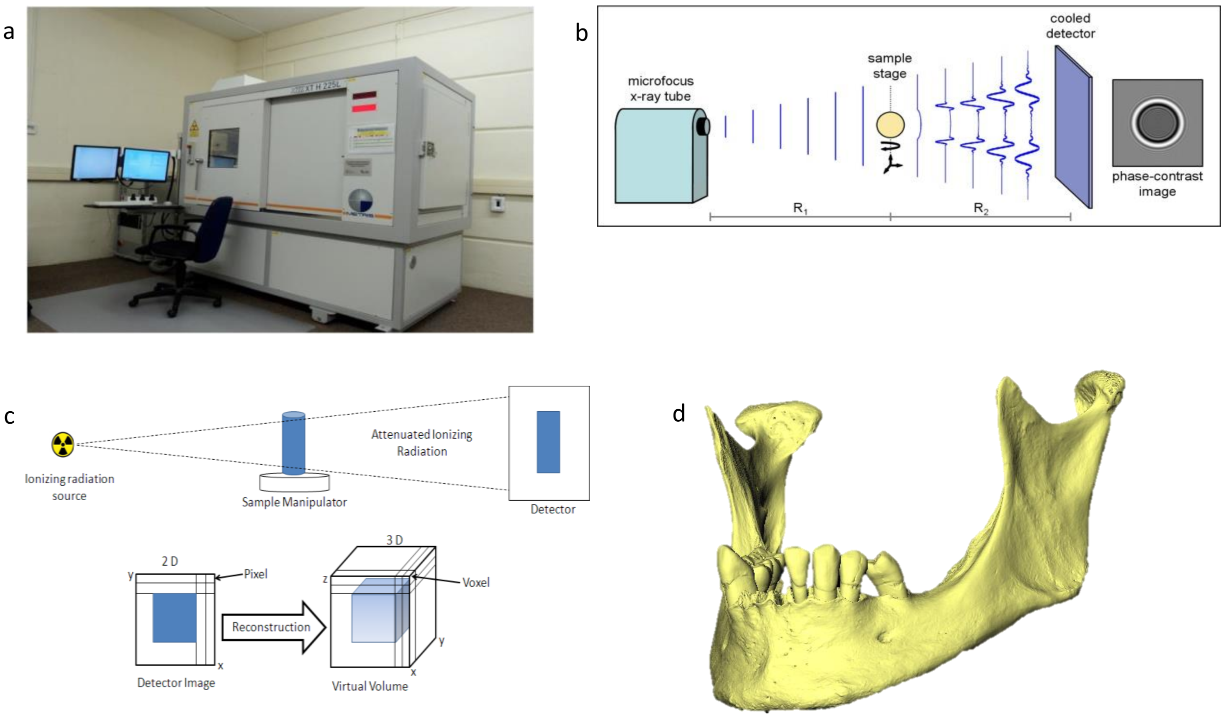

Figure 2.7 a) Micro-XCT scanner, MIXRAD, Necsa*, b) schematic illustration of specimen location and micro-XCT scanning procedure#, c) micro-XCT scanning process, MIXRAD facility, Necsa*, d) micro-XCT 3D reconstruction of mandible.
* Source: 18th World Congress on Nondestructive Testing, 2012. With kind permission by Dr de Beer, Necsa.
# (Zysk et al. 2012)

2.2.3 Anatomical landmarks

When shape analysis and accurate measurements involving anatomical landmarks are performed, precise landmarks are essential. Anatomical landmarks are used for measurements and allow the extraction of shape information, to be used for GMM (Wärmländer et al. 2019) for the present study. However, the uniformity and repeatability of landmark placement remain an issue (Wärmländer et al. 2019), whether landmarks are collected in dry bone, in 2D or in 3D (Caple and Stephan 2016; Wärmländer et al. 2019) to quantify and analyse shape. Shape, defined as *"all the geometric information that results from eliminating the effects of the position, scale and rotation of an object"* (Kendall 1977), can be measured, quantified and objectively and repeatably described by using anatomical landmarks (Weber and Bookstein 2011). Shape can be analysed in dry skulls with craniometric landmarks or on the soft-tissue face with capulometric landmarks (Caple and Stephan 2016).

Standardisation of craniometric landmarks was undertaken repeatedly in the early 1900s (Papillault 1906; MacCurdy 1912; Papillault 1919). In 1991, Bookstein proposed the definition of three types of landmarks, according to their positions and settings: type I representing a location on a juxtaposition of tissues, type II on maximal curvatures or processes, and type III are extremal points without a precise location, defined by a distance such as 'farthest distance from' or 'midpoint between' (Bookstein 1991). Bookstein himself referred to type III landmarks as 'deficient' as they miss precise coordinates (Bookstein 1991). Thus, type III landmarks are especially prone to placement error due to the relative imprecision of definition (Lagravère et al. 2010). Examples of type III landmarks used in this research are the gnathion and the gonion. The gnathion is defined as the *"median point between pg and me"* (Krogman and Sassouni 1957) and subsequently depends on the location of both, the pogonion (pg) and the menton (me), with the pogonion, per definition, being rather variable in location. The definition of the gonion is diverse (Figure 2.8) (Martin 1928; Martin and Knussmann 1988; Lagravère et al. 2010; Miloro et al. 2014) and places the landmark on a varying site on the mandibular angle.

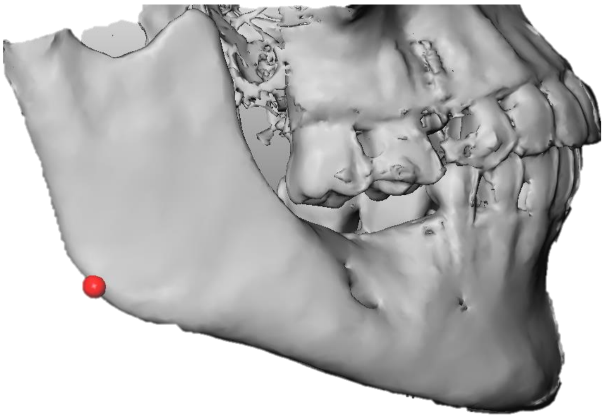

Figure 2.8 Landmark on the mandibular angle indicating the possible gonion placement.

Over time, the three landmark types became equivalent to good or precise (type I) and to bad or unprecise (type III) (Wärmländer et al. 2019). With a further expansion of the landmark types from three to six (Weber and Bookstein 2011), the uniformity of the landmark placement did not improve, and considerable confusion regarding landmark types became manifest in research papers (Cummaudo et al. 2013; Wärmländer et al. 2019). Therefore, Wärmländer and colleagues question the use of landmark types and rather encourage researchers to explain the purpose of their landmarks (be they craniometric or capulometric) and to be transparent on the intra- and interobserver errors (Wärmländer et al. 2019).

Anatomical landmarks may be placed manually (Schlager and Rüdell 2015) on a 3D surface, or they can also be placed automatically (Ridel 2019; Ridel et al. 2020), or when using a microscribe device (Nagasaka 2003). Especially in large samples, manual landmarking would be tedious and the repeatability in the manual process is lower than with the automatic process (Guyomarc'h et al. 2014; Ridel et al. 2018; Ridel et al. 2020). As the geometry of the measured landmark configuration is preserved by the set of landmark coordinates, GMM allows for effective visual representations of statistical results as actual shapes or shape deformations (Bookstein 1991; Slice 2007; Mitteroecker and Gunz 2009).

2.3 FORENSIC ANTHROPOLOGY

At the University of Pretoria, the Forensic Anthropology Research Centre (FARC) has been closely collaborating with the South African Police Service (SAPS) and their Victim Identification Centre (VIC) to alleviate the challenge of the high number of unidentified human remains in South Africa. Biological profiling is of paramount importance in forensic anthropological practice; it is based on the analysis of human variation for estimation of the demographic parameters, ancestry, sex, age and stature (İşcan and Steyn 2013). The forensic anthropologist is motivated to quantify ancestry-related shape variation in a medico-legal setting (Stull et al. 2014).

The estimation of ancestry is based on geographical origin and patterns of shape variation within a population (Brace 1995; Church 1995; Ousley 2009; L'Abbé 2011; Sholts et al. 2011; İşcan and Steyn 2013; Spradley 2016; Oettlé et al. 2017). The estimation of sex is expressed as the female and male biological sexes; 'gender' is not expressed in the genetic makeup of an individual and is thus not a category used in the field of forensic anthropology (İşcan and Steyn 2013). Sex estimation in subadult individuals is a challenge, as the expression of sex-discriminating traits develops for a short time during early childhood and, after that, only during young adulthood (Franklin et al. 2007; Hutchinson et al. 2012).

In the estimation of skeletal age, forensic anthropologists distinguish between biological and chronological age (Acsádi and Nemeskéri 1970). The latter refers to the actual number of years lived by an individual as recorded in personal identification documents, and constitutes the age sought by the forensic anthropologist. The former, in contrast, describes the physiological condition of the individual, which may differ from the number of years lived. Biological age depends on a number of influencing factors such as genetic disposition, nutrition, body mass index and level of physical activity (İşcan and Steyn 2013). Hence, chronological age is estimated based on the influence that unidentifiable factors could have on the ageing process of an individual (İşcan and Steyn 2013). The estimation of age is considered to be an inherently non-metric procedure and based on morphoscopic methods only (Spradley 2016).

In addition to ancestry, sex and age, the estimation of stature can be achieved in two different ways: by measuring one or several long bones and deduct stature of the living or by adding up the length of all bones in a skeleton contributing to the individual's stature in life (Fully 1956). A value is then added to make up for the loss of soft-tissues such as cartilage, intervertebral discs and the skin (İşcan and Steyn 2013).

Biological profiles are traditionally done by applying morphoscopic, metric or GMM methodologies (see section 2.3.1) to assess the expression of a trait (İşcan and Steyn 2013; Spradley 2016) and should, if possible, be based on many individuating traits on the skeleton in order to maximise probabilities of correct profiling. If, however, the entire skeleton is not available for analysis, biological profiles must be carried out on partial skeletons or single bones, even if this results in lower probabilities of correct profiling (İşcan and Steyn 2013). Moreover, biological profiles should be carried out, if and where possible, using multivariate approaches (Spradley 2016).

2.3.1 Shape variation assessment

Methods to analyse shape variation in forensic anthropology include morphoscopic, metric and GMM techniques. Morphoscopic methods refer to non-metric assessments of shape; visually by comparing a shape to a drawing or photo, or tactilely by feeling the expression of a trait and classifying it, according to a description, into ordinal data. More generally speaking, scores of trait expressions are used to bring the individual within a range of morphological variation (Todd 1920; Acsádi and Nemeskéri 1970; İşcan et al. 1984a; İşcan et al. 1984b; İşcan et al. 1985; Bruzek 2002; Walker 2008; Klales et al. 2012).

For metric techniques, standardised bone measurements are taken and entered into software programs such as FORDISC, for example, for the estimation of ancestry and sex (Ousley and Jantz 1996; Jantz and Ousley 2005). The applicability of a morphoscopic or metric method to a new population should be validated before introducing it on a larger scale (Krüger et al. 2015) as trait expressions can be population-specific (Walker 2008).

Geometric morphometrics can make use of data in a coordinate system, derived from 2D or 3D images, and are a mathematical means to analyse shape variation using landmarks and semilandmarks (Hennessy et al. 2002; Schlager and Rüdell 2015; Ridel et al. 2018; Noble et al. 2019).

2.3.1.1 Morphoscopic methods applied to chin shape variation: the Walker method

Morphoscopic methods for biological profiling are widely used by forensic anthropologists, even though they involve a certain degree of observer subjectivity (Walker 2008; İşcan and Steyn 2013), which may influence both the intra- and the interobserver errors (Garvin and Ruff 2012), and may even influence induced cognitive bias (Nakhaeizadeh et al. 2014).

The mandible is generally a useful bone for biological profiles; being a robust and durable bone, it is often preserved in a forensic context, even under adverse circumstances (Oettlé et al. 2009a), and the chin shape is generally deemed suitable for the estimation of sex, both morphoscopically and metrically (Walker 2008; Byrnes et al. 2017).

The shape of the chin can be assessed morphoscopically by holding the mandible so as to view it from a superior perspective. Assessment of the chin shape can be done by scoring the chin as *"blunt (smoothly rounded), pointed (the chin comes to a distinct point), square (the chin has a nearly straight front), or bilobate (the chin has a distinct central sulcus)"* (Byrnes et al. 2017). The accuracy of results when assessing both ancestry and sex, as reported in the study by Byrnes and colleagues (2017), is dependent on the level of observer experience; the authors report a higher accuracy when the assessment is done metrically (Byrnes et al. 2017).

The morphoscopic method published by Walker (2008) to assess an individual's sex according to the chin shape is widely used, and based on the original publication by Acsádi and Nemeskéri (1970), further developed by Buikstra and Ubelaker (1994). Five traits on the human skull (nuchal crest, mastoid process, supraorbital ridge/glabella, supraorbital margin and mental eminence) are scored from 1 to 5 according to their expression when compared to a line drawing and a description. Score 1 is defined as *"minimal expression"*, score 5 as *"maximal expression"* of each of the five traits (Walker 2008). *"Minimal expression"* in the mental eminence is equal to: *"Area of mental eminence is smooth. There is little or no projection of the mental eminence above the surrounding bone"*, while *"maximal expression"* is *"a massive mental eminence that occupies most of the anterior* *portion of the mandible"* (Walker 2008). While the author refers to the method as being 'visual' (Walker 2008), the scoring process is, at least in part, a tactile procedure. For three of the five described traits (nuchal crest, orbital margin and mental eminence), the observer is asked to move a hand or finger across the skull region in question and feel the expression of the trait (Walker 2008). Using a logistic regression model, the results of all five traits combined assume a high probability of correct sex estimation (88%) when carried out according to the description by Walker (Walker 2008; Krüger et al. 2015; Dereli et al. 2018). None of the five traits should, however, be studied in isolation; results obtained from the analysis of the mental eminence, for instance, show a low reliability (Krüger et al. 2015; Lewis and Garvin 2016). In this study, the Walker (2008) method was used to test the method's applicability to micro-XCT scans in two South African populations. The test was done by comparing the scores given to the same specimens in bone and 3D surfaces and by comparing the observers' performance.

The Walker method was previously applied to bones from the Pretoria Bone Collection (PBC), housed at the Department of Anatomy, University of Pretoria (L'Abbé et al. 2005; Krüger et al. 2015), resulting in a discrepancy between sexual dimorphism in North American and South African populations; the degree of sexual dimorphism was lower in South Africans as compared to the populations studied by Walker (McDowell et al. 2012; L'Abbé et al. 2013). Krüger and colleagues (2015) have adapted the formula to South African populations, thus highlighting the need for a population-specific formula. Coefficients were introduced for any combination of the cranial traits, specific for a South African sample. Before the present study, however, there was no certainty how observer performance of the mental eminence compares between bones and 3D scan surfaces.

2.3.1.2 Geometric morphometric methods applied to mandibular shape variation

Since the 1990s, many of the commonly used morphoscopic methods have been challenged with the surge of GMM (İşcan and Steyn 2013; Klingenberg 2016; Noble et al. 2019). Geometric morphometrics is a mathematical means of exploring and quantifying shape to further knowledge in the fields of medical diagnostics, evolutionary biology, forensics or functional morphology (Weber and Bookstein 2011). In contrast to traditional (non-geometric) morphometric approaches based on linear distances, ratios and angles (Braun et al. 2004; Pretorius et al. 2006; Mitteroecker and Gunz 2009; Thackeray and Dykes 2016), GMM methods are based on the Cartesian coordinates (x, y, z) of measurement points, the anatomical landmarks. Geometric morphometric methods provide an objective way to quantify the shape of morphological features for statistical comparisons between groups (Hennessy and Stringer 2002; Franklin et al. 2007). In GMM, the shape and the size of a morphological structure are separated. The shape of an object is determined by the geometric properties that are unaffected by size, orientation or positioning (Bookstein 1991; Dryden and Mardia 2016). The size is measured most frequently as the centroid size (CS), which represents the average (arithmetic mean) of all landmarks (Bookstein 1991; Dryden and Mardia 2016). It is calculated as the square root of the summed squared distance between all landmarks and their CS (Bookstein 1991; Dryden and Mardia 2016).

Thus far, GMM have been used in a number of studies related to forensic anthropology and biological profiling (Pretorius et al. 2006; Franklin et al. 2007; Claes et al. 2012; Stull et al. 2014; Garvin and Stock 2016). For example, the estimation of ancestry, applying GMM in South African populations on the cranium, was studied and found to be very accurate, even in South African Coloureds, a highly admixed population group (Stull et al. 2014). Geometric morphometrics were also reliably used to estimate sex from the gonial eversion in South African black females and males (Oettlé et al. 2009a). When studying the mandibular ramus flexure, however, less reliable results were obtained when applying GMM (Oettlé et al. 2005; Pretorius et al. 2006) as opposed to the original morphoscopic analyses (Loth and Henneberg 1996). Examples for the successful application of GMM and the forensic sex estimation in a recent Italian population (Nuzzolese et al. 2019) and a modern Czech sample (Bejdová et al. 2013) show the wide range of applications of this relatively new technology to mandibles. Geometric morphometrics can also be applied to both, the hard- and soft-tissue facial shapes. The nasal shape and size in black and white South Africans were analysed employing GMM, and a significant difference between the ancestries was found in all of the hard- and soft-tissue measurements (Ridel et al. 2018).

Although in addition to the literature cited above, extensive research has been done on the mandible regarding the estimation of ancestry, sex, and age (Jensen and Palling 1954; De Villiers 1968; Acsádi and Nemeskéri 1970; Tobias 1974; Loth 1996; İşcan and Steyn 1999; Xie and Ainamo 2004; Oettlé et al. 2009a; 2009b; Thayer and Dobson 2010; İşcan and Steyn 2013), a comprehensive analysis of chin shape variation among ancestral, sex and age groups as well as allometry, employing GMM on dentate South African blacks and whites, had not been performed before the present study. Moreover, specimens in skeletal collections are often edentulous (Hutchinson et al. 2015), thus limiting the possibility to study dentate individuals. This further increased the need to include 3D images in this study. The development of newer imaging modalities, i.e. CBCT, has opened the possibility of including living individuals with a wider spectrum of dentition into research pertaining to the chin. By assessing the applicability of a morphoscopic sex estimation technique to micro-XCT scans, and by investigating the chin shape variation using CBCT scans, the present study contributed to the quantifiable biological profiling methods involving 3D imaging techniques in South Africa.

CHAPTER 3 MATERIALS AND METHODS

The materials and methods applied in both parts of this study will be outlined below. The first or morphoscopic part of the study entails the sexing of the mandible by scoring the mental eminence according to the Walker method (Walker 2008) in bone and the applicability of the method to micro-focus X-ray computed tomography (micro-XCT) scan surfaces. The second part focusses on the chin shape variation study employing geometric morphometrics (GMM) and carried out on cone beam computed tomography (CBCT) scans.

3.1 WALKER METHOD ON THE MENTAL EMINENCE

3.1.1 Materials

Data acquisition

In the morphoscopic part of the study, 105 mandibles from black and white South Africans of known ancestry, age and sex were included from the Pretoria Bone Collection (PBC). The sex estimation method (Walker 2008) assessing the expression of the mental eminence was applied to these 105 mandibles and then to the micro-XCT surfaces of the same bones.

The micro-XCT scans were obtained between 2015 and 2017 at the Nuclear Energy Corporation South Africa (Necsa). The surfaces were segmented using the surface determination module of VGStudio MAX-3.0 software (Hoffman and De Beer 2012;

http://volumegraphics.com) at Necsa. Acquisition parameters were: 1000 projections per 360°, 90-120 kV, 70-220 mA. The resolution was between 0.066 and 0.100 µm. Three-dimensional surfaces were created and extracted in .ply format in order to visualise them in any software.

Sample

The sample consisted of black and white South African mandibles, with the following sample structure (Table 3.1): 34 black females (BF), 43 black males (BM), 8 white females (WF) and 20 white males (WM). Age at death ranged between 21 and 98 years, with the sample mean age at 52.6 years; 49.6 years for the black and 61.0 years for the white South Africans. For the purpose of this study, the same age groups were used here as for the chin shape variation study of this dissertation; young adults (18-29), adult group 1 (30-44), adult group 2 (45-59) and mature (≥60). The full list of specimens is given in Table 1, Appendix A.

Table 3.1 Sample structure of the 105 individuals for the Walker study.

Ancestry	Sex	Age range in years	Mean age	18-29	30-44	45-59	≥60	N
Black	Female	24-80	47.2	5	10	11	8	34
Black	Male	26-98	51.5	2	16	12	13	43
White	Female	21-81	53.9	1	0	5	2	8
White	Male	31-80	63.8	0	1	6	13	20
Overall		21-98	52.6	8	27	34	36	105

The foremost selection criterion for the sample was the dentition pattern of the individuals. Only individuals with dentition patterns A1, A2, A3, B1, B2 and B3 of the Eichner Index (Eichner 1955) were included as the shape of the chin and mental eminence and the mandibular angle in (almost) edentulous specimens are often altered (Oettlé et al. 2009b; Oettlé 2014) due to decreased masticatory performance. The latter is lost to a large degree between dentition groups B3 and B4 (Ikebe et al. 2010), hence the cut-off at dentition pattern B3 for this study. Dentition patterns B1, B2 and B3 consist of three, two and one posterior occlusal zone(s), respectively, with at least one premolar or molar in the maxilla and mandible in occlusion. Beyond dentition pattern B3, there is no posterior occlusal zone.

3.1.2 Methods

In this section, the methodological approach to the Walker (2008) part of this study will be described. This includes the description of the scoring process and the tests carried out on the data. The subsequent qualitative part of the methodology will highlight the observers' perception of the scoring process.

Reliability of trait scores (1-5) associated with the mental eminence

The method originally published by Walker (2008) is traditionally used on bone to estimate an individual's sex. All five traits described and observed on the human skull (nuchal crest, supraorbital ridge/glabella, mastoid process, supraorbital margin and mental eminence) are scored according to their expression and a sex estimation is deducted from the combined scores. Each of the five traits is observed in the skull and compared to a figure in the article by Walker (Walker 2008) depicting the trait expression. In Figure 3.1, the scoring of the mental eminence is shown with the score description as follows: score 1: female; score 2: probably female; score 3: ambiguous sex; score 4: probably male and score 5: male Buikstra and Ubelaker article (1994, pp. 21). Score 3 was categorised separately from "female" (scores 1 and 2) and "male" (scores 4 and 5).

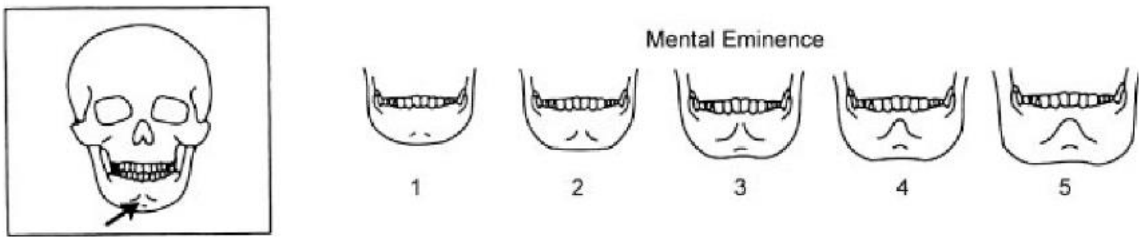

Figure 3.1 Standard for scoring the mental eminence. Source: Am J Phys Anthropol 2008;136:39-50. With kind permission by Wiley.

The Walker method (Walker 2008) was applied to the mental eminence in isolation. The mental eminence is defined as *"the triangular eminence, or bony chin, at the base of the corpus in the anterior symphyseal region. It is separated from the alveolar margins of the incisors by a pronounced incurvation or 'mental sulcus' […]."* (White and Folkens 2005, pp. 123) (Figures 2.2 and 2.3). Five scores can be attributed to the characteristic of the trait: score 1 relates to *"little or no projection of the mental eminence"*. By contrast, score 5 is described as *"a massive mental eminence that occupies most of the anterior portion of the mandible"* (Walker 2008, pp. 42). The scoring process, although usually referred to as being 'visual' (Walker 2008), is at least in part a tactile procedure. In the publication by Walker, the method is described as *"Hold the mandible between the thumbs and index fingers on either side of the mental eminence. Move the thumbs medially until they delimit the lateral borders of the mental eminence"* (Buikstra and Ubelaker 1994, pp. 20; Walker 2008, pp. 42). Feeling the bony surface in this way, researchers score the mental eminence and hence estimate the individual's sex (Figure 3.2).

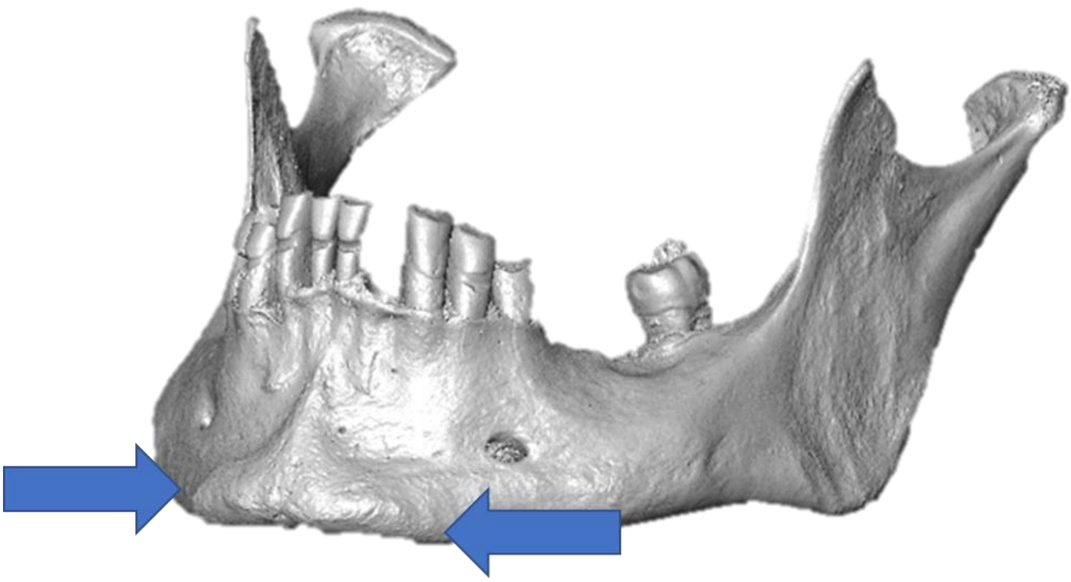

Figure 3.2 Mental eminence in a mandible; blue arrows show approximate thumb placement in the sex estimation on bone.

Intraobserver and interobserver tests

The principal investigator carried out an intraobserver error test (intraOE) on 25 randomly selected specimens out of the 105 (Table 2, Appendix A). The specimens were scored twice, each, in bone and three-dimensional (3D) surfaces at an interval of two weeks.

The blinded interobserver error test (interOE) on the 105 specimens was done by four observers of different levels of experience, in both modalities, bone and 3D surfaces, including the principal investigator; observers 1 and 3 had the highest level of experience applying the Walker (2008) traits to bones, while observer 2 had the lowest and observer 4 was the principal investigator who had done the largest amount of reading on the subject.

For the scoring process in bone, the 105 mandibles were laid out on a table in random order. Figure 1 (pp. 41) and Table 1 (pp. 42) in the Walker (Walker 2008) article were used by all observers for the scoring process in bones as well as 3D surfaces. Scores were entered into an excel file; the scores were not shared among observers at the time of observation.

The scoring of the 3D surfaces was done with myVGL viewer software (Volume Graphics, https://www.volumegraphics.com/de/produkte/myvgl.html) (Hoffman and De Beer 2012). Observers viewed the surfaces and were free to manipulate the surfaces (rotation and zoom) according to their comfort and preference. Again, scores were entered into an excel file and scores were shared only after completion of all observations. In addition, all observers answered questions asked in writing by the principal investigator and connected to the process of scoring of bones as well as 3D surfaces (Table 3.2). The questions referred to the observers' experience during the scoring processes for both modalities, bone and 3D surfaces. The purpose of the qualitative part was to assess a possible difference in the observers' experience when scoring the two modalities. All observers answered the questions independently by email, after the scoring process in both modalities was completed. The questions were the following:

Table 3.2 Questions to all observers referring to the scoring experience in both modalities.

1 – Which modality took you longer to score; bone or 3D surfaces?
2 – Which modality did you find harder to score; bone or 3D surfaces?
3 – Which score(s) (1, 2, 3, 4 and/or 5) did you find the hardest to do, both, in bone and 3D surfaces?
4 – How did you score the mandible (comparing the mental eminence to other mandibles, etc.)?
5 – How did you score the 3D surfaces (zoom, rotation, etc.)?

Statistical analysis

The interOE agreement of all four observers' scores in both modalities was tested with Fleiss Kappa (Fleiss 1971). The intra- and pairwise interOE were tested using Cohen's Kappa (Krüger et al. 2015). Likewise, for the comparisons of bone versus 3D surface scores per observer Cohen's Kappa was used. The interpretation of the *κ-values* (Fleiss and Cohen's Kappa) is given in Table 3.3, according to Landis and Koch (Landis and Koch 1977). The median of each observer's scores was calculated. The next step was to compare the scores for bone and 3D surfaces per observer. As scores are classified ordinal data, non-normality was assumed, and non-parametric Wilcoxon Signed-Rank tests were used (Liddell and Kruschke 2017; Villa 2017). Similar tests were applied for the intraOE tests. Statistical analyses were done using R psych package (Revelle 2019) and irr package (Gamer et al. 2019). Statistical significance was assumed for a *p-value* equal to or smaller than 0.05.

Table 3.3 Kappa values and their interpretation according to Landis and Koch 1977.

Kappa value	Interpretation
<0.00	Poor
0.00 to 0.20	Slight
0.21 to 0.40	Fair
0.41 to 0.60	Moderate
0.61 to 0.80	Substantial
0.81 to 1.00	(Almost) perfect

Further analyses

As one of the aims was to compare the scores in bones with those in 3D surfaces, the sample was analysed overall and split between the observers as well as the subsamples (ancestry, sex and age groups). Furthermore, the score frequency per observer was studied.

3.2 CHIN SHAPE VARIATION IN SOUTH AFRICANS

3.2.1 Materials

For the GMM part of the study, CBCT scans from 291 patients were used. The scans originated from the Oral and Dental Hospital, University of Pretoria where patients were scanned between 2015 and 2018. Patients were scanned once, for medical reasons, not for reasons related to this study. The patient data were anonymised, and only ancestry, sex and age at scanning were recorded for the purposes of this study (Table 3, Appendix A).

Scanning took place in a seated position with eyes closed and a relaxed facial expression. Criteria for exclusion of scans were distorting conditions such as pathologies or anomalies of the facial bones, current or healed fractures of the bones in question as well as tooth loss. All included specimens had the dentition pattern A1, A2, A3, B1, B2 and B3 of the Eichner Index (Eichner 1955). Only subjects of the age above 18 years were considered as the adolescent, growing mandible was not the focus of this study. The sample structure is given in Table 3.4.

Table 3.4 Sample structure of the 291 subjects for the chin shape analysis.

Group	Age in years	Ancestry	Sex	N
Young adults	18-29	Black	Female	12
			Male	24
		White	Female	27
			Male	14
Adult group 1	30-44	Black	Female	21
			Male	22
		White	Female	30
			Male	12
Adult group 2	45-59	Black	Female	11
			Male	41
		White	Female	12
			Male	20
Mature	≥60	Black	Female	3
			Male	28
		White	Female	1
			Male	13
Total				291

All CBCT scans were obtained using a CBCT scanner (Planmeca ProMax ® 3D, Planmeca OY, Helsinki, Finland) with the following properties: 90 kV, 11.2 mA, voxel size of 0.4 mm and field of view of 230 x 260 mm at the Oral and Dental Hospital, University of Pretoria. The CBCT images in DICOM format were imported into MeVisLab © v. 2.7.1 software for segmentation and 3D surface mesh generation.

3.2.2 Methods

The method used in the present study is based on the proposed procedures suggested by Claes (2007) and first tested and published by Ridel and colleagues (2020). This method includes the segmentation of CBCT images, the subsequent 3D surface mesh generation, followed by an initialisation process to align the 3D surfaces in the same Cartesian coordinate system, and a non-rigid registration process allowing an automatic landmarking on all hard-tissue 3D surfaces using a template. The individual steps in this procedure are depicted in Figure 3.3 and outlined in detail thereafter.

Segmentation

The segmentation process preceding the following procedures describes the separation of soft- and hard-tissue of the patient scans acquired at the Oral and Dental Hospital, Pretoria. As only the hard-tissue is analysed in the current study, the soft-tissue is eliminated in the segmentation process. For this purpose, CBCT images in DICOM format are exported into MeVisLab © v. 2.7.1 software. Following the segmentation process, 3D surface meshes were generated.

The segmentation process was based on grey values, which represent the density of the observed tissue. As in regular x-ray images, a higher grey value implies a greater tissue density. For the segmentation process, grey values between 1 100 and 1 300 were chosen in MeVisLab © v. 2.7.1 software for optimal output. The so-called threshold-segmentation included the definition of the ideal grey value per scan, thus allowing the observer to obtain the best hard-tissue image according to the "Half Maximum Height" (HMH) thresholding method (Spoor et al. 1993).

With the chosen grey values, the software calculated a 3D image of the scanned skull. As the CBCT scans consist of a great number of individual slices, the software calculated the spaces in-between.

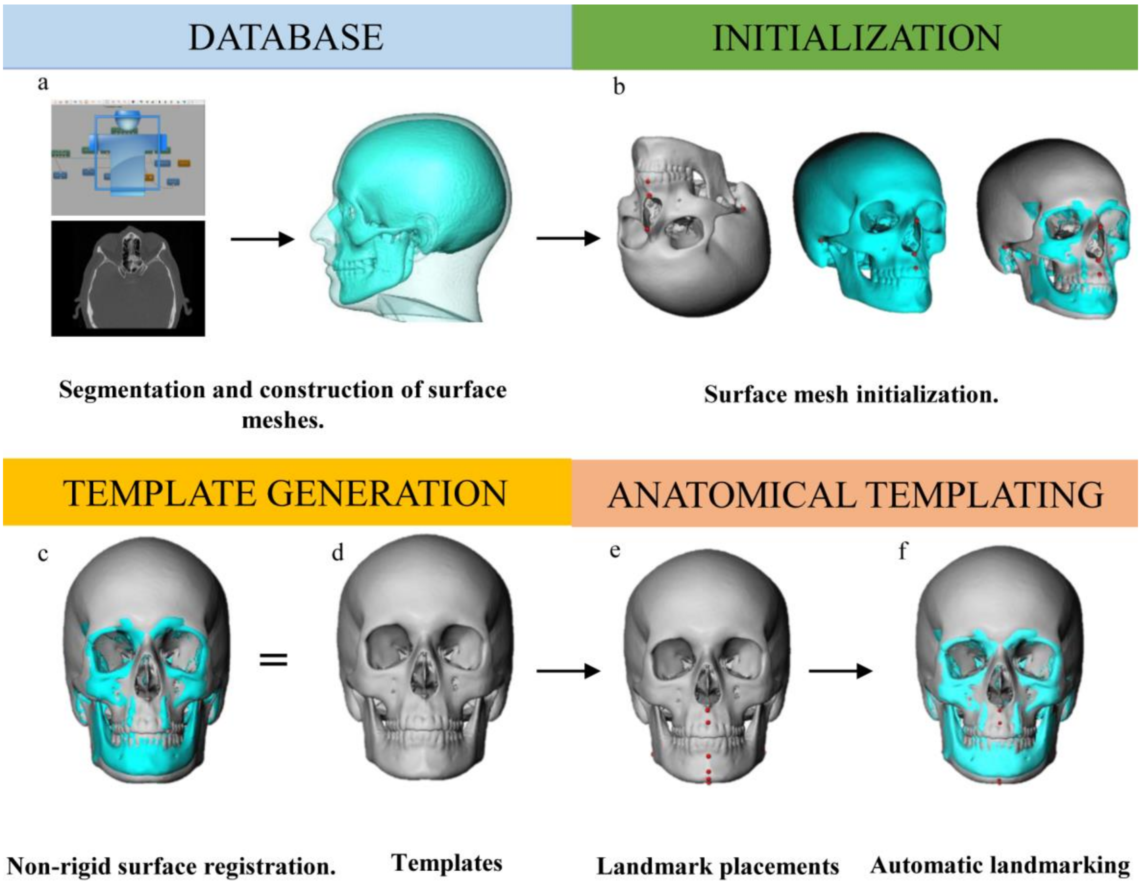

Figure 3.3 Workflow of the automatic landmarking used in this study (Ridel et al. 2020); scans are segmented, surface mesh is constructed (a); initialisation of surface mesh (b); non-rigid surface registration (c) results in a template (d) on which craniometric landmarks are placed manually (e); automatic landmarking (f) places craniometric landmarks on the 3D surfaces. Figure courtesy Dr AF Ridel.

Surface mesh initialisation

The crucial point in the next step is the alignment of all the 3D surfaces into a uniform Cartesian coordinate system. This process is called surface mesh initialisation (Ridel et al. 2020). The floating surface, referring to the template from Ridel (Ridel 2019), must be brought into close proximity of the target surface (specimen used in this study) before the registration process can be initiated. The initialisation process is done by manually placing a set of five landmarks on the maxilla and the mandible (Figure 3.4) on the floating as well as target hard-tissue surfaces and subsequently bringing them into closer and aligned proximity.

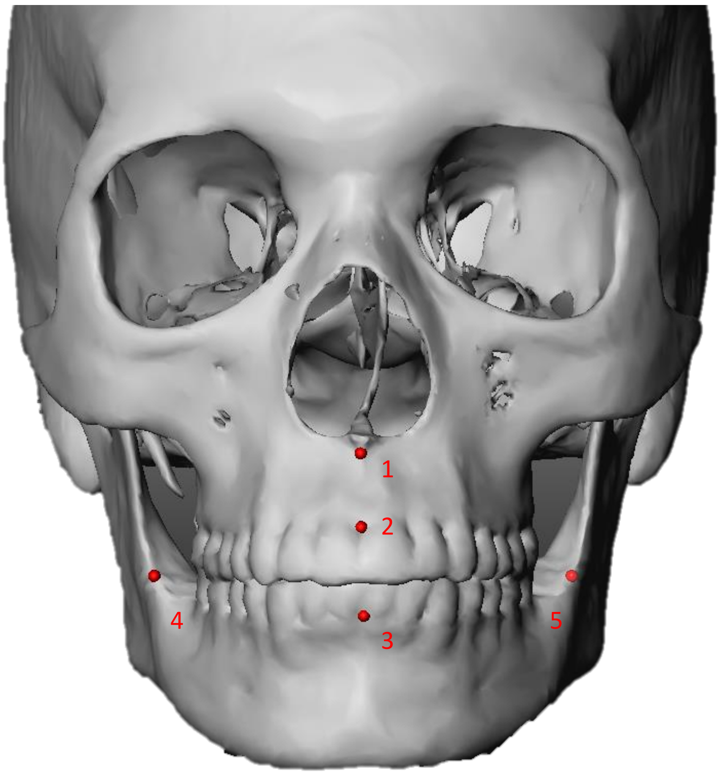

Figure 3.4 Landmarks used for surface mesh initialisation process (template skull generated in MeVisLab © v. 2.7.1 software).

This transformation in space resulted in the coordinates of each landmark of the floating surface into the space of the target surface. The quality of the preceding initialisation process determines the outcome of the surface registration.

Hard-tissue template generation using a non-rigid surface registration process

The reference templates are created in an iterative fashion, akin to the generation of the mean shape in a General Procrustes Analysis (GPA) procedure (Kendall 1984; Slice 2001), the main difference being the insertion of a point-correspondence establishment step determined by the non-rigid registration process (Claes 2007; Ridel et al. 2018). Surface registration refers to the establishment of the geometrical relationship between surfaces that aligns the surfaces between them as closely as possible (Claes 2007). Then, every individual surface is "templated" (named the warped surfaces) such that every point on all 3D surfaces is associated with the anatomically corresponding point on the reference template. In a last step, landmarks are indicated once on the reference templates. Every landmark placed on the template is associated with the anatomically corresponding point on the warped surfaces (Ridel et al. 2018).

Anatomical templating

During an anatomical templating process, the reference template is warped non-rigidly to every subject's anatomically corresponding surface (target surface) (Ridel et al. 2018). The non-rigid (robust) surface registration software used for this warping was developed using the MeVisLab © v. 2.7.1 software (Snyders et al. 2014). The warping is performed iteratively starting with a rigid alignment, and gradually following with more flexible registration steps (Ridel et al. 2018). At the end of this process every landmark of the template is projected onto every subject's surface, thus establishing a dense point-based anatomical correspondence among all subjects (Ridel et al. 2018). Therefore, the coordinates of all subjects are recorded within a common coordinate system, which may be used for statistical analysis (Ridel et al. 2018).

The use of anatomical craniometric landmarks is the basis for research in this area. Thus, reliable and uniform placement of the craniometric landmarks was essential. For the present study, the definitions of all nine craniometric landmarks as presented in Caple and Stephan (Caple and Stephan 2016) were used. The landmarks selected were first placed on the template and then placed automatically on the mandible as well as on the maxilla, enabling the consistent study of the hard-tissue region of the chin and anchoring the bony menton in the face (Table 3.5).

Table 3.5 Definitions, abbreviations, nature and type of landmarks used for the surface meshes initialisation.

Landmark	Position	Abbrev.	Nature	Definition	Original source
Subspinale / A Point	1	ss	Unilateral	The deepest point seen in the profile view below the anterior nasal spine.	(Howells 1937, 1973)
Prosthion	2	pr	Unilateral	Median point between the central incisors on the anterior most margin of the maxillary alveolar rim.	(Martin 1928; Martin and Knussmann 1988)
Infradentale	3	id	Unilateral	Median point at the superior tip of the septum between the mandibular central incisors.	Buikstra and Ubelaker 1994
Supramentale / B Point	4	sm	Unilateral	Deepest median point in the groove superior to the mental eminence.	(Phulari 2013; George 1993)
Pogonion	5	pg	Unilateral	Most anterior median point on the mental eminence of the mandible.	(Martin 1928, Martin and Knussmann 1988)
Menton	6	me	Unilateral	Most inferior median point of the mental symphysis (may not be the inferior point on the mandible as the chin is often clefted on the inferior margin).	(Krogman and Sassouni 1957)
Gnathion	7	gn	Unilateral	Median point halfway between pg and me.	(Krogman and Sassouni 1957)
Mental tubercle	8, 9	mt	Bilateral	Rounded projections forming the inferior angles at the base of triangular mental protuberance.	(Oettlé 2014)
Gonion	10, 11	go	Bilateral	Point on the rounded margin of the angle of the mandible, bisecting two lines; one following vertical margin of the ramus and one following horizontal margin of corpus of mandible.	(Martin 1928; Martin and Knussmann 1988)

The sequence of craniometric landmarks placement in both, manual and automatic procedures, was as follows: 1 subspinale (ss), 2 prosthion (pr), 3 infradentale (id), 4 supramentale (sm), 5 pogonion (pg), 6 menton (me), 7 gnathion (gn), 8 mental tubercle left (mt lft), 9 mental tubercle right (mt rgt), 10 gonion left (gn lft), 11 gonion right (gn rgt) (Figure 3.5). They were placed in the MeVisLab © v. 2.7.1 software by zooming and rotating the 3D surface to the best position in order to best detect the location.

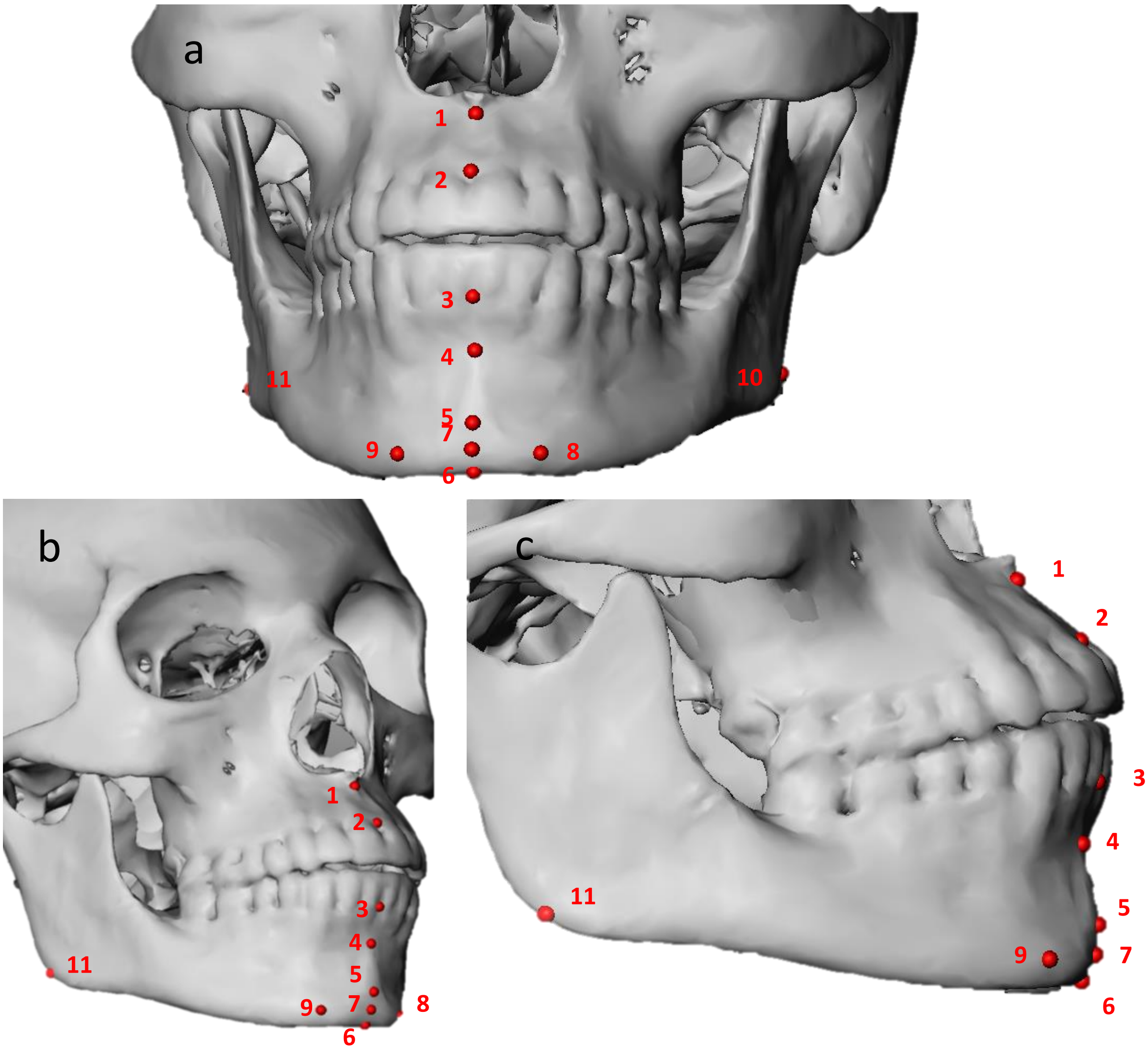

Figure 3.5 Landmarks used for this study; frontal (a), diagonal (b) and lateral (c) view. The sequence of landmarks is listed in Table 3.5 (template skull generated in MeVisLab © v. 2.7.1 software).

The craniometric landmarks on the entire sample were placed automatically by positioning the pre-defined craniometric landmarks on the template surface and projecting them onto each surface in the subsample (Figure 3.3). The coordinates of the craniometric landmarks were saved in an excel file for statistical analysis.

The craniometric landmarks were placed manually and automatically in an intra- and interobserver dispersion test (intraOD and interOD) on ten surfaces from a previous study sample (Table 4, Appendix A), in order to test the repeatability of both methods (Ridel et al. 2018).

Statistical analysis

The statistical analysis of this study was concerned with the chin shape variation and the possible influencing factors ancestry, sex, age and allometry. The evaluation and the quantification of shape differences attributed to known factors (ancestry, sex and age) were performed on hard-tissue shapes using GMM. The first analyses as described below were carried out on all nine craniometric landmarks while in a second analysis, only selected craniometric landmarks on the bony menton (Figure 3.6) were looked at (1 infradentale, 2 supramentale, 3 pogonion, 4 menton, 5 gnathion, 6 mental tubercle left and 7 mental tubercle right). The selection criterion was the specific analysis of the morphology of the bony menton only, without the landmarks on the maxilla and the gonia.

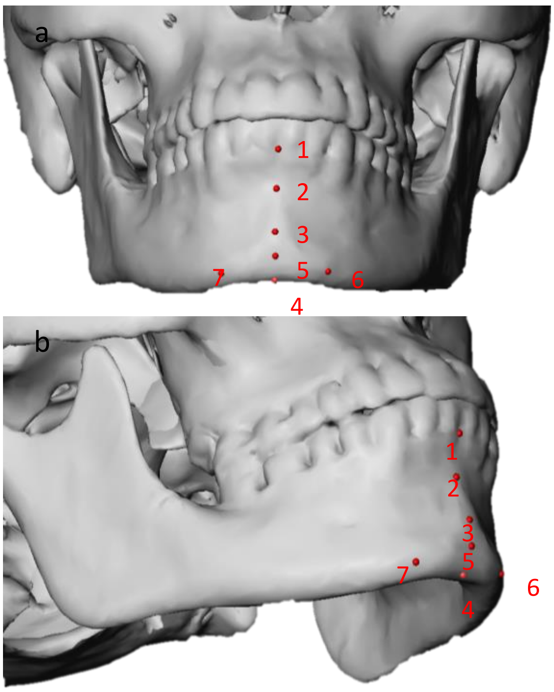

Figure 3.6 Selected craniometric landmarks used for this study; frontal (a) and diagonal (b) view (template skull generated in MeVisLab © v. 2.7.1 software).

Before analysing chin shape variation and the factors influencing it, reproducibility testing of the manual versus automatic landmark placement as well as the intraOD and interOD test were performed to evaluate the landmark dispersion between observers and methods (manual and automatic). Geometric morphometric methods involving GPA and Principal Component Analysis (PCA) to create principal component (PC) scores, were the underlying methodologies used in the study of shape variation between methods, observers and with influencing factors.

General Procrustes Analysis

Preceding the statistical analysis, a GPA (Goodall 1991; Dryden and Mardia 2016) was performed on the hard-tissue raw Cartesian coordinates to obtain pose-invariant shape coordinates (Kendall 1984; Klingenberg and McIntyre 1998; Slice 2001; Klingenberg et al. 2002). The raw landmark coordinates not only contain information on size and shape of the landmark configurations, but also on their position and orientation. The most common approach for separating shape from size and the "nuisance parameters" position and orientation is GPA (Rohlf and Slice 1990). This method comprises three steps: translating all landmark configurations to the same centroid, scaling all configurations to the same coordinate system, and iteratively rotating all configurations until the summed squared distances between the landmarks and their corresponding sample average are a minimum. The coordinates of the resulting superimposed landmark configurations are called Procrustes shape coordinates as they only contain information about the shape of the configurations.

Reproducibility testing

The reproducibility of the manual versus automatic landmark placement was tested with an intra- and an interOD. For this purpose, ten scans from the sample were randomly selected. Two observers placed the craniometric landmarks on the template (interOD); the principal investigator placed them twice (intraOD), at an interval of two weeks. The same observers carried out the manual and the automatic landmarking procedures. The manual and the automatic landmark placement were carried out using MeVisLab © v. 2.7.1 software. The Cartesian coordinates of both procedures were saved in excel files for further analysis.

The manual placement of landmarks was performed by indicating the eleven craniometric landmarks on the ten scans individually. For the automatic landmarking procedures, the same ten scans were used as for the manual craniometric landmark placement. For the automatic placement, the observers placed the craniometric landmarks once on the template; the software then placed them on each scan automatically.

The analysis of the precision of the manual versus automatic landmarking took place by calculating the dispersion of each landmark using the dispersion Δ_{ij} for each landmark *i* and individual *j*. Dispersion is defined as the Mean Euclidean Distance (MED) of the sample landmark $\boldsymbol{p}_{ijk}$ to the mean $\overline{\boldsymbol{p}}_{ij}$ of the (x,y,z)-coordinates of landmark *i* over all observations *k* (intra- and interOD) for subject *j*:

$$\Delta_{ij} = \sum_{k=1}^{K} \left\| \boldsymbol{p}_{ijk} - \overline{\boldsymbol{p}}_{ij} \right\| / K \text{, with } \overline{\boldsymbol{p}}_{ij} = \sum_{k=1}^{K} \boldsymbol{p}_{ijk} / K$$

Boxplots of MED values are generated for automatic and manual landmarking separately, displaying the dispersion. Precision is then reported as the global (averaged over all landmarks) mean (μ_Δ) and median (m_Δ) of the per landmark mean ($\mu_{\Delta \mathrm{i}}$) and median ($m_{\Delta \mathrm{i}}$) values over all scans.

Principal Component Analysis

Data reduction was achieved by PCA to reduce data dimensionality and to create independent principal component (PC) scores that quantify the different shapes studied. Statistical testing was performed using the PC scores covering 95% of the sample's overall variance. The PCA involves the examination of axes that reflect maximum variation and covariation. The data is transformed to a new coordinate system, such that the greatest variance of the data lies on the first transformed new variable (the first PC) and the second greatest variance on the second transformed variable. The orthogonal axes of the PCA summarise variation decreasing in order. Individual observation was plotted along axes. The score of a given observation on a given axis corresponds to the projection of the data on that axis. Examining variation on the first axis provides a way to reduce the variable space to dimensions that express most variation. Each axis corresponds to a linear combination of original variables. The first corresponds to the main direction of the variance covariance structure of individual observations.

Multivariate normality

For this study, multivariate normality testing was performed on the GMM-derived hard-tissue PC scores distribution by interpreting Q-Q-plots (Scrucca 2000), which allows the presumption that the variables are distributed according to the distribution tested. The graphical output shows the actual values of squared Mahalanobis distances plotted versus those of an ideal multivariate normal distribution. The closer the values are to the diagonal line, the more probable is a multivariate normal distribution.

Univariate / Multivariate analysis of variance and standard discriminant function analysis

First, the impacts of both ancestry and sex on the hard-tissue within the complete sample were assessed separately. Then, in order to identify significant ancestry-specific differences, the impact of sex, the ageing process and allometry were analysed on each subsample (blacks and whites) separately. The entire workflow for the statistical analyses is shown in Figure 3.7. Multiple analysis of variance (MANOVA) was run to evaluate differences between populations, sexes and with ageing on hard-tissues. A MANOVA is an extension of the univariate analysis of variance (ANOVA). MANOVA takes into account multiple continuous dependent variables and bundles them together into a weighted linear combination or composite variables. The MANOVA will compare whether the newly created combination differs among groups or levels of the independent variable. In this way, the MANOVA essentially tests whether the independent grouping variable simultaneously explains a statistically significant amount of variance in the dependent variable. MANOVA was applied using the R-package geomorph (Adams et al. 2018). Two non-parametric tests were also applied in order to double-check the results from the parametric test: 50-50 MANOVA and permutation testing (all permutation tests were run with 10 000 rounds). A 50-50 MANOVA (Langsrud 2002; Langsrud et al. 2007) is a modified version of a MANOVA, designed for many (potentially correlated) response variables. The 50-50 MANOVA was applied using the R-package ffmanova (Langsrud and Mevik 2012). Permutation testing permits calculation and comparison to values gained from the same sample where group membership is randomly reassigned repeatedly. As a result, the number of resampled values exceeding the "true" one is divided by the number of permutation rounds. If the value to be tested falls within the range of random grouping, the null hypothesis cannot be rejected because the measured value is not exceeding the one generated by chance. Permutation testing was performed using the R-package morpho (Schlager 2013). Significance of age effects were also assessed using standard MANOVA (parametric test) and 50-50 MANOVA (non-parametric test). Standard Discriminant Function Analysis (DFA) was also performed for ancestry and sex classification purposes and the classification accuracy estimated by conducting a leave-one-out cross-validation. A DFA finds linear variables that describe intergroup differences. These combinations define linear discriminant functions. The linear discriminant coefficients are defined from the non-null eigenvectors of the between-group variance-covariance "scaled" by the within-group variance-covariance. The DFA in this study was calculated using the R-package morpho (Schlager 2013).

Hard-tissue raw coordinates

Generalised Procrustes Analysis –
Principle Component Analysis –
Multivariate normality analysis

Principle Component scores

Statistical analysis:

A) Ancestry (MANOVA; 50-50 MANOVA; PERMUTATION TEST)

B) Sex, Age, Allometry (MANCOVA, 50-50 MANOVA) and covariates (ancestry*sex*age; ancestry*allometry)

Figure 3.7 Workflow of statistical shape variation analysis.

The statistical analysis was performed with R studio software version 1.0.44-®2009-2016 for Windows (R Core Team 2012). Statistical significance was assumed for *p-values* equal to or smaller than 0.05.

CHAPTER 4 RESULTS

4.1 WALKER METHOD

The analyses of the morphoscopic Walker method (2008) scores in bone and three-dimensional (3D) surfaces are explained. First, the intra- and interobserver error tests are stated, followed by an analysis of the score frequency and the comparison of the scores assigned by the four observers to the two modalities. The scores were obtained in bone and in 3D surfaces and were compared within the ancestral groups, the sex groups, the age groups, as well as with combinations of these groups: ancestral-sex and ancestral-sex-age groups. The main attention of the analyses lay on the observers' performance in relation to known sex and on performance compared between bone and 3D surfaces. The qualitative analysis section focussed on the observers' experience during the scoring process of both modalities, bone and 3D surfaces.

4.1.1 Intraobserver and interobserver tests

Before comparing the scoring between modalities and analysing the accuracy of sexing in both modalities, repeatability between observations by the principal investigator (intraOE) and between observations by four different observers (interOE) are reported. The Cohen's Kappa test results for the intraobserver error (intraOE) and the Fleiss Kappa test results for the interobserver error (interOE) are given in Table 4.1. The Cohen's Kappa test for intraOE was moderate with κ=0.448 for bone and substantial, κ=0.799, for 3D surfaces.

The interOE agreement of all four observers' scores as calculated by the Fleiss Kappa tests, were minimal both in bone (κ=0.163) and in 3D surfaces (κ=0.169).

Table 4.1 Cohen's Kappa results of the intraOE and Fleiss Kappa results of the interOE.

	intraOE	interOE
Bone	κ=0.448	κ=0.163
3D surfaces	κ=0.799	κ=0.169

Regarding the results of the Cohen's Kappa test for the 12 comparisons among the four observers and the two modalities (Table 4.2), only one (κ=0.332) had a fair correlation (observer 2 versus observer 3 in 3D surfaces) and two (κ=0.626 for bone and κ=0.748 for 3D surfaces) had a substantial correlation (observers 1 and 4 in both modalities). The remaining nine comparisons were moderate, between κ=0.432 and κ=0.546. The mean value of all Cohen's Kappa results of the interOE in bone was κ=0.521 while that of 3D surfaces was κ=0.489; both are moderate.

Table 4.2 Cohen's Kappa results of the interOE and interpretation (Landis and Koch 1977).

InterOE	Modality	*κ-values*	Interpretation
1 vs. 2	Bone	0.546	moderate
	3D surface	0.464	moderate
1 vs. 3	Bone	0.516	moderate
	3D surface	0.481	moderate
1 vs. 4	Bone	**0.626**	**substantial**
	3D surface	**0.748**	**substantial**
2 vs. 3	Bone	0.432	moderate
	3D surface	0.332	fair
2 vs. 4	Bone	0.488	moderate
	3D surface	0.462	moderate
3 vs. 4	Bone	0.517	moderate
	3D surface	0.447	moderate
Mean	Bone	0.521	moderate
	3D surfaces	0.489	moderate

Bold figures highlight the highest/substantial *κ-values*.

Medians were calculated for all observers and are shown in Table 4.3. There was little variation in the medians among the four observers. While observers 1 and 4 presented with a slight difference between the modalities (3 and 2, 2 and 3, respectively), observers 2 and 3 showed the same values (3 and 2, respectively) for both modalities.

Table 4.3 Medians of scores in bone (b) and 3D surfaces (3D), of each observer (obs.).

	Obs. 1	Obs. 2	Obs. 3	Obs. 4
Median (b)	3	3	2	2
Median (3D)	2	3	2	3

The comparisons of scores in bone and 3D surfaces for all four observers and the two intraOE tests were done with a Wilcoxon Signed-Rank test in R and resulted in the *p-values* listed in Table 4.4. The statistically significant *p-values* for all (excluding the intraOE 2 test) indicated the diversity of the scores. The non-significant *p-value* for the intraOE 2 test (0.183) indicated the relative similarity of the scores between bone and 3D surfaces.

Table 4.4 Wilcoxon comparison of scores in bone versus 3D surfaces per observer (obs.).

	Obs. 1	Obs. 2	Obs. 3	Obs. 4	Intra 1	Intra 2
p-value	<0.001	0.018	0.026	0.016	0.005	**0.183**

Bold figure highlights non-significant *p-value*.

4.1.2 Score frequency in bone versus 3D surfaces

Frequencies for the ordinal scores assigned to the mental eminences according to the system described by Walker (2008) are given below in Tables 4.5 and 4.6 for bone and 3D surfaces, respectively. The tables per ancestral-sex subsamples highlight the frequency of scores assigned per observer and as combined, across the four observers, for bone and 3D surfaces, respectively. The distribution of score frequency showed that black females (BF) were most often given score 2 by all four observers although not all observers concurred on this score. When looking at black males (BM) and white females (WF), a score 3 was most often given in bone by all observers, while in 3D surfaces, score 2 was given to BM and score 3 to WF. Score 5 was most often given to white males (WM) in bone while in 3D surfaces, WM were most often assigned a score 3.

Table 4.5 Score frequency per observer (obs.) and combined for all observers, in bone.

	Subsample	Score 1		Score 2		Score 3		Score 4		Score 5		Total	
		N	%	N	%	N	%	N	%	N	%	N	%
Obs. 1	BF	3	8.9	**13**	**38.2**	11	32.4	6	17.6	1	2.9	34	100.0
	BM	3	7.0	**17**	**39.5**	15	34.9	5	11.6	3	7.0	43	100.0
	WF	0	0.0	1	12.5	2	25.0	1	12.5	**4**	**50.0**	8	100.0
	WM	2	10.0	3	15.0	2	10.0	4	20.0	**9**	**45.0**	20	100.0
Obs. 2	BF	1	2.9	7	20.6	12	35.3	**14**	**41.2**	0	0.0	34	100.0
	BM	3	7.0	6	14.0	**18**	**41.9**	14	32.6	2	4.5	43	100.0
	WF	0	0.0	1	12.5	2	25.0	**3**	**37.5**	2	25.0	8	100.0
	WM	0	0.0	3	15.0	3	15.0	5	25.0	**9**	**45.0**	20	100.0
Obs. 3	BF	3	8.9	**24**	**70.6**	7	20.5	0	0.0	0	0.0	34	100.0
	BM	3	7.0	**17**	**39.5**	15	34.9	6	14.0	2	4.6	43	100.0
	WF	1	12.5	0	0.0	**5**	**62.5**	2	25.0	0	0.0	8	100.0
	WM	1	5.0	4	20.0	**8**	**40.0**	5	25.0	2	10.0	20	100.0
Obs. 4	BF	**14**	**41.3**	12	35.3	6	17.6	1	2.9	1	2.9	34	100.0
	BM	6	14.0	**17**	**39.5**	11	25.6	5	11.6	4	9.3	43	100.0
	WF	2	25.0	0	0.0	1	12.5	**3**	**37.5**	2	25.0	8	100.0
	WM	2	10.0	3	15.0	2	10.0	2	10.0	**11**	**55.0**	20	100.0
All obs.	BF	21	15.4	**56**	**41.2**	36	26.5	21	15.4	2	1.5	136	100.0
	BM	15	8.7	57	33.1	**59**	**34.3**	30	17.4	11	6.5	172	100.0
	WF	3	9.3	2	6.3	**10**	**32.3**	9	28.1	8	25.0	32	100.0
	WM	5	6.3	13	16.2	15	18.8	16	20.0	**31**	**38.7**	80	100.0

Highest values in bold.

Table 4.6 Score frequency per observer (obs.) and combined for all observers, in 3D surfaces.

	Subsample	Score 1		Score 2		Score 3		Score 4		Score 5		Total	
		N	%	N	%	N	%	N	%	N	%	N	%
Obs. 1	BF	3	8.9	**21**	**61.8**	8	23.4	2	5.9	0	0.0	34	100.0
	BM	6	14.0	**23**	**53.5**	9	20.9	2	4.6	3	7.0	43	100.0
	WF	1	12.5	0	0.0	**3**	**37.5**	1	12.5	**3**	**37.5**	8	100.0
	WM	2	10.0	5	25.0	2	10.0	4	20.0	**7**	**35.0**	20	100.0
Obs. 2	BF	4	11.8	7	20.6	**14**	**41.3**	8	23.4	1	2.9	34	100.0
	BM	0	0.0	11	25.6	**19**	**44.2**	9	20.9	4	9.3	43	100.0
	WF	0	0.0	2	25.0	1	12.5	**4**	**50.0**	1	12.5	8	100.0
	WM	1	5.0	2	10.0	**9**	**45.0**	6	30.0	2	10.0	20	100.0
Obs. 3	BF	**12**	**35.3**	**12**	**35.3**	6	17.6	4	11.8	0	0.0	34	100.0
	BM	9	21.0	**17**	**39.5**	12	27.9	3	7.0	2	4.6	43	100.0
	WF	1	12.5	2	25.0	**3**	**37.5**	2	25.0	0	0.0	8	100.0
	WM	1	5.0	5	25.0	**10**	**50.0**	4	20.0	0	0.0	20	100.0
Obs. 4	BF	6	17.6	**17**	**50.0**	6	17.6	5	14.8	0	0.0	34	100.0
	BM	6	14.0	**14**	**32.6**	12	27.8	9	21.0	2	4.6	43	100.0
	WF	1	12.5	0	0.0	2	25.0	1	12.5	**4**	**50.0**	8	100.0
	WM	1	5.0	4	20.0	2	10.0	1	5.0	**12**	**60.0**	20	100.0
All obs.	BF	25	18.4	**57**	**41.9**	34	25.0	19	14.0	1	0.7	136	100.0
	BM	21	12.2	**65**	**37.8**	52	30.2	23	13.4	11	6.4	172	100.0
	WF	3	9.4	4	12.5	**9**	**28.1**	8	25.0	8	25.0	32	100.0
	WM	5	6.2	16	20.0	**23**	**28.8**	15	18.6	21	26.4	80	100.0

Highest values in bold.

The average scores assigned by each observer as well as the difference between the scores for bone as compared to 3D surfaces are given in Table 4.7 to highlight any under- or over-scoring by the observers. While observers 1, 2 and 3 scored bones on average slightly higher than 3D surfaces (by 0.2, 0.3 and 0.4 scores), the fourth observer scored rather higher in 3D surfaces (0.2) than in bone. Thus, in three of the four observers there was a tendency to sexing the specimens more feminine (on average 0.3 scores), while one observer tended to sex the specimens more male (0.2 scores).

Table 4.7 Average of scores for all observers for bone (b) and 3D surfaces (3D) and score difference between modalities.

Observer	Average score b	Average score 3D	Score difference between modalities
1	3.0	2.6	-0.4
2	3.4	3.1	-0.3
3	2.6	2.4	-0.2
4	2.7	2.9	+0.2

4.1.3 The application of the Walker method to sexing the mandible

When considering the application of the Walker method (2008) in terms of correctly sexing the specimens, scores were categorised into female, ambiguous and male, following the description of the scoring method by Buikstra and Ubelaker (1994). First, scores on the entire sample of the 105 mandibles and corresponding 3D surfaces were analysed in view of how they compared to known sex. Then ancestral groups were analysed separately, followed by the comparison of scores to sex groups and ancestral-sex groups. Finally, age groups were considered, together with ancestry and sex, when compared to scores per observer.

Analysis of the complete sample

It was found that in both modalities (bones and 3D surfaces), percentages of correct sexing on the complete sample per observer were in general lower than chance (<50 %). See Tables 4.8 and 4.9 for the comparative highest values and percentages of correct sexing in bone and 3D surfaces. Of the 420 observations (four observers and 105 specimens), only observer 4 assigned the correct score most often, as opposed to an incorrect or ambiguous score, in both modalities (47.6% in bone and 45.7% in 3D surfaces). Observers 1, 2 and 3 sexed the sample most often correctly in bone (correct percentages ranging between 36.2% and 47.6%), but not in 3D surfaces.

Analysis per ancestral group

When considering the ancestries separately (Tables 4.8 and 4.9), sexing by the observers seemed to be less often correct in black as compared to white South Africans. Observers 1 and 2 scored black South Africans mostly incorrectly or ambiguously in bone. Observers 3 and 4 displayed the highest percentage of correct sexing (45.5% each) in black South Africans in bone but differed in 3D surfaces; only observer 4 showed the highest percentage of correctly sexing black South Africans in 3D surfaces (44.2%) while observers 1, 2 and 3 had their highest percentages in incorrectly and ambiguously sexing black South Africans.

In bone for white South Africans, in contrast, only observer 3 did not display the highest correctly sexing percentage. In 3D surfaces, again observer 3 differed from the other three observers by most often ambiguously sexing white South Africans.

Analysis per sex group

The results of the score analysis within the female and male subsamples, disregarding ancestry, are shown in Tables 4.8 and 4.9 in bone and 3D surfaces, respectively. Three of the four observers scored females most often correctly in both modalities (between 40.5% and 66.6% in bone and between 57.1% and 64.2% in 3D surfaces). The same three observers sexed the male subsample most often incorrectly in bone as well as in 3D surfaces (ranging between 39.7% and 46.0% in bone and 39.7% and 57.1% in 3D surfaces). Only one observer sexed the females most often incorrectly (in bone) and ambiguously (in 3D surfaces), and the males most often correctly (in bone) and ambiguously (in 3D surfaces).

Table 4.8 Comparison of scores to known sex in the complete sample, per ancestral group, per sex group and per ancestral-sex group, respectively, per observer, in bone.

		Complete sample		Black		White		Females		Males		BF		BM		WF		WM	
Obs.	Cat.	N	%	N	%	N	%	N	%	N	%	N	%	N	%	N	%	N	%
1	Corr.	**38**	**36.2**	24	31.2	**14**	**50.0**	**17**	**40.5**	21	33.3	**16**	**47.1**	8	18.6	1	12.5	**13**	**65.0**
	Amb.	30	28.6	26	33.8	4	14.3	13	31.0	17	27.0	11	32.4	15	34.9	2	25.0	2	10.0
	Inc.	37	35.2	**27**	**35.0**	10	35.7	12	28.5	**25**	**39.7**	7	20.5	**20**	**46.5**	**5**	**62.5**	5	25.0
	N	105	100.0	77	100.0	28	100.0	42	100.0	63	100.0	34	100.0	43	100.0	8	100.0	20	100.0
2	Corr.	**39**	**37.1**	24	31.2	**15**	**53.6**	9	21.5	**30**	**47.6**	8	23.5	16	37.2	1	12.5	**14**	**70.0**
	Amb.	35	33.3	**30**	**39.0**	5	17.8	14	33.3	21	33.3	12	35.3	**18**	**41.9**	2	25.0	3	15.0
	Inc.	31	29.6	23	29.8	8	28.6	**19**	**45.2**	12	19.1	**14**	**41.2**	9	20.9	**5**	**62.5**	3	15.0
	N	105	100.0	77	100.0	28	100.0	42	100.0	63	100.0	34	100.0	43	100.0	8	100.0	20	100.0
3	Corr.	**43**	**41.0**	**35**	**45.5**	8	28.6	**28**	**66.6**	15	23.8	**27**	**79.4**	8	18.6	1	12.5	7	35.0
	Amb.	35	33.3	22	28.6	**13**	**46.4**	12	28.5	23	36.5	7	20.6	15	34.9	**5**	**62.5**	**8**	**40.0**
	Inc.	27	25.7	20	25.9	7	25.0	2	4.7	**25**	**39.7**	0	0.0	**20**	**46.5**	2	25.0	5	25.0
	N	105	100.0	77	100.0	28	100.0	42	100.0	63	100.0	34	100.0	43	100.0	8	100.0	20	100.0
4	Corr.	**50**	**47.6**	**35**	**45.5**	**15**	**53.6**	**28**	**66.6**	22	34.9	**26**	**76.5**	9	20.9	2	25.0	**13**	**65.0**
	Amb.	19	18.1	18	23.4	2	7.1	7	16.7	12	19.1	6	17.6	11	25.6	1	12.5	1	5.0
	Inc.	36	34.3	24	31.1	11	39.3	7	16.7	**29**	**46.0**	2	5.9	**23**	**53.5**	**5**	**62.5**	6	30.0
	N	105	100.0	77	100.0	28	100.0	42	100.0	63	100.0	34	100.0	43	100.0	8	100.0	20	100.0

Highest values in bold. Correct (corr.), ambiguous (amb.) and incorrect (inc.) categories are used.

Table 4.9 Comparison of scores to known sex in the complete sample, per ancestral group, per sex group and per ancestral-sex group, respectively, per observer, in 3D surfaces.

		Complete sample		Black		White		Females		Males		BF		BM		WF		WM	
Obs.	Cat.	N	%	N	%	N	%	N	%	N	%	N	%	N	%	N	%	N	%
1	Corr.	41	39.0	29	37.6	**12**	**42.9**	**25**	**59.5**	16	25.4	**24**	**70.6**	5	11.6	1	12.5	**11**	**55.0**
	Amb.	22	21.0	17	22.1	5	17.8	11	26.2	11	17.5	8	23.5	9	20.9	3	37.5	2	10.0
	Inc.	**42**	**40.0**	**31**	**40.3**	11	39.3	6	14.3	**36**	**57.1**	2	5.9	**29**	**67.5**	**4**	**50.0**	7	35.0
	N	105	100.0	77	100.0	28	100.0	42	100.0	63	100.0	34	100.0	43	100.0	8	100.0	20	100.0
2	Corr.	34	32.3	24	31.1	**10**	**35.7**	13	31.0	21	33.3	11	32.4	13	30.2	2	25.0	8	40.0
	Amb.	**43**	**41.0**	**33**	**42.9**	**10**	**35.7**	**15**	**35.7**	**28**	**44.4**	**14**	**41.2**	**19**	**44.2**	1	12.5	**9**	**45.0**
	Inc.	28	26.7	20	26.0	8	28.6	14	33.3	14	22.3	9	26.4	11	25.6	**5**	**62.5**	3	15.0
	N	105	100.0	77	100.0	28	100.0	42	100.0	63	100.0	34	100.0	43	100.0	8	100.0	20	100.0
3	Corr.	36	34.3	29	37.7	7	25.0	**27**	**64.2**	9	14.3	**24**	**70.6**	5	11.6	**3**	**37.5**	4	20.0
	Amb.	31	29.5	18	23.4	**13**	**46.4**	9	21.5	22	34.9	6	17.6	12	27.9	**3**	**37.5**	**10**	**50.0**
	Inc.	**38**	**36.2**	**30**	**38.9**	8	28.6	6	14.3	**32**	**50.8**	4	11.8	**26**	**60.5**	2	25.0	6	30.0
	N	105	100.0	77	100.0	28	100.0	42	100.0	63	100.0	34	100.0	43	100.0	8	100.0	20	100.0
4	Corr.	**48**	**45.7**	**34**	**44.2**	**14**	**50.0**	**24**	**57.1**	24	38.1	**23**	**67.6**	11	25.6	1	12.5	**13**	**65.0**
	Amb.	22	21.0	18	23.4	4	14.3	8	19.1	14	22.2	6	17.6	12	27.9	2	25.0	2	10.0
	Inc.	35	33.3	25	32.4	10	35.7	10	23.8	**25**	**39.7**	5	14.8	**20**	**46.5**	**5**	**62.5**	5	25.0
	N	105	100.0	77	100.0	28	100.0	42	100.0	63	100.0	34	100.0	43	100.0	8	100.0	20	100.0

Highest values in bold. Correct (corr.), ambiguous (amb.) and incorrect (inc.) categories are used.

Analysis per ancestral-sex group

The analysis of scores within the ancestral-sex groups showed differences among the observers. The detailed results for all four observers for the ancestral-sex groups are given in Tables 4.8 and 4.9 for bone and 3D surfaces, respectively. Observers 1, 3 and 4 concurred in their scores in both modalities for the BF, sexing it most often correctly. Correct percentages ranged between 47.1% and 79.4%. Observer 2 scored the BF less often correctly. For the BM, observers 1, 3 and 4 concurred in most often incorrectly sexing this subsample in bone and in 3D surfaces (percentages ranging between 46.5% and 67.5%). Observer 2 sexed the BM most often ambiguously in both modalities. In the WF, observers 1, 2 and 4 concurred in most often incorrectly sexing this subsample (between 50.0% and 62.5%) in both modalities while observer 3 sexed the WF most often ambiguously and correctly (62.5% in bone and 37.5% in 3D surfaces). In the WM, observers 1 and 4 concurred in most often sexing this subsample correctly in both modalities; in bone, observer 2 also concurred (ranging between 65.0% and 70.0%). In 3D surfaces, observers 1 and 4 concurred in most often correctly sexing the WM (55.0% and 65.0%, respectively) while observers 2 and 3 sexed the WM most often ambiguously.

Thus, BF generally had better chances of being sexed correctly while the chances for BM and WF were lower. In the latter subsamples, the highest percentages were for incorrect sex; three of the four observers were consistent in this scoring. In WM, again three out of four observers agreed on the highest percentage of correctly sexing this subsample. The distribution of correct sexing in bones and 3D surfaces was the same. While BF and WM were sexed correctly by almost all observers, BM and WF were sexed incorrectly in both modalities by three of the four observers.

Analysis per ancestral-sex-age group

Thus far, ancestral and sex groups were analysed separately as well as combined (ancestral-sex groups). In addition to ancestry and sex, age at death was tested to assess any possible influence on the applicability of the Walker method (Walker 2008) to 3D surfaces on the mental eminence. The tests for correct sexing of the specimens, divided into the age groups 18 to 29, 30 to 44, 45 to 59, and over 60 years, delivered the results as shown in Tables 4.10 and 4.11 for bone and 3D surfaces, respectively. Observers 1 and 4 concurred in their scoring by most often correctly sexing BF and WM, across the age groups and in both modalities (correct percentages ranging between 47.1% and 76.5% in bone and 55.0% and 70.6% in 3D surfaces). Observer 3 showed a similar trend as observers 1 and 4 in correctly or incorrectly sexing the ancestral-sex-age groups but was not as consistent; the scoring of the BF and BM concurred with observers 1 and 4 (BF most often correct, BM most often incorrect in both modalities) while the WF and WM differed and were scored most often ambiguously by observer 3. Observer 2 was less consistent in the scoring of the subsamples across the age groups, and scores concurred only in the WM across all age groups with the other observers in correct sexing. The scoring of the other subsamples differed from the other three observers.

Age at death had no influence on the outcome of the scoring of the mental eminence neither in bone nor in 3D surfaces, as shown in Tables 4.8 and 4.9.

Table 4.10 Comparison of scores to known ancestry, sex and age at death per observer (obs.) and category (cat.), in bone.

		BF					BM					WF					WM				
Obs.	Cat.	18-29	30-44	45-59	≥60	%	18-29	30-44	45-59	≥60	%	18-29	30-44	45-59	≥60	%	18-29	30-44	45-59	≥60	%
1	Corr.	1	**7**	**4**	**4**	**47.1**	0	5	1	2	18.6	0	0	0	**1**	12.5	0	**1**	**4**	**8**	**65.0**
	Amb.	**3**	3	3	2	32.4	**1**	**7**	2	5	34.9	0	0	2	0	25.0	0	0	2	0	10.0
	Inc.	1	0	**4**	2	20.5	**1**	4	**9**	**6**	**46.5**	**1**	0	**3**	**1**	**62.5**	0	0	0	5	25.0
	N	5	10	11	8	100.0	2	16	12	13	100.0	1	0	5	2	100.0	0	1	6	13	100.0
2	Corr.	**2**	3	3	0	23.5	**1**	6	4	**5**	37.2	0	0	0	**1**	12.5	0	**1**	**5**	**8**	**70.0**
	Amb.	1	2	3	**6**	35.3	0	**8**	**5**	**5**	**41.9**	0	0	2	0	25.0	0	0	1	2	15.0
	Inc.	**2**	**5**	**5**	2	**41.2**	**1**	2	3	3	20.9	**1**	0	**3**	**1**	**62.5**	0	0	0	3	15.0
	N	5	10	11	8	100.0	2	16	12	13	100.0	1	0	5	2	100.0	0	1	6	13	100.0
3	Corr.	**4**	**9**	**8**	**6**	**79.4**	0	4	0	4	18.6	0	0	0	**1**	12.5	0	**1**	**2**	4	35.0
	Amb.	1	1	3	2	20.6	**1**	4	**7**	3	34.9	0	0	**5**	0	**62.5**	0	0	**2**	**6**	**40.0**
	Inc.	0	0	0	0	0.0	**1**	**8**	5	**6**	**46.5**	**1**	0	0	**1**	25.0	0	0	**2**	3	25.0
	N	5	10	11	8	100.0	2	16	12	13	100.0	1	0	5	2	100.0	0	1	6	13	100.0
4	Corr.	**3**	**9**	**8**	**6**	**76.5**	0	3	2	4	20.9	0	0	1	**1**	25.0	0	**1**	**4**	**8**	**65.0**
	Amb.	1	1	2	2	17.6	**1**	4	3	4	27.9	0	0	1	0	12.5	0	0	1	0	5.0
	Inc.	1	0	1	0	5.9	**1**	**9**	**7**	**5**	**51.2**	**1**	0	**3**	**1**	**62.5**	0	0	1	5	30.0
	N	5	10	11	8	100.0	2	16	12	13	100.0	1	0	5	2	100.0	0	1	6	13	100.0

Bold figures highlight the highest values and percentages. Correct (corr.), ambiguous (amb.) and incorrect (inc.) categories are used.

Table 4.11 Percent correct sexing of ancestry, sex and age at death per observer, in 3D surfaces.

Obs.		BF					BM					WF					WM				
		18-29	30-44	45-59	≥60	%	18-29	30-44	45-59	≥60	%	18-29	30-44	45-59	≥60	%	18-29	30-44	45-59	≥60	%
1	Corr.	**3**	**8**	**9**	**4**	**70.6**	0	3	1	1	11.6	0	0	0	1	12.5	0	1	**3**	**7**	**55.0**
	Amb.	1	1	2	**4**	23.5	1	3	1	4	20.9	0	0	**3**	0	37.5	0	0	1	1	10.0
	Inc.	1	1	0	0	5.9	1	**10**	**10**	**8**	**67.5**	1	0	2	1	**50.0**	0	0	2	5	35.0
	N	5	10	11	8	100.0	2	16	12	13	100.0	1	0	5	2	100.0	0	1	6	13	100.0
2	Corr.	2	3	4	2	32.4	1	4	3	5	30.2	0	0	1	1	25.0	0	1	1	**6**	40.0
	Amb.	**3**	3	**6**	2	**41.2**	1	5	**6**	**7**	**44.2**	0	0	1	0	12.5	0	0	**4**	5	**45.0**
	Inc.	0	**4**	1	**4**	26.4	0	**7**	3	1	25.6	1	0	**3**	1	**62.5**	0	0	1	2	15.0
	N	5	10	11	8	100.0	2	16	12	13	100.0	1	0	5	2	100.0	0	1	6	13	100.0
3	Corr.	**2**	**9**	**8**	**5**	**70.6**	0	1	0	4	11.6	0	0	**2**	0	25.0	0	0	2	2	20.0
	Amb.	1	1	2	2	17.6	1	7	3	1	27.9	1	0	1	1	**37.5**	0	0	**3**	**7**	**50.0**
	Inc.	**2**	0	1	1	11.8	1	**8**	**9**	**8**	**60.5**	0	0	**2**	1	**37.5**	0	1	1	4	30.0
	N	5	10	11	8	100.0	2	16	12	13	100.0	1	0	5	2	100.0	0	1	6	13	100.0
4	Corr.	**4**	**8**	**6**	**5**	**67.6**	1	5	1	4	25.6	0	0	0	1	12.5	0	1	**4**	**8**	**65.0**
	Amb.	0	1	3	2	17.6	0	3	5	4	27.9	1	0	1	0	25.0	0	0	1	1	10.0
	Inc.	1	1	2	1	14.8	1	**8**	**6**	**5**	**46.5**	0	0	**4**	1	**62.5**	0	0	1	4	25.0
	N	5	10	11	8	100.0	2	16	12	13	100.0	1	0	5	2	100.0	0	1	6	13	100.0

Bold figures highlight the highest numbers and percentages. Correct (corr.), ambiguous (amb.) and incorrect (inc.) categories are used.

4.1.4 Qualitative analysis

In the qualitative part of the study, the questions posed to all four observers after completion of the scoring process in bones and 3D surfaces are listed in Appendix B, followed by the observers' answers.

The observers' answers indicate a general tendency to feel more uncomfortable when scoring 3D surfaces as opposed to bone and a general uncertainty with the intermediate scores 2, 3 and 4 while scores 1 and 5 were perceived to be less of a challenge. Observers handled the 3D surfaces differently in the scoring process; some used the zooming tool, while others just rotated the 3D surfaces on the screen to better discern the eminence, in the absence of the tactile experience.

4.1.5 Summary of results

1. The overall observer performance in the two modalities was very similar even though a slight tendency to underscore the specimens in 3D surfaces was detected.

2. Scoring performance in the intraOE test was best among all pairwise comparisons.

3. Complete sample: observers showed high agreement in correctly sexing the specimens in bone but lower in 3D surfaces.

4. Within ancestral groups: white South Africans were more likely to be correctly sexed than black South Africans, in bone as well as 3D surfaces.

5. Within sex groups: females were more likely to be correctly sexed than males, in bone as well as 3D surfaces.

6. Within ancestral-sex groups: BF and WM were more likely to be correctly sexed than BM and WF, in either of the two modalities.

7. Within ancestral-sex-age groups: As in the ancestral-sex groups, BF and WM were more often correctly sexed than BM and WF, regardless of age at death.

8. In the qualitative section, the observers were almost unanimous about which scores were harder to allocate (2, 3 and 4) than others (1, 5). Observers were more uncomfortable scoring 3D surfaces than bones.

4.2 CHIN SHAPE VARIATION IN SOUTH AFRICANS

In the following section, the results of the chin shape variation geometric morphometrics (GMM) are provided, starting with the reproducibility test of the manual versus automatic landmarking, followed by the analysis of the influence of the factors, ancestry, sex, age and allometry, on the bony chin shape of black and white South Africans.

4.2.1 Reproducibility test: manual versus automatic landmarking

In Table 4.12, automatic landmarking had high reproducibility of the craniometric landmarks in the interOD. The mean interobserver dispersion (interOD) of landmarks in the interOD 1 test was 7.00 mm and somewhat less in the interOD 2 test with 5.73 mm. The mean interOD for the automatic landmarking resulted in 0.52 mm and 0.60 mm in the interOD 1 and 2, respectively. Even though the manual intraobserver dispersion (intraOD) resulted in only 2.08 mm average dispersion of the eleven craniometric landmarks, automatic landmarking resulted in 0.21 mm dispersion. In Figures 4.1 and 4.2, the reproducibility for each craniometric landmark with a manual and an automatic placement are given. For this study, the automatic landmarking process was used.

Table 4.12 Global mean of the inter- and intraobserver dispersion (in mm) of the manual versus automatic landmark placement.

Method	InterOD 1	InterOD 2	IntraOD
Manual	7.00	5.73	2.08
Automatic	0.52	0.60	0.21

For each craniometric landmark separately in the manual placement analysis, best reproducibility (<2 mm) was found for landmark 1 (subspinale), 2 (prosthion) and 3 (infradentale) as well as for craniometric landmark 6 and 7 (menton and gnathion) for the intraOD and the interOD tests (Figure 4.1). The mental tubercles (8 and 9) and both gonia (10 and 11) were less reproducible in interOD 1 and intraOD (>2 mm) but were more reproducible in interOD 2 (<2 mm). A low reproducibility could be seen in 4 and 5, namely the supramentale and pogonion, in the intraOD and in interOD 1 (>2 mm), while a higher reproducibility was achieved in interOD 2 (<2 mm).

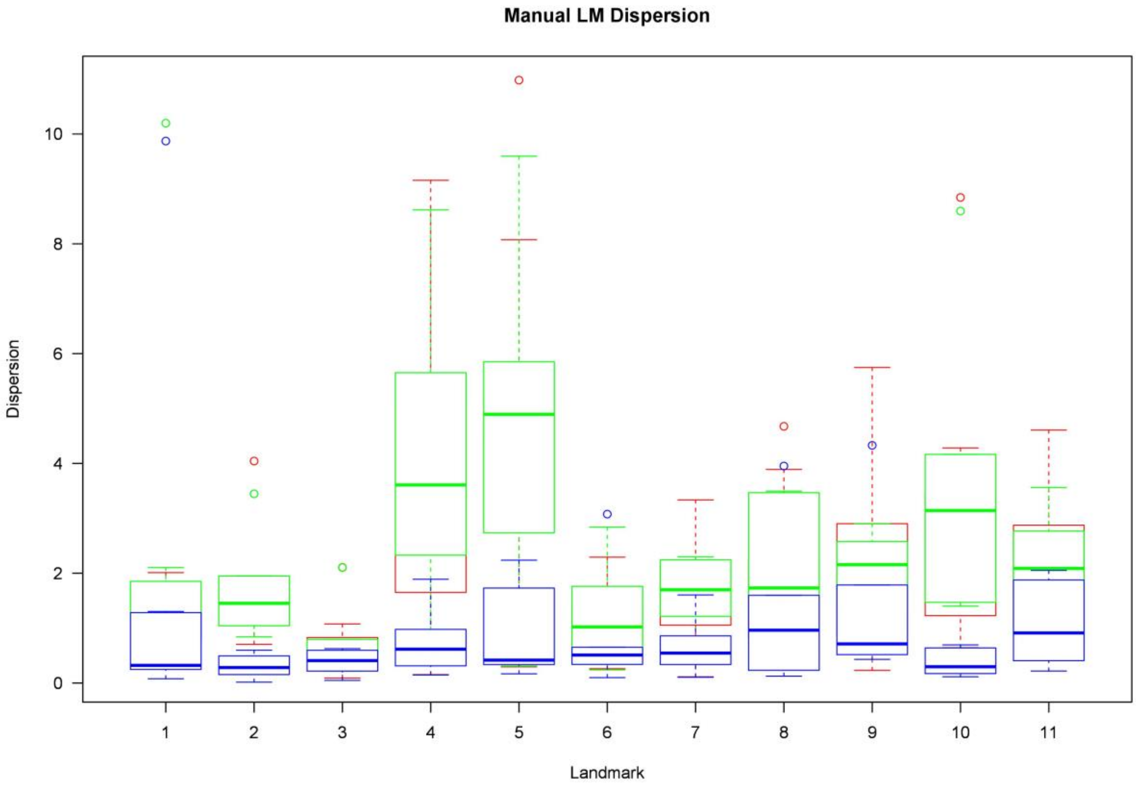

Figure 4.1 Boxplots of the dispersion (in mm) for manual landmarking; interOD 1 (green); interOD 2 (blue); intraOD (red). Numbering of landmarks in Table 3.5.

In the automatic craniometric landmark placement, the intraOD (red) showed the best reproducibility of all the tests (Figure 4.2) while interOD 2 (blue) was slightly less reproducible than interOD 1 (green). Interestingly, the craniometric landmarks with the best reproducibility (<0.2 mm) was 8 (mental tubercle left) while craniometric landmark 9 (mental tubercle right) showed the lowest reproducibility in the interOD tests (>1 mm). The gonia (10 and 11) were equally reproducible as, for example, 4 and 5 (supramentale and pogonion); <0.2 mm for the intraOD and <1 mm for both interOD tests. The latter two craniometric landmarks also showed the lowest reproducibility in the manual landmarking process. As in the manual landmarking, craniometric landmarks 1, 2 and 3 (subspinale, prosthion and infradentale) exhibited relatively good reproducibility (<0.6 mm).

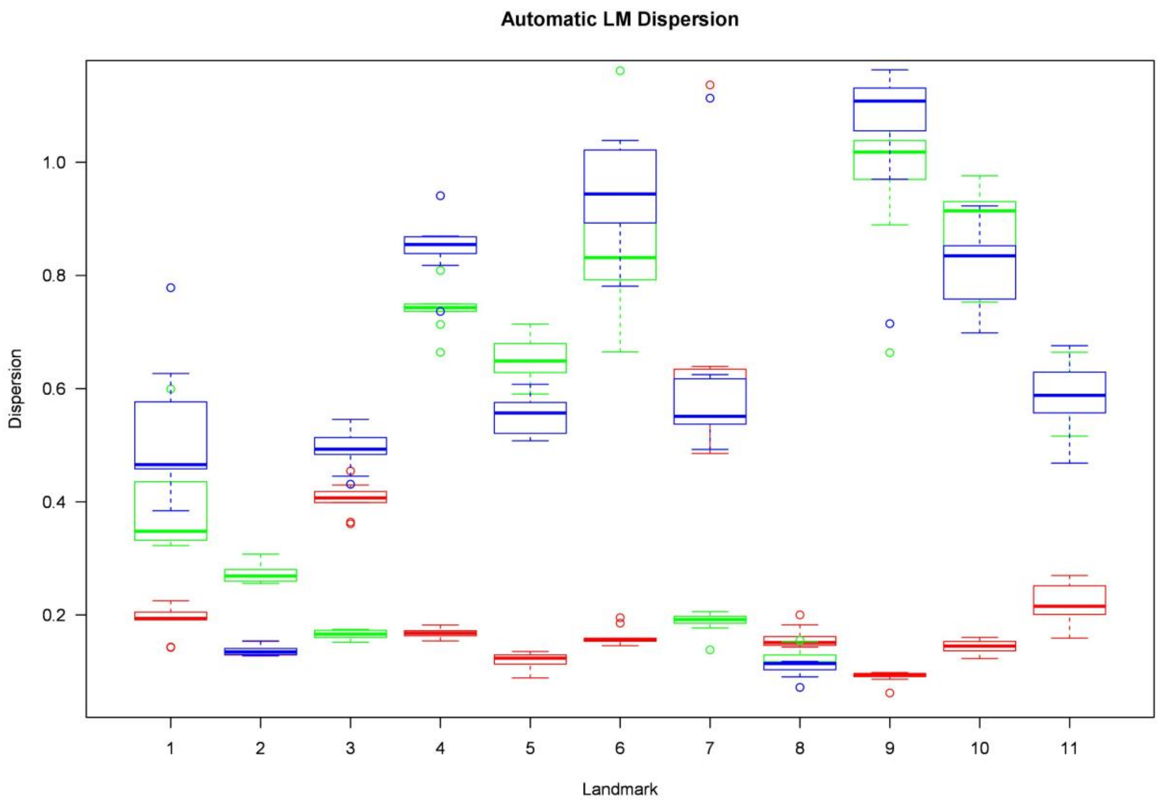

Figure 4.2 Boxplots of the dispersion (in mm) for automatic landmarking; interOD 1 (green); interOD 2 (blue); intraOD (red). Numbering of landmarks in Table 3.5.

Overall, craniometric landmarks 1, 2, 3 and 7 (subspinale, prosthion, infradentale and gnathion) showed high reproducibility in both the manual and the automatic placement procedures, as opposed to craniometric landmarks 4, 5, 9 and 10 (supramentale, pogonion, mental tubercle right and gonion left). Craniometric landmarks 6, 8 and 11 (menton, mental tubercle left and gonion right) performed differently in the two placement procedures with an overall lower reproducibility in the manual placement procedure.

4.2.2 Multivariate normality analysis

The normality distribution of the entire sample (n=291) is given in Figure 4.3. The Q-Q-plot demonstrates some degree of non-normal distribution of the data, the points forming a curve deviating slightly from the straight line. Thus, for the sake of thoroughness, both parametric and non-parametric tests were carried out on the data.

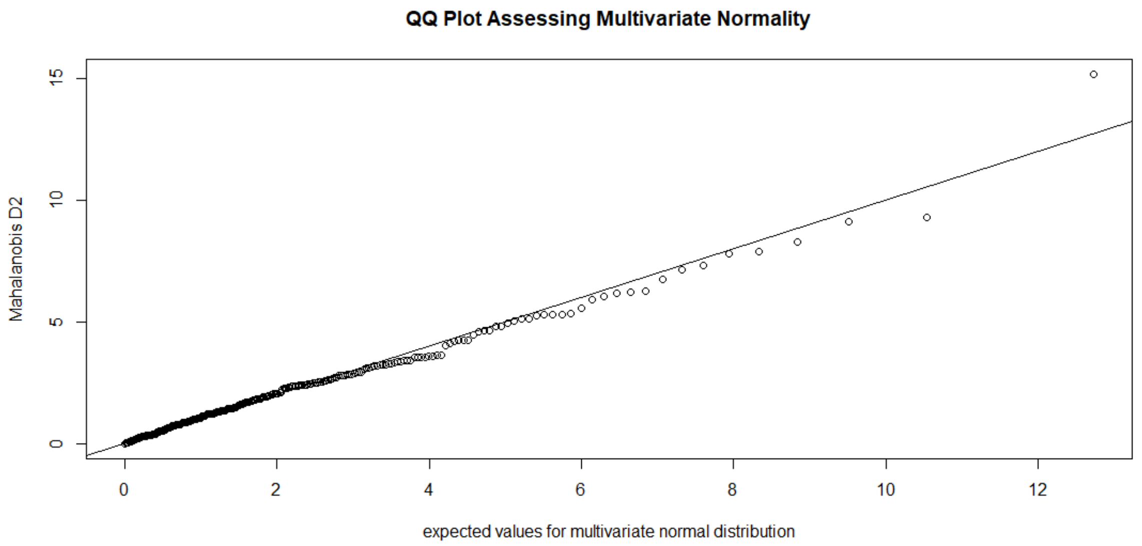

Figure 4.3 Multivariate normality of the sample; Q-Q-plot of the linear model of the hard-tissue shape of the sample.

4.2.3 Chin shape analysis

In this section, the results of the analysis of the parameters ancestry, sex, age and allometry are reported in view of their influence on the chin shape. This influence was tested in the complete sample for each parameter, as well as in ancestral-sex, ancestral-sex-age, allometry-ancestral, and allometry-ancestral-sex groups.

4.2.3.1 Ancestry

Complete sample

Testing the ancestry-related shape variation in the complete sample (n=291), mandibular shape differences were statistically significant among the two ancestral groups, as can be seen in Figure 4.4. The lower margin of the mandibular body and the gonial angle in red indicate the visibility of the template mandible of white South Africans whereas the rest of the mandible is brown, pointing at the pronounced mandible of black South Africans. The mental tubercles, however, are more developed, and the chin at the mental symphysis is slightly higher in white than in black South Africans. However, the greater parts of the mandible and maxilla are more prominent in black than in white South Africans, as seen in Figure 4.4.

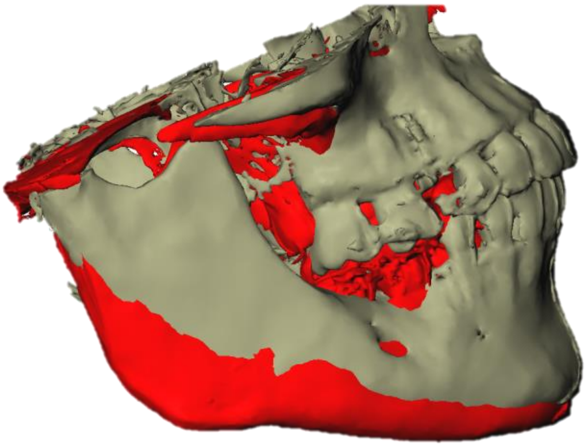

Figure 4.4 Mandibular shape differences between ancestral averages (black South Africans: brown; white South Africans: red). Template skulls of black and white South Africans generated in MeVisLab © v. 2.7.1 software.

Principal Component 1, accounting for 28.36% of shape variation versus PC 2, accounting for 25.48% of shape variation, are shown in Figure 4.5, indicating the extent of shape changes (minimum and maximum). The maximum shape reflecting the extreme of white South Africans displayed a wider distance between the gonia and a greater width between the mental tubercles, as compared to the minimum shape. However, when comparing the mean shapes per ancestry from frontal and diagonal views as depicted in

Figures 4.6a, c, d and f, differences between ancestral groups are not obvious. The obtained *p-value* of the MANOVA was 0.001. The 50-50 MANOVA test resulted in a *p-value* of <0.001, the permutation test in a *p-value* of 0.001. Discriminant function analysis of black and white South Africans in connection with ancestry as a shape-influencing factor resulted in 86.9% (Table 4.13). Ancestry was thus a shape-influencing factor on the hard-tissue chin in black and white South Africans (Figure 4.27).

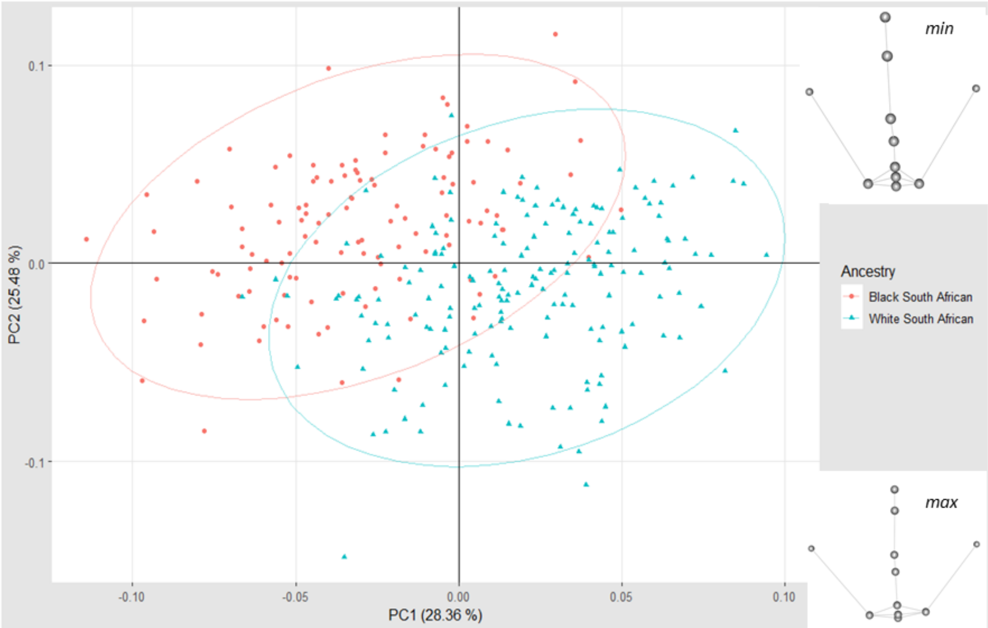

Figure 4.5 PC 1 versus PC 2 of the complete sample for ancestry on all landmarks indicating the minimum and maximum shapes along PC1.

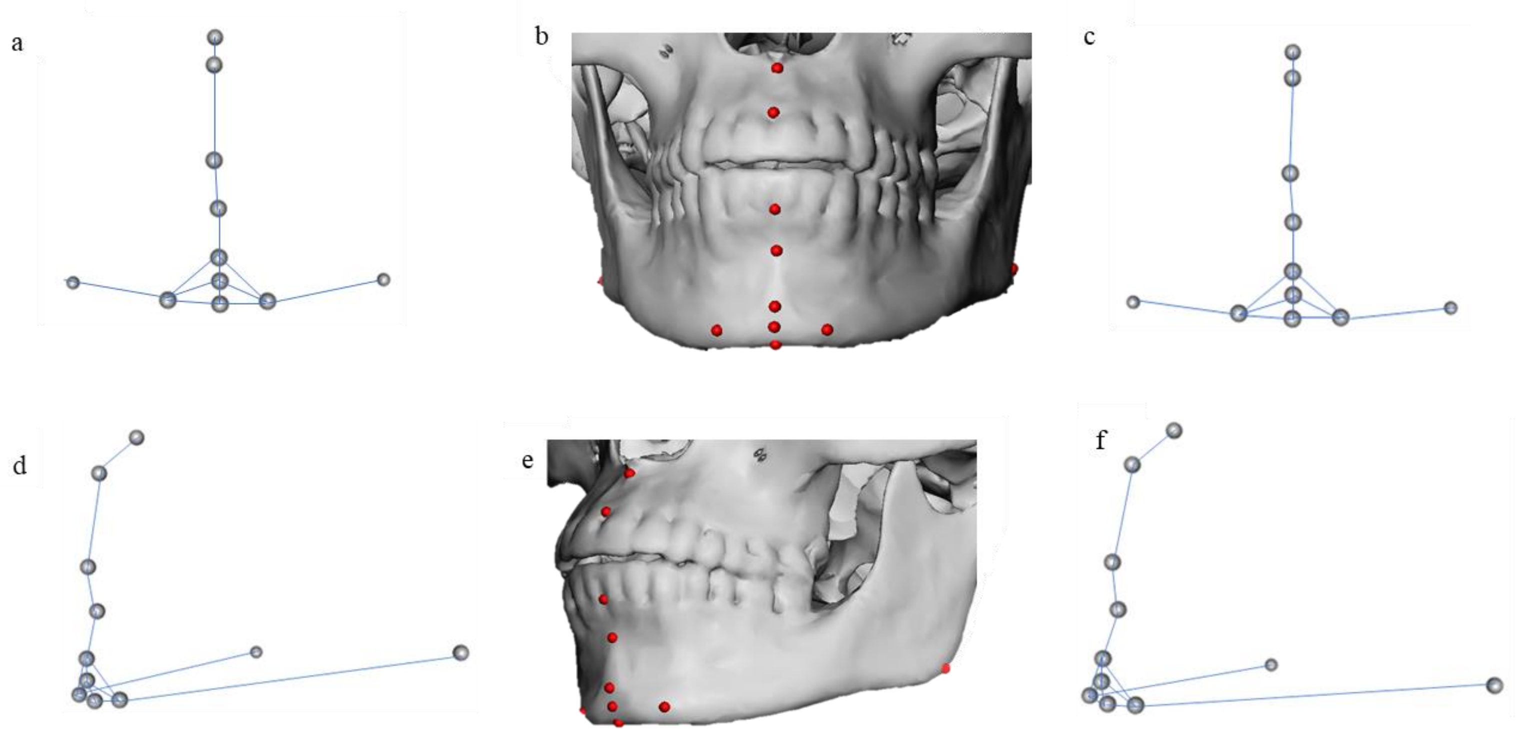

Figure 4.6 Frontal and diagonal views of the mean shapes in black and white South Africans, respectively, on all craniometric landmarks; a) black, frontal view; b) template, frontal view; c) white, frontal view; d) black, diagonal view; e) template, diagonal view; f) white, diagonal view.

In Figure 4.7, the extent of ancestry-related shape variation for the selected craniometric landmarks is depicted by plotting PC 1 (71.69%) versus PC 2 (11.74%), indicating a greater shape variation in the bony menton in white as opposed to black South Africans. The main difference between the minimum and the maximum shapes along the PC 1 axis was the width between the mental tubercles and height between the menton and the infradentale. The mean shapes of both subsamples are given in Figure 4.8a, c, d and f (from frontal and diagonal views), highlighting the greater dimensions between pogonion, gnathion and menton as well as between the mental tubercles in whites. The actual distances were also considerably larger in white than in black South Africans. When the selected craniometric landmarks for the hard-tissue chin were analysed, the statistically significant (Figure 4.28) results showed a MANOVA *p-value* of 0.001, a 50-50 MANOVA *p-value* of <0.001, a permutation test of 0.001 and a Discriminant Function Analysis (DFA) outcome of 91.7% (Table 4.13). Thus, ancestry-related shape variation was significant in both sets of data, all the landmarks, including the gonia and the maxillary landmarks, as well as the selected landmarks on the bony chin.

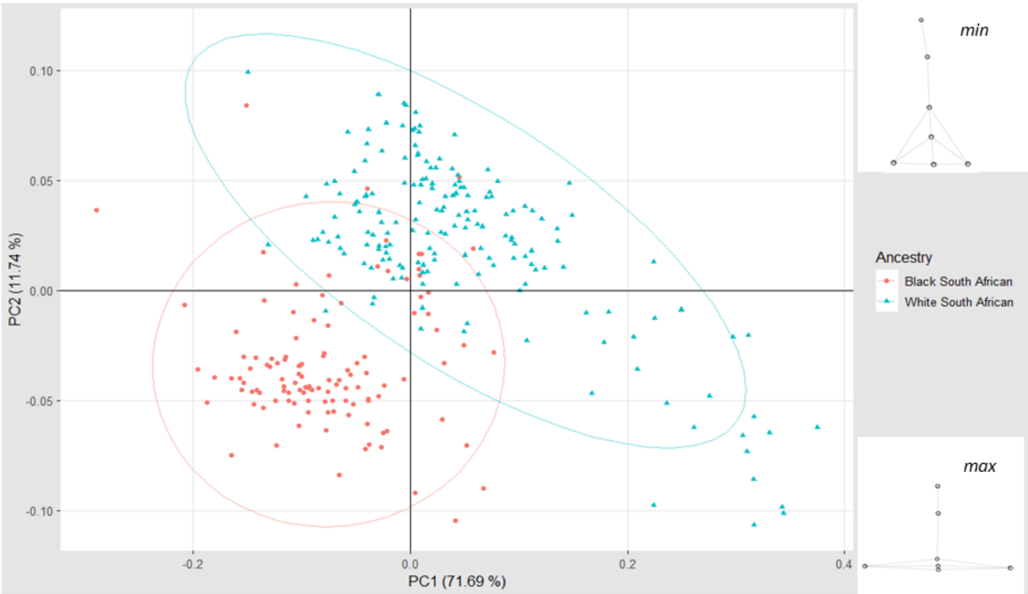

Figure 4.7 PC 1 versus PC 2 of the complete sample for ancestry on the seven selected landmarks indicating the minimum and maximum shapes along PC1.

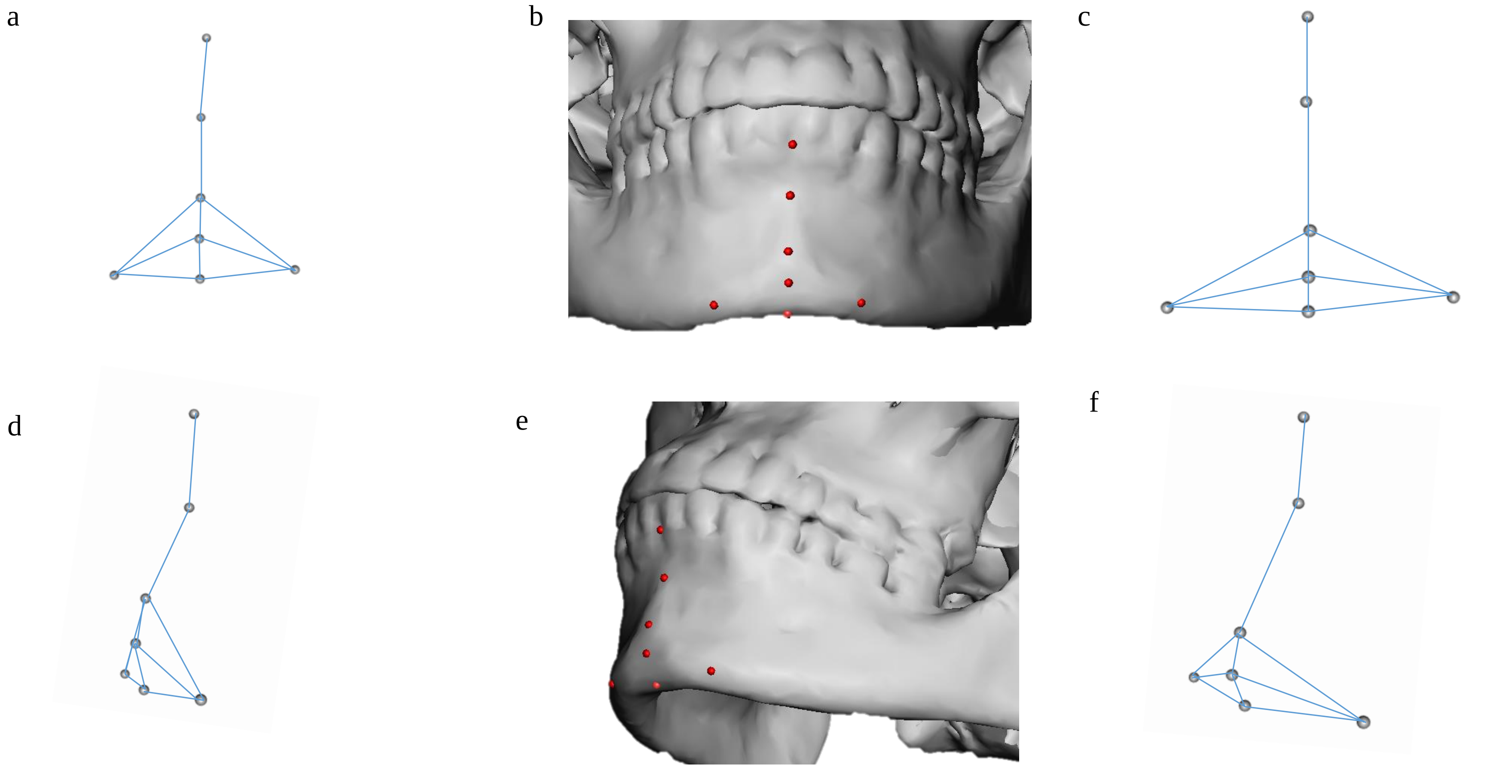

Figure 4.8 Frontal and diagonal views of the mean shapes in black and white South Africans, respectively, on the selected craniometric landmarks; a) black, frontal view; b) template, frontal view; c) white, frontal view; d) black, diagonal view; e) template, diagonal view; f) white, diagonal view.

*Ancestry*Males*

When all black and white males in the sample (black males n=70, white males n=59; total n=129) were analysed for the influence of ancestry on the chin shape, the obtained *p-values* were all statistically significant (0.001) for all tests (MANOVA *p-value*, 50-50 MANOVA *p-value* and permutation test) (Figure 4.27). The DFA was 87.2% (Table 4.13). Principal Component 1 (31.05%) versus 2 (20.91%) are depicted in Figure 4.9, showing a distinct shape variation between the male subsamples. As for the complete black sample, black males also exhibited a narrower chin but a slightly larger distance between pogonion and menton, compared to white males.

As in the above analysis of all craniometric landmarks, the selected craniometric landmarks resulted in a statistically significant value of 0.001 for all statistical tests performed (Figure 4.28). The DFA was 88.3% (Table 4.13). Principal Component 1 (70.46%) versus 2 (12.47%) are given in Figure 4.10 below, depicting the distinct shape variation on the chin between black and white males, and highlighting the greater shape variation within white as opposed to the black South Africans when analysing the bony menton only. The maximum shape reflected the extreme shape, pointing to white South African males having a much wider chin and lower distance between pogonion and menton than the minimum shape, which reflects black South African males whose chin was narrower and taller.

The mean shapes of both black and white males are depicted in Figures 4.11a, c, d and f. In white males, the distance between pogonion, gnathion and menton was smaller than in black males, where the distribution of the craniometric landmarks in the vertical line (infradentale to menton) were more evenly spaced than in white males. The distance between the mental tubercles was larger in white males as opposed to black males, enhancing the perception of the squarer chin in white South Africans.

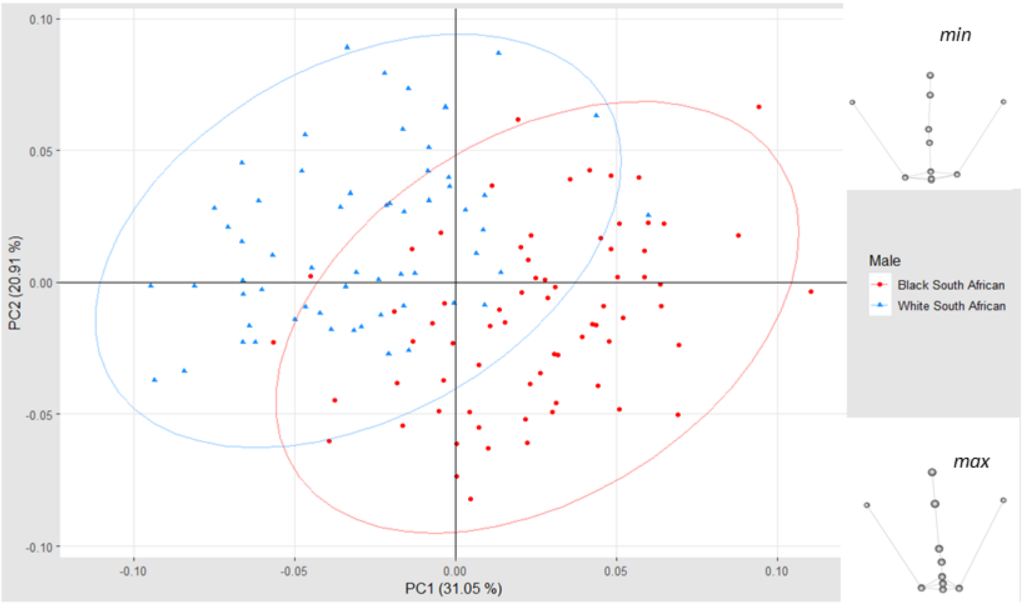

Figure 4.9 PC 1 versus PC 2 of the complete sample for males on all landmarks indicating the minimum and maximum shapes along PC1.

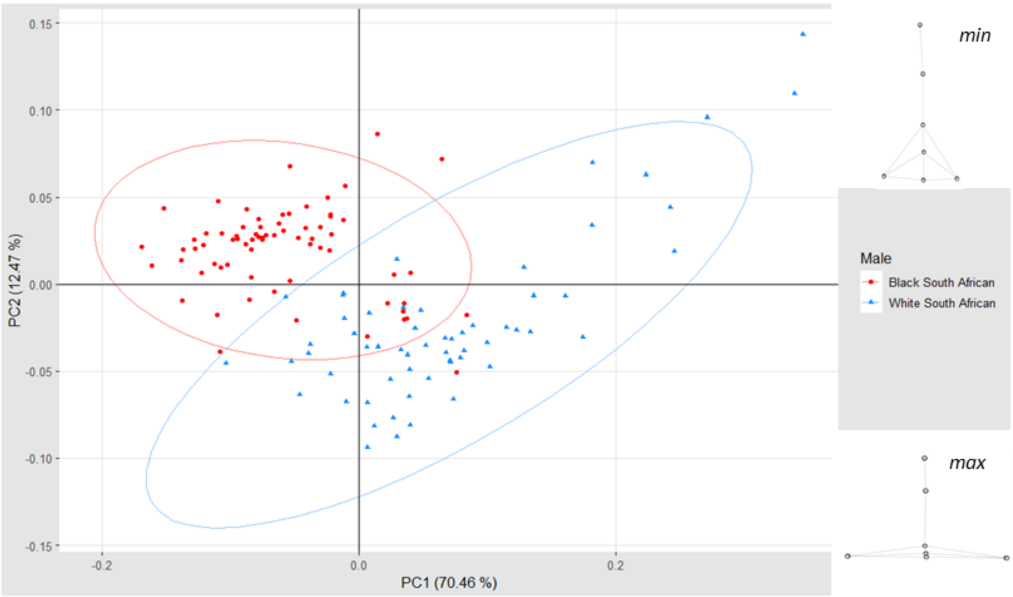

Figure 4.10 PC 1 versus PC 2 of the complete sample for males on the seven selected landmarks indicating the minimum and maximum shapes along PC1.

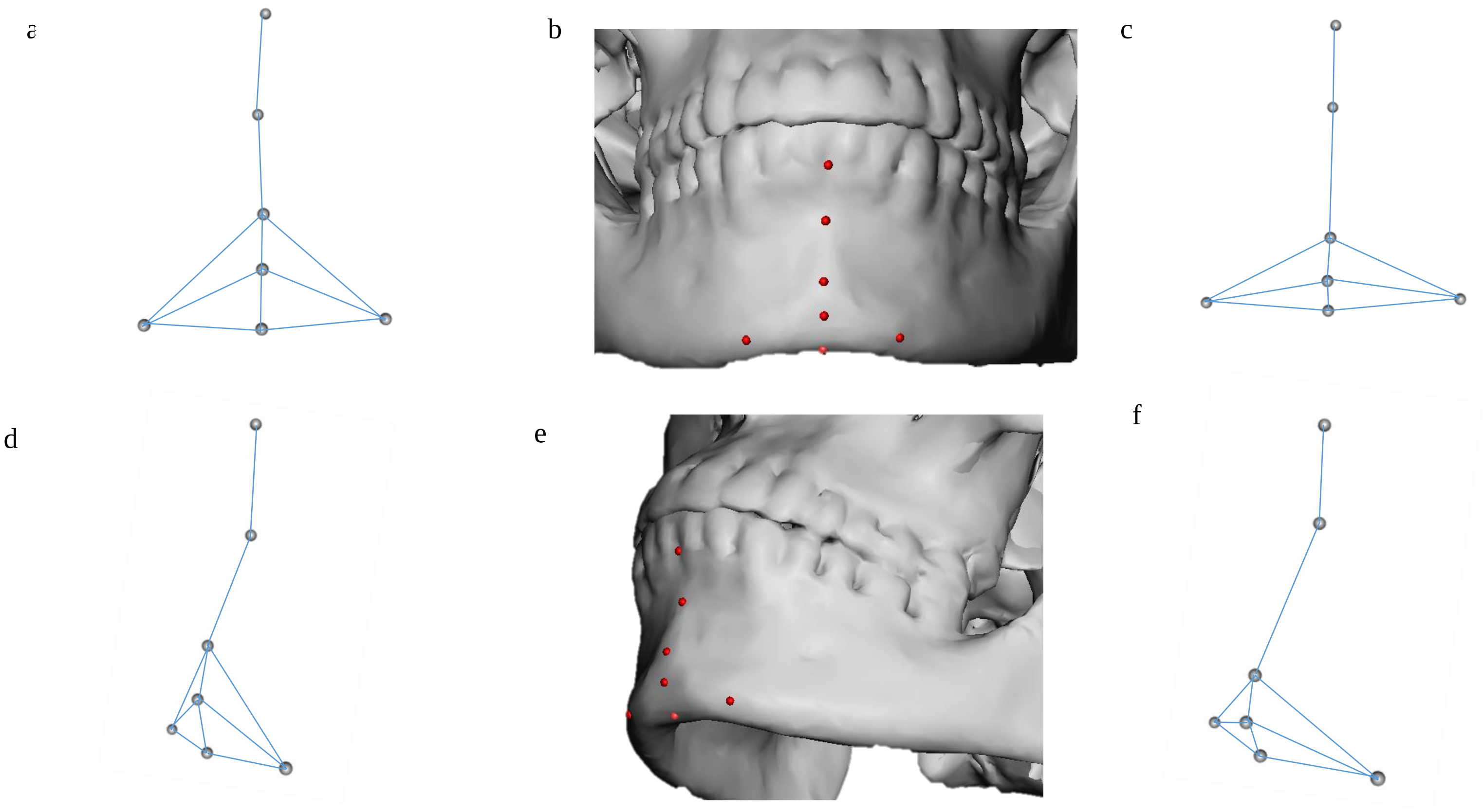

Figure 4.11 Frontal and diagonal views of the mean shapes in black and white South African males, respectively, on the selected craniometric landmarks; a) black, frontal view; b) template, frontal view; c) white, frontal view; d) black, diagonal view; e) template, diagonal view; f) white, diagonal view.

*Ancestry*Females*

The analysis of ancestry-related shape variation among all black and white females in the sample (black females n=47, white females n=115; total n=162) resulted in statistically significant values of 0.001 (MANOVA *p-value*, 50-50 MANOVA and permutation test). The DFA was 86.4% (Table 4.13, Figure 4.27). Principal Component 1 (29.20%) versus 2 (27.03%) are shown in Figure 4.12. The figure highlights the different shapes between black and white females, with the maximum shape of the chin being narrower between the mental tubercles and slightly higher between the pogonion and the menton than the minimum shape.

The same statistically significant results (MANOVA: 0.001, 50-50 MANOVA: 0.001, permutation test: 0.001 and DFA: 95.6%) were obtained for the selected craniometric landmarks (Table 4.13, Figure 4.28). Principal Component 1 (73.47%) versus 2 (10.16%) are shown in Figure 4.5f, highlighting the distinct shapes between black and white females. White females presented with a greater shape variation of the selected craniometric landmarks on the bony menton, than black females. However, shape did not vary to the extent seen in black and white males (Figure 4.13). Mean shapes of black and white females are given in Figures 4.14a, c, d and f. As seen in the analyses of ancestry across the complete sample and in black and white males, the distance between pogonion, gnathion and menton as well as between the mental tubercles is larger in white than in black females. The curvature between infradentale, supramentale and pogonion in white females is more pronounced than in black females, thus enhancing the perception of the prominent chin in white South Africans.

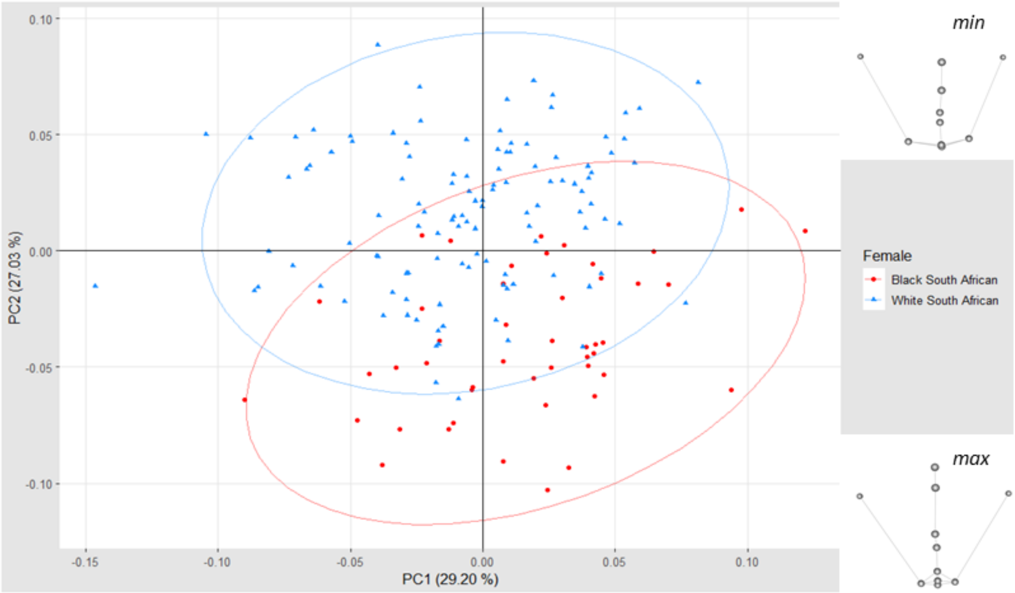

Figure 4.12 PC 1 versus PC 2 of the complete sample for females on all landmarks indicating the minimum and maximum shapes along PC1.

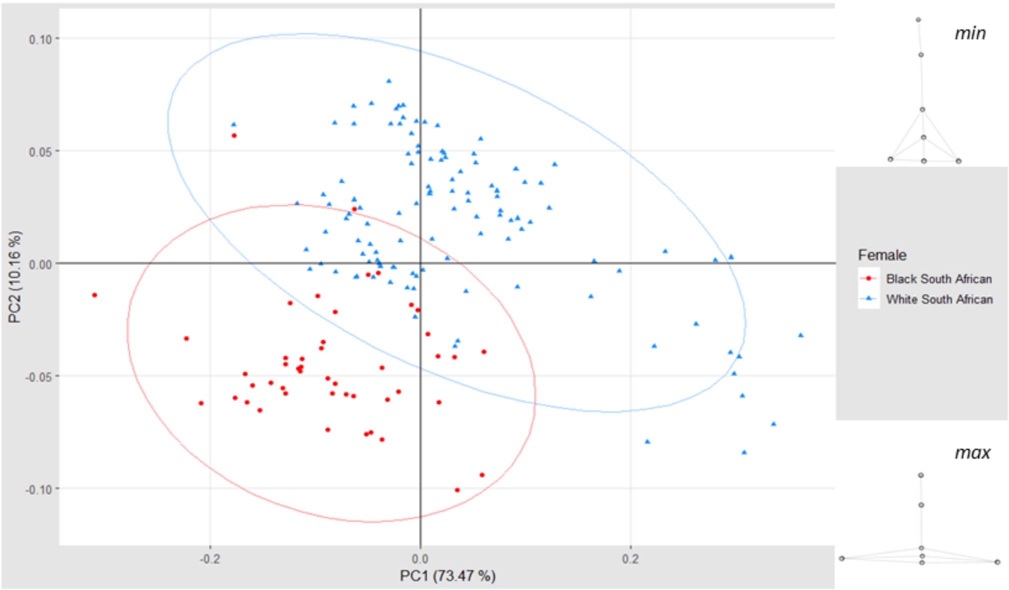

Figure 4.13 PC 1 versus PC 2 of the complete sample for females on the seven selected landmarks indicating the minimum and maximum shapes along PC1.

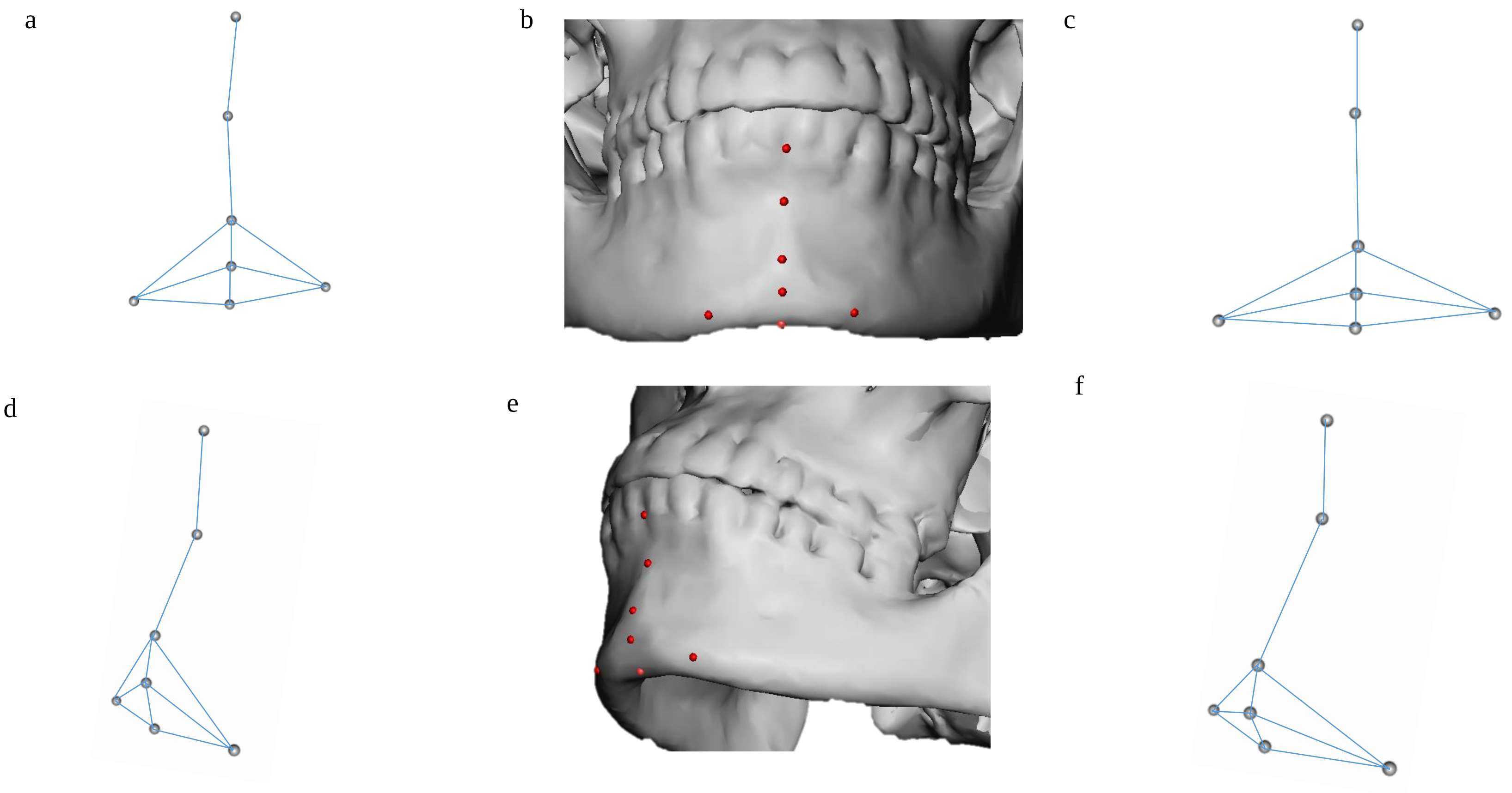

Figure 4.14 Frontal and diagonal views of the mean shapes in black and white South African females, respectively, on the selected craniometric landmarks; a) black, frontal view; b) template, frontal view; c) white, frontal view; d) black, diagonal view; e) template, diagonal view; f) white, diagonal view.

4.2.3.2 Sex

Complete sample

When sex as a chin shape-influencing factor was analysed across the complete sample (females n=162, males n=129), the analysis did not result in significant values: a MANOVA *p-value* of 0.067, a 50-50 MANOVA *p-value* of 0.052, a permutation test of 0.066 and a DFA outcome of 57.3% (Table 4.13, Figure 4.27). The minimum and maximum shapes are given in Figure 4.15, with PC 1 accounting for 28.36% and PC 2 for 25.48% of shape variation between sexes. Shape variation between the minimum and maximum mainly concerned the distance between pogonion and menton.

On the selected craniometric landmarks, in contrast, the analysis of sex in the complete sample was significant. It resulted in a MANOVA *p-value* of 0.003, a 50-50 MANOVA *p-value* of 0.001, a permutation test of 0.001 and a DFA outcome of 63.9% (Table 4.13, Figure 4.28). The influence of PC 1 and PC 2 was 71.69% and 11.74%, respectively. The shape variation in Figure 4.16 mainly concerns the width and height of the chin (distance between the mental tubercles and pogonion and menton, respectively).

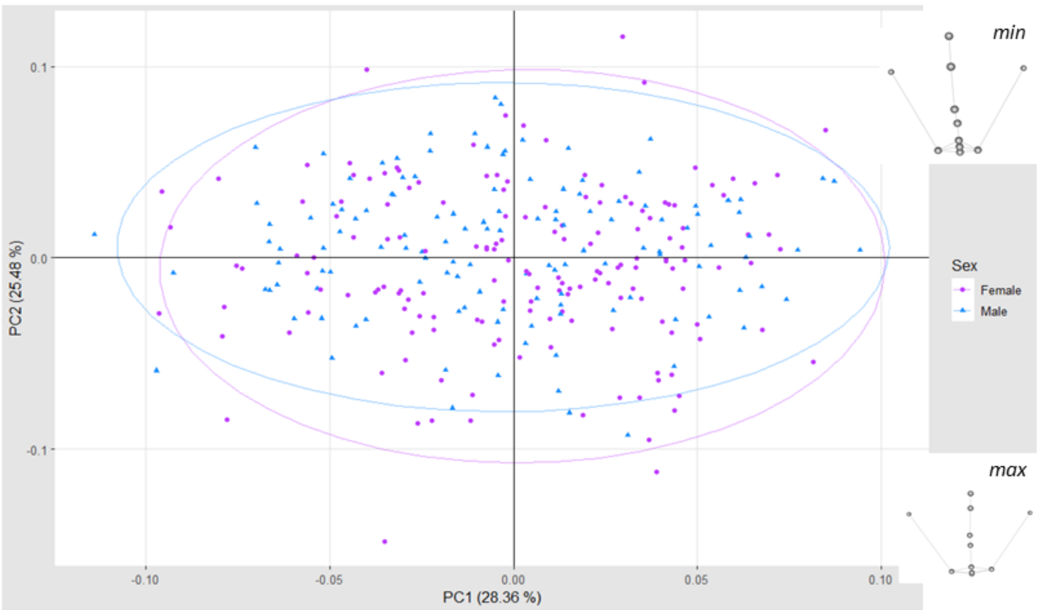

Figure 4.15 PC 1 versus PC 2 of the complete sample for sex on all landmarks indicating the minimum and maximum shapes along PC1.

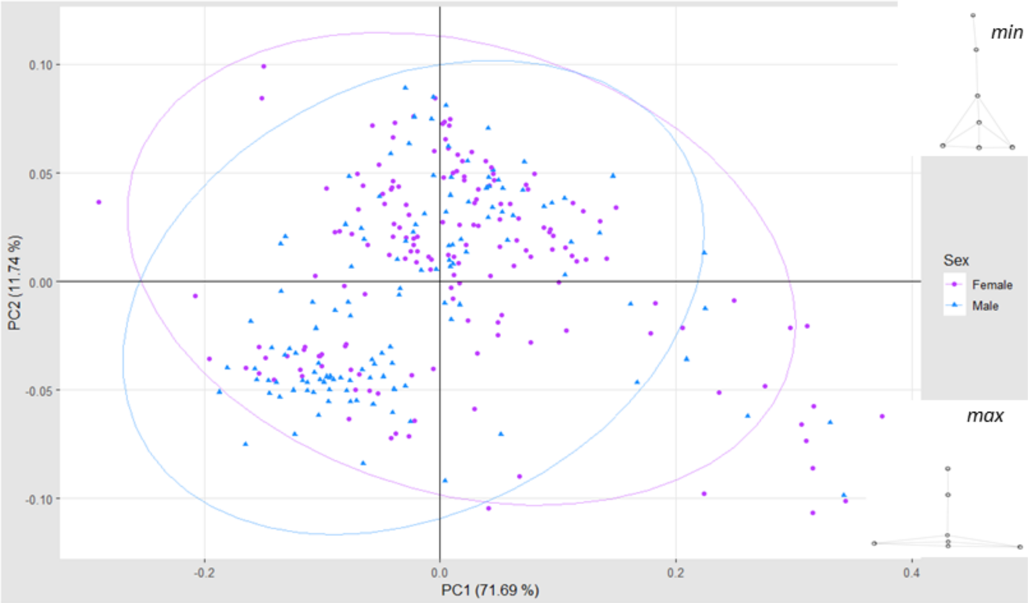

Figure 4.16 PC 1 versus PC 2 of the complete sample for sex on the seven selected landmarks indicating the minimum and maximum shapes along PC1.

4.2.3.3 Age

Complete sample

Before analysing the ancestral subsamples for the influence of age, the complete sample (n=291) was tested for the influence of age on the chin shape. Principal Component 1 (28.36%) versus 2 (25.48%) are displayed in Figure 4.17. The obtained results were a MANCOVA *p-value* of <0.001 and a 50-50 MANOVA *p-value* of <0.001, thus, both statistically significant (Table 4.13, Figure 4.27). The shape change from minimum to maximum referred to an increasing distance between pogonion and menton, between supramentale and pogonion as well as a slightly wider distance between the gonia.

The age analysis on the selected craniometric landmarks (Figure 4.18) resulted in equally statistically significant *p-values*: a MANCOVA of <0.001 and a 50-50 MANOVA of <0.001 (Table 4.13, Figure 4.28). Principal Component 1 accounted for 71.69% and PC

2 accounted for 11.74% of shape difference, which mainly concerned the width and the height of the chin.

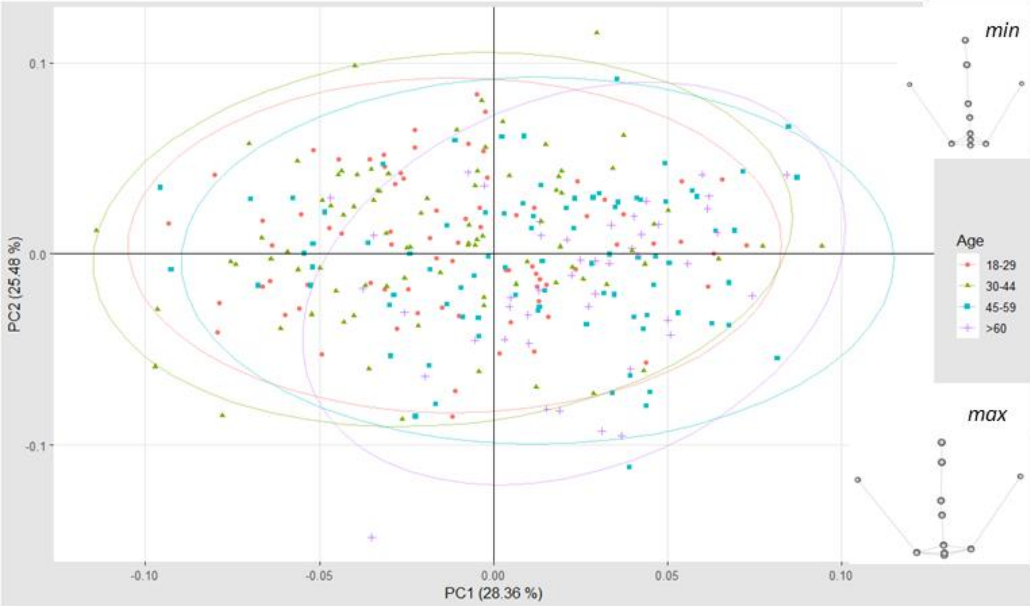

Figure 4.17 PC 1 versus PC 2 of the complete sample for age on all landmarks indicating the minimum and maximum shapes along PC1.

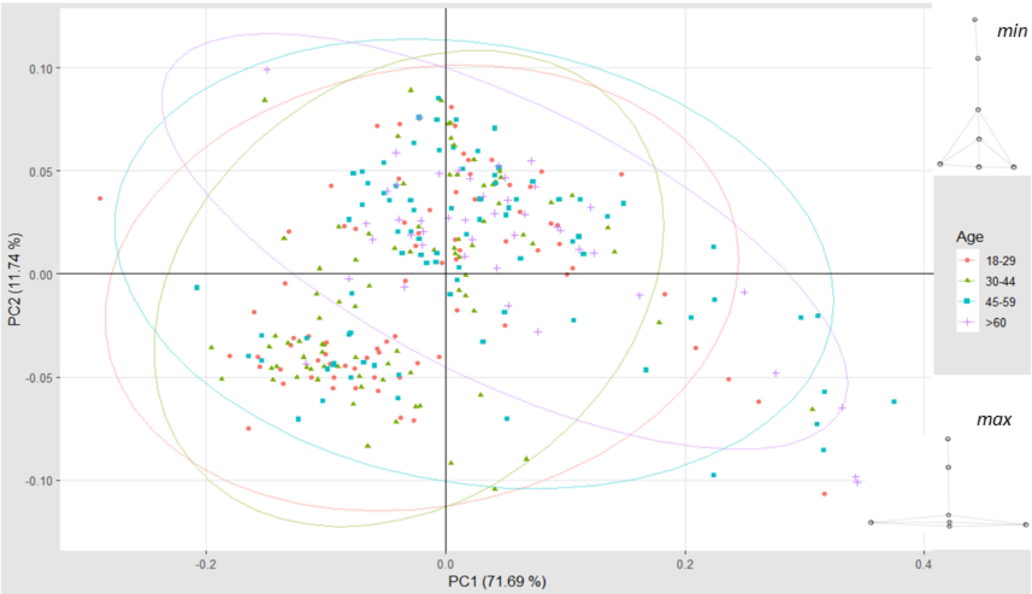

Figure 4.18 PC 1 versus PC 2 of the complete sample for age on the seven selected landmarks indicating the minimum and maximum shapes along PC1.

*Sex*Whites*

For the analysis of sex in white South Africans, PC 1 (31.48%) versus PC 2 (19.08%) are shown in Figure 4.19. The figure depicts some extent of overlap and little shape variation between the sexes in white South Africans. The chin shape variation of sex in this subsample (females n=115 and males n=59, total n=174) resulted in a MANOVA *p-value* of 0.282, the 50-50 MANOVA *p-value* in 0.238. The permutation test showed a value of 0.266 and the DFA test resulted in 65.2% (Table 4.13). Overall, sex did not significantly influence the shape of the bony chin (Figure 4.27). The chin shape changes between females and males in white South Africans differed slightly regarding the mandibular body length from the mental tubercles to the gonia and the distance from pogonion to menton.

As for all the craniometric landmarks, when analysing the selected craniometric landmarks of the hard-tissue chin, the obtained results were not significant (a MANOVA value of 0.417, a 50-50 MANOVA of 0.085 and a permutation test of 0.404). The DFA value was 66.1% (Table 4.13, Figure 4.28). Principal Component 1 (77.19%) versus 2 (10.44%), depicting great overlap in the shape, are shown in Figure 4.20, highlighting the non-significant shape variation of sex in white South Africans, when looking at the selected craniometric landmarks. Thus, irrespective of all eleven versus the seven selected craniometric landmarks, sex in white South Africans did not significantly influence the chin shape despite the visible difference between the minimum and maximum shapes, with the maximum exposing a much shorter distance between the mental tubercles and a larger distance between pogonion and menton. In addition, the distance between the supramentale and the pogonion was considerably larger than in the minimum shape.

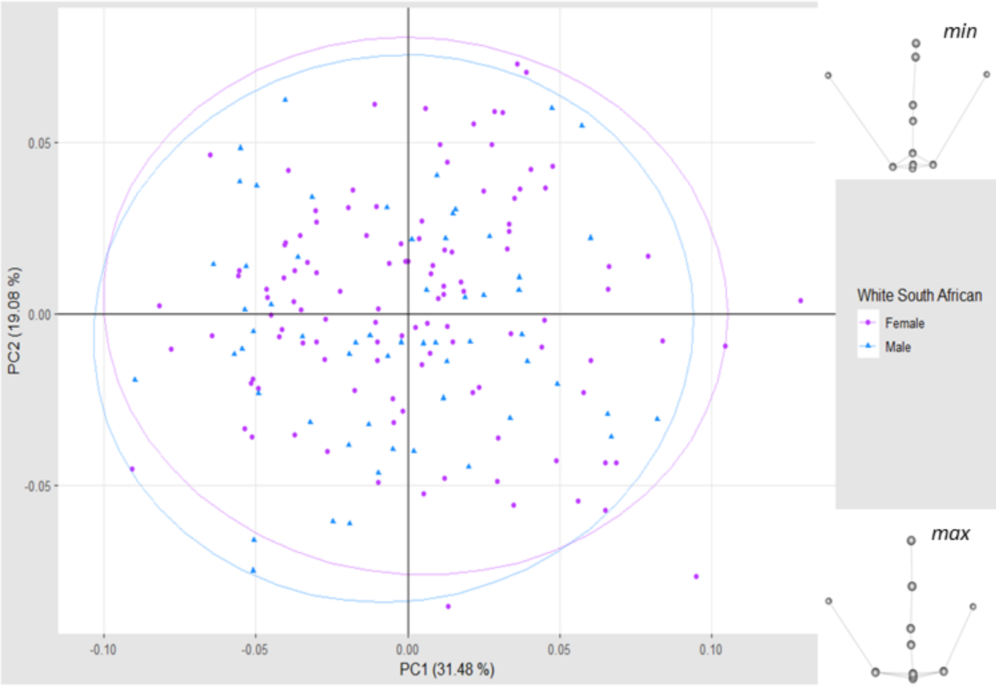

Figure 4.19 PC 1 versus PC 2 of white South Africans on all landmarks indicating the minimum and maximum shapes along PC1.

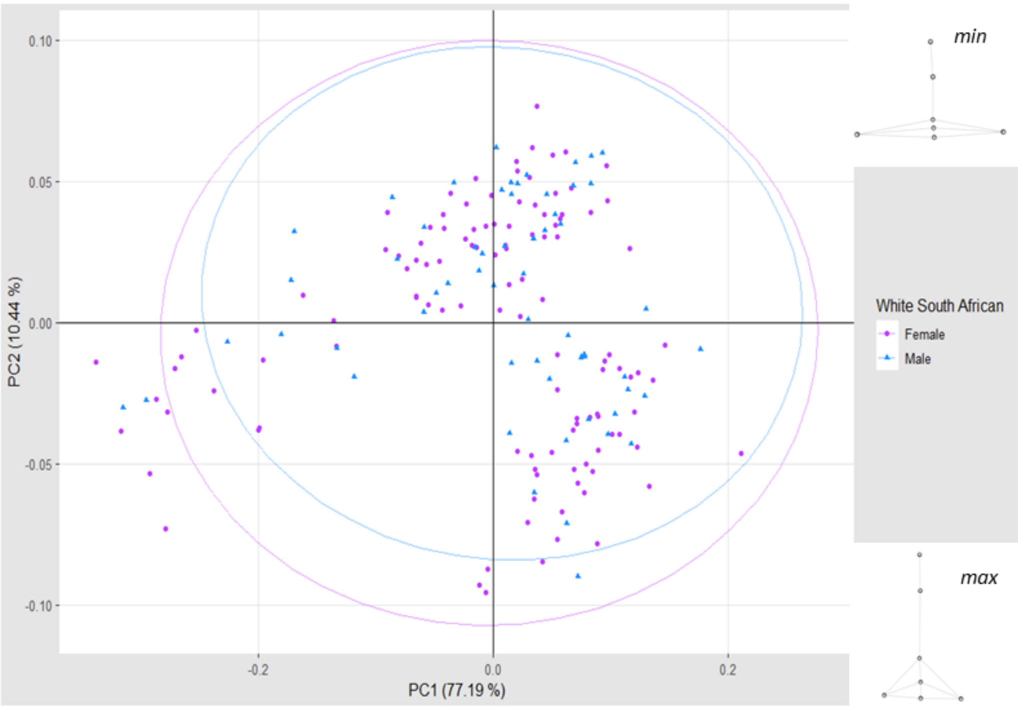

Figure 4.20 PC 1 versus PC 2 of white South Africans on the seven selected landmarks indicating the minimum and maximum shapes along PC1.

*Sex*Blacks*

For the analysis of sex in black South Africans, PC 1 (38.51%) versus PC 2 (19.97%) are given in Figure 4.10c. The chin shape variation of the factor sex in black South Africans (females n=47 and males n=70, total n=117) is not statistically significant (Figure 4.27), as can be seen in the great overlap of shape between females and males (Figure 4.21); the MANOVA *p-value* was 0.638 and the 50-50 MANOVA *p-value* was 0.745. Permutation test resulted in 0.800, equally non-significant. The DFA test was 59.8% (Table 4.13), thus very similar to the DFA test result in white South Africans above. Hence, the influence of sex on the shape of the chin in black and white South Africans was minimal.

As for all craniometric landmarks, the analysis of the selected craniometric landmarks in black South Africans resulted in non-significant values: a MANOVA *p-value* of 0.341, a 50-50 MANOVA of 0.267, a permutation test value of 0.350 and a DFA of 60.6% (Table 4.13, Figure 4.28). Principal Component 1 (61.34%) versus 2 (19.35%) are given in Figure 4.22, showing great overlap in the shape of the selected craniometric landmarks in black females and males, despite the visible shape change between minimum and maximum. The maximum shape displayed a shorter distance between the mental tubercles and a larger distance between pogonion and menton.

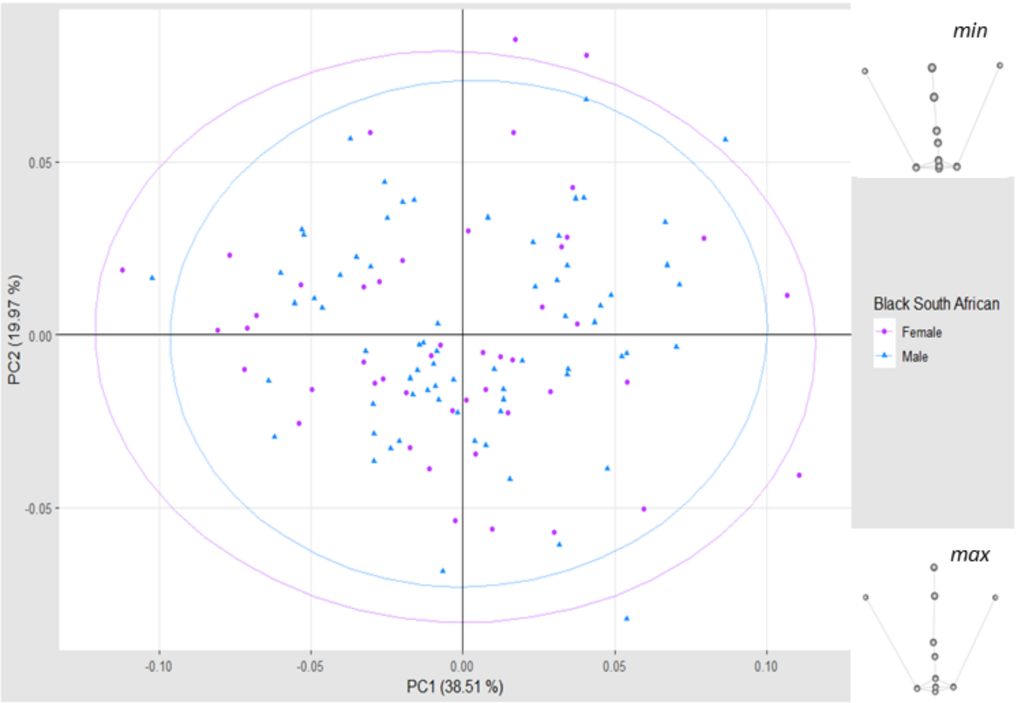

Figure 4.21 PC 1 versus PC 2 of black South Africans on all landmarks indicating the minimum and maximum shapes along PC1.

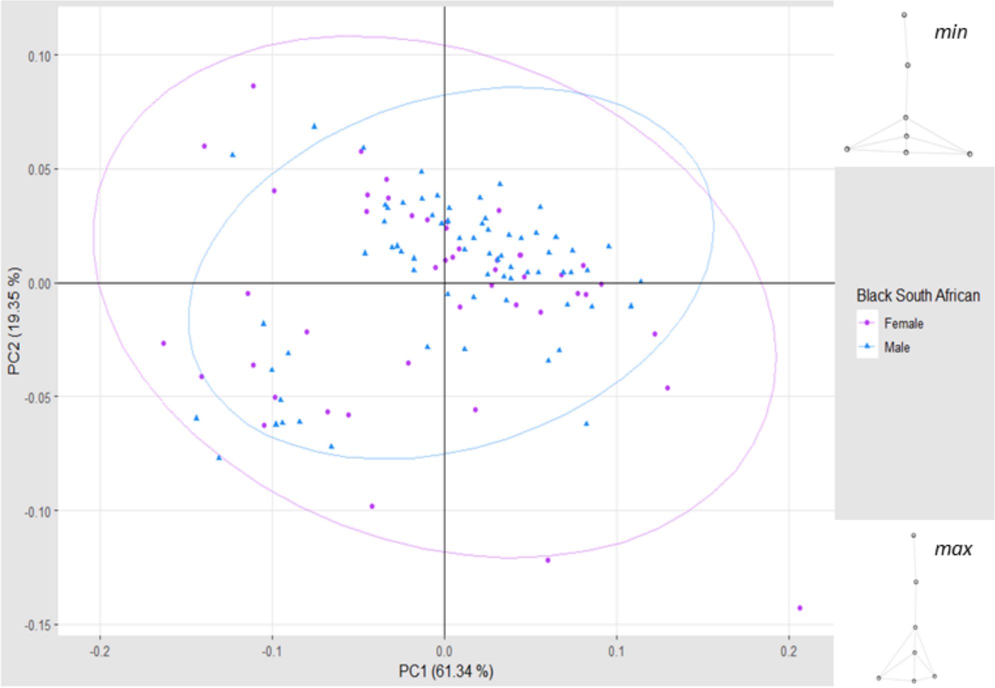

Figure 4.22 PC 1 versus PC 2 of black South Africans on the seven selected landmarks indicating the minimum and maximum shapes along PC1.

*Age*Whites*

For the analysis of age in white South Africans (18-29 n=38, 30-44 n=34, 45-59 n=61, ≥60 n=41, total n=174), PC 1 (31.48%) versus PC 2 (19.8%) are given in Figure 4.23, highlighting some shape variation in the width of the chin and also in the distance between subspinale and prosthion. This analysis of age in white South Africans resulted in a MANCOVA *p-value* of 0.011 and a 50-50 MANOVA of 0.002 (Table 4.13); both values are statistically significant (Figure 4.27).

The analysis of the selected craniometric landmarks resulted in a MANCOVA *p-value* of 0.069 and a 50-50 MANOVA of 0.055 (Table 4.13, Figure 4.28), which was not statistically significant. The first two PC scores (with 77.19% and 10.44% shape influence, respectively) are given in Figure 4.24, depicting the extent of shape variation which concerned the width and the height of the chin (distance between the mental tubercles as well as between pogonion and menton), and also the distance between supramentale and pogonion.

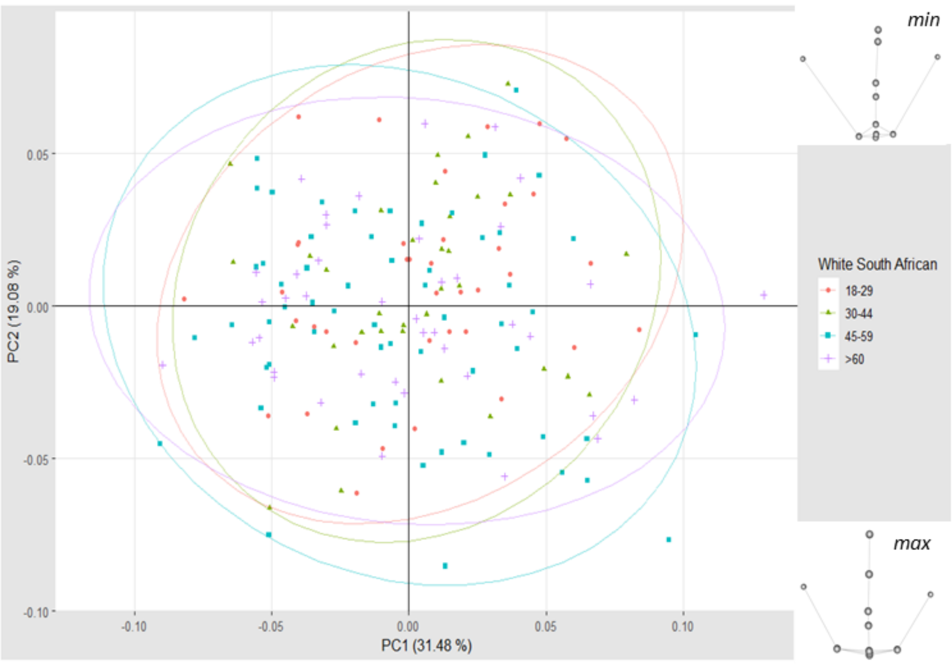

Figure 4.23 PC 1 versus PC 2 of white South Africans for age on all landmarks indicating the minimum and maximum shapes along PC1.

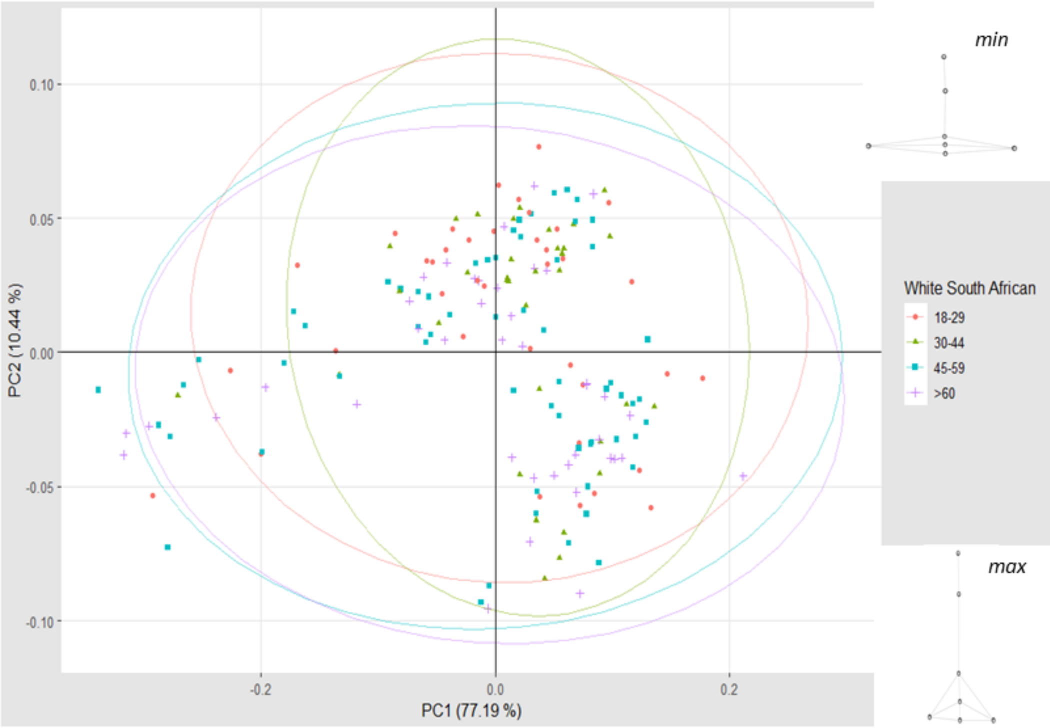

Figure 4.24 PC 1 versus PC 2 of white South Africans for age on the seven selected landmarks indicating the minimum and maximum shapes along PC1.

*Age*Blacks*

For the analysis of age as a shape-influencing factor on black South Africans (18-29 n=39, 30-44 n=51, 45-59 n=23, ≥60 n=4, total n=117), the first two PC scores (with 38.51% and 19.97% shape influence, respectively) are given in Figure 4.25, highlighting the small extent of shape variation in the distance between pogonion and menton. The chin shape variation analysis (MANCOVA) of age in black South Africans resulted in a *p-value* of 0.468, the 50-50 MANOVA a *p-value* of 0.408 and was thus not statistically significant (Table 4.13, Figure 4.27).

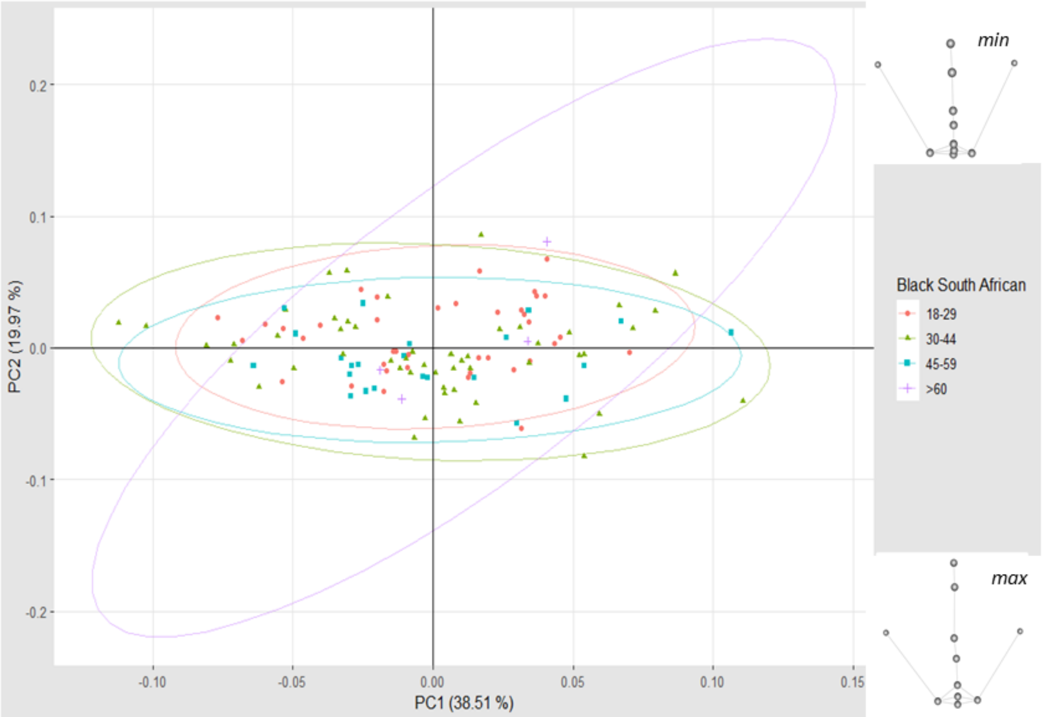

Figure 4.25 PC 1 versus PC 2 of black South Africans for age on all landmarks indicating the minimum and maximum shapes along PC1.

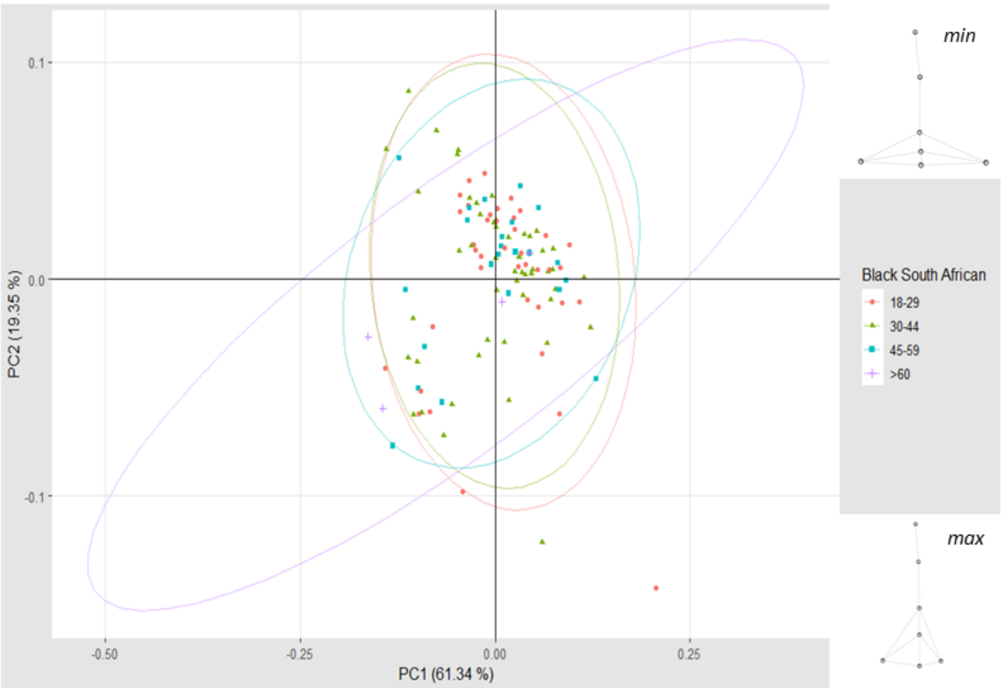

Figure 4.26 PC 1 versus PC 2 of black South Africans for age on the seven selected landmarks indicating the minimum and maximum shapes along PC1.

On the selected craniometric landmarks, the same analysis resulted in a MANCOVA *p-value* of 0.359 and a 50-50 MANOVA of 0.282 (Table 4.13), neither of which is statistically significant (Figure 4.28). Principal Component 1 (61.34%) versus 2 (19.35%) are given in Figure 4.26, highlighting the small extent of shape variation in black South Africans in relation to age, referring to the width and the height of the chin (distance between the mental tubercles and distance between pogonion and menton).

*Sex*Age*Whites*

The combination of age with sex was statistically non-significant in white South Africans (n=174). The MANCOVA resulted in a *p-value* of 0.174, the 50-50 MANOVA in 0.177 (Table 4.13, Figure 4.27).

In the selected craniometric landmarks, the analysis resulted in a MANCOVA value of 0.176 and a 50-50 MANOVA of 0.061 (Table 4.13, Figure 4.28), thus not statistically significant.

*Sex*Age*Blacks*

As in white South Africans, the analysis of age combined with sex in black South Africans (n=117) was not statistically significant with a MANCOVA *p-value* of 0.365 and a 50-50 MANOVA of 0.344 (Table 4.13, Figure 4.27).

When the selected craniometric landmarks were analysed, the MANCOVA value was 0.326, and the 50-50 MANOVA value was 0.361 (Table 4.13, Figure 4.28), thus not statistically significant.

4.2.3.4 Allometry

Complete sample

The analysis of the complete sample for allometry resulted in a MANCOVA *p-value* of <0.001 and a 50-50 MANOVA of <0.001, and were thus both statistically significant.

*Allometry*Whites*

The chin shape variation of allometry as a chin shape-influencing factor in white South Africans (n=174) showed a MANCOVA *p-value* of <0.001 and a 50-50 MANOVA *p-value* of <0.001 (Table 4.13); both were statistically significant (Figure 4.27).

The analysis of the selected craniometric landmarks resulted in a MANCOVA value of <0.001 and a 50-50 MANOVA value of likewise <0.001 (Table 4.13). Allometry was a statistically significant shape-influencing factor in whites (Figure 4.28).

*Allometry*Blacks*

The chin shape variation with allometry as a factor in black South Africans (n=117) resulted in a MANCOVA *p-value* of 0.002 and an equal, statistically significant 50-50 MANOVA *p-value* of 0.002 (Table 4.13, Figure 4.27).

The analysis of the selected craniometric landmarks showed a MANCOVA value of <0.001 and a 50-50 MANOVA value of likewise <0.001 (Table 4.13), both statistically significant (Figure 4.28). Hence, as in white South Africans, allometry in black South Africans influenced shape for all landmarks as well as for the selected landmarks.

*Allometry*Sex*Whites*

Allometry combined with sex in white South Africans (n=174) was not statistically significant (Figure 4.27); the MANCOVA *p-value* was 0.797, equal to the 50-50 MANOVA *p-value* of 0.797 (Table 4.13).

The non-significant results obtained in the same subsample on the selected craniometric landmarks were a MANCOVA value of 0.142 and a 50-50 MANOVA value of, likewise, 0.142 (Table 4.13, Figure 4.28).

*Allometry*Sex*Blacks*

The analysis of the allometry-sex combination in black South Africans (n=117) showed statistically non-significant results (Figure 4.27); the MANCOVA *p-value* was 0.155; the 50-50 MANOVA *p-value* was 0.180 (Table 4.13).

The analysis of the selected craniometric landmarks resulted in a MANCOVA value of 0.133 and a 50-50 MANOVA of 0.859 (Table 4.13), thus allometry in combination with sex did not influence the shape of the chin (Figure 4.28).

Table 4.13 Compilation of results, chin shape variation in South Africans with the influencing factors ancestry, sex, age and allometry; MANOVA; 50-50 MANOVA; MANCOVA; permutation test and discriminant function analysis (DFA).

Chin shape (all landmarks)	MANOVA	50-50 MANOVA	PERMUT. TEST	DFA	Bony menton shape (selected landmarks)	MANOVA	50-50 MANOVA	PERMUT. TEST	DFA
Ancestry	**0.001**	**<0.001**	**0.001**	86.9%	Ancestry	**0.001**	**<0.001**	**0.001**	91.7%
Ancestry*Males	**0.001**	**0.001**	**0.001**	87.2%	Ancestry*Males	**0.001**	**0.001**	**0.001**	88.3%
Ancestry*Females	**0.001**	**0.001**	**0.001**	86.4%	Ancestry*Females	**0.001**	**0.001**	**0.001**	95.6%
Sex	0.067	0.052	0.066	57.3%	Sex	**0.003**	**0.001**	**0.001**	63.9%
Sex*Whites	0.282	0.238	0.266	65.2%	Sex*Whites	0.417	0.085	0.404	66.1%
Sex*Blacks	0.638	0.745	0.800	59.8%	Sex*Blacks	0.341	0.267	0.350	60.6%
Chin shape (all landmarks)	**MANCOVA**	**50-50 MANOVA**			**Bony menton shape (selected landmarks)**	**MANCOVA**	**50-50 MANOVA**		
Age	**<0.001**	**<0.001**			Age	**<0.001**	**<0.001**		
Age*Whites	**0.011**	**0.002**			Age*Whites	0.069	0.055		
Age*Blacks	0.468	0.408			Age*Blacks	0.359	0.282		
Sex*Age*Whites	0.174	0.177			Sex*Age*Whites	0.176	0.061		
Sex*Age*Blacks	0.365	0.344			Sex*Age*Blacks	0.326	0.361		
Allometry	**<0.001**	**<0.001**							
Allometry*Whites	**<0.001**	**<0.001**			Allometry*Whites	**<0.001**	**<0.001**		
Allometry*Blacks	**0.002**	**0.002**			Allometry*Blacks	**<0.001**	**<0.001**		
Allometry*Sex*Whites	0.797	0.797			Allometry*Sex*Whites	0.142	0.142		
Allometry*Sex*Blacks	0.155	0.180			Allometry*Sex*Blacks	0.133	0.859		

Significant values in bold.

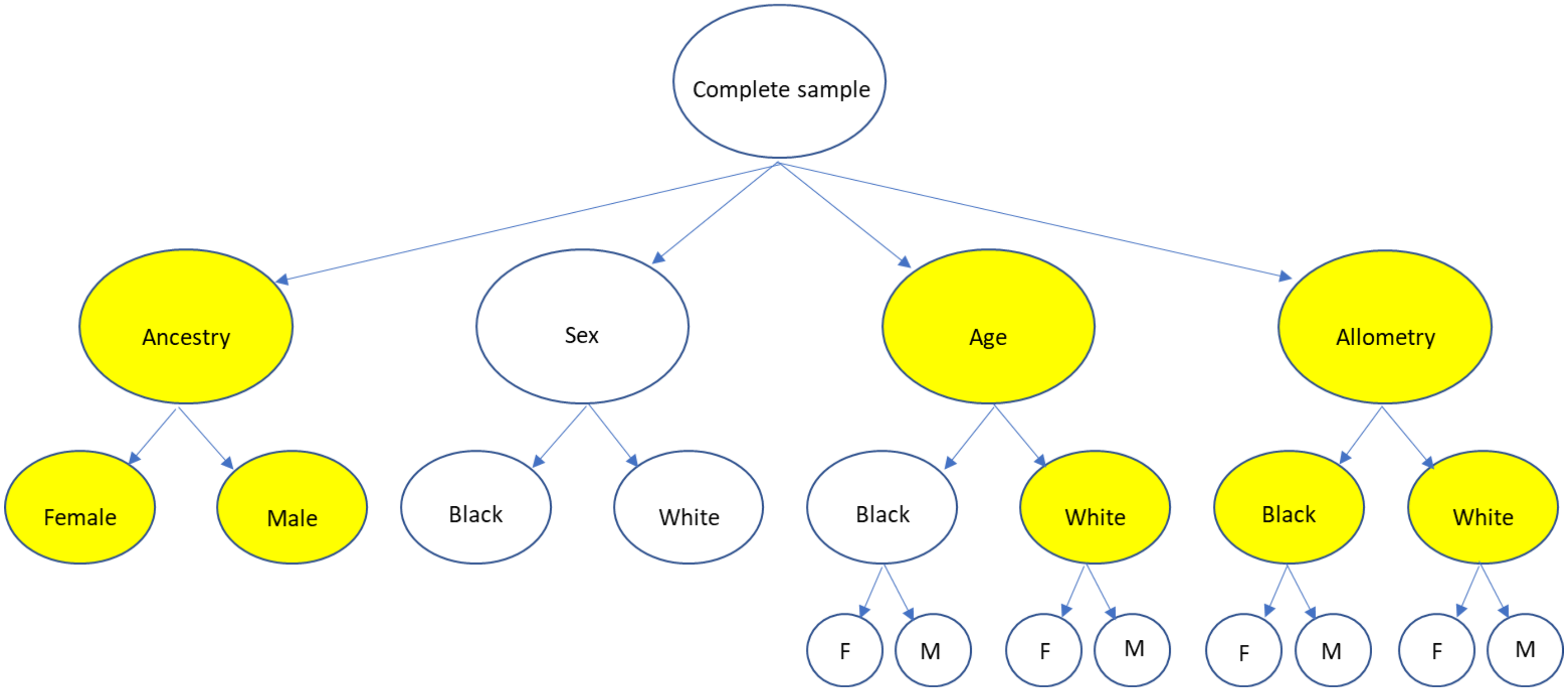

Figure 4.27 Summary of significant (yellow) and non-significant (white) results in the analysis of all eleven craniometric landmarks.

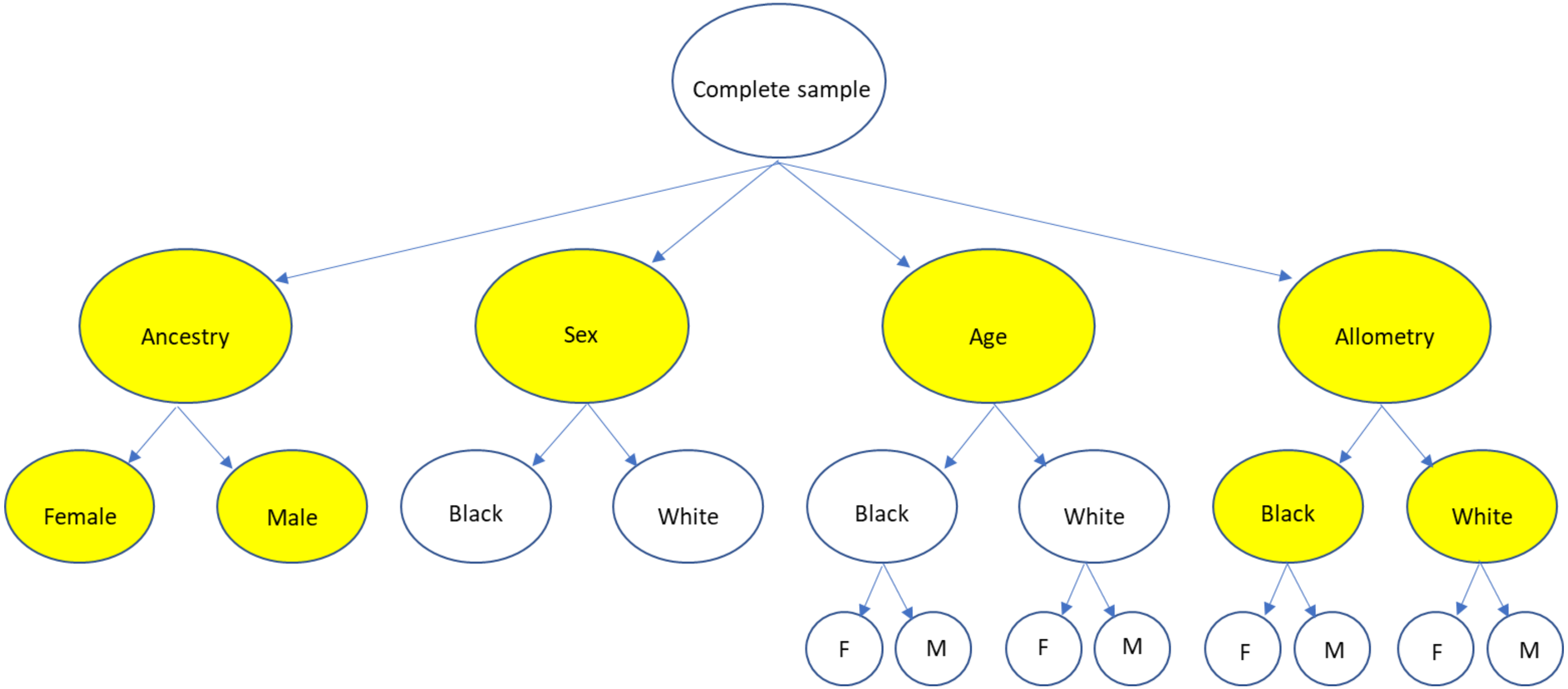

Figure 4.28 Summary of significant (yellow) and non-significant (white) results in the analysis of the selected seven craniometric landmarks.

4.2.4 Summary of results

1. The manual landmarking process resulted in lower reproducibility than the automatic landmarking.

2. Ancestry, age and allometry in the complete sample influenced the shape of the chin.

3. Ancestry significantly influenced the chin shape within sex groups.

4. Sex was statistically significant in the complete sample, but only on the seven selected landmarks (bony menton). Sex had no significant influence on chin shape within the ancestral groups.

5. Age in black South Africans was not significant, while in the complete sample, as well as in white South Africans, it was significant. However, in white South Africans only when analysing all craniometric landmarks. Age did not influence the chin shape, when analysed in combination with ancestry and sex.

6. Allometry influenced the shape of the chin in the complete sample, as well as in black and white South Africans. However, sex combined with allometry and ancestry did not influence the chin shape.

7. No difference was observed in the analysed parameters between all eleven versus the seven selected craniometric landmarks, except for sexual dimorphism in the complete sample, and age in whites.

CHAPTER 5 DISCUSSION

The human mandible is often preserved in skeletal remains (Oettlé et al. 2009a). It is a useful bone for the assessment of ancestry (L'Abbé et al. 2011; Stull et al. 2014) and sexual dimorphism (Garvin and Ruff 2012), the latter being detectable in early childhood (Hutchinson 2010), and in adult age (Franklin et al. 2007; Garvin and Ruff 2012). Hence, the mandible lends itself for research related to population- and sex-specific standards for biological profiling in South Africa. However, less is known regarding the role of the chin in forensic anthropological assessments; thus, the chin was the focus of this study. The expression of sexual dimorphism in the mental eminence as part of the morphoscopic assessment described by Walker (2008) was analysed, as well as the applicability of the method to three-dimensional scan surfaces (3D surfaces), especially as the trait is felt, rather than visually observed, in bone. Scores in bone and 3D surfaces per observer were compared.

Furthermore, the study analysed the influence of the factors ancestry, sex, age and size (allometry) on the human chin shape, using craniometric landmarks and applying geometric morphometric (GMM) methods. A previous study found that the mandible undergoes non-significant morphological changes with increasing age (Windhager et al. 2019). After the eruption of the third molar at approximately 18 years of age (İşcan and Steyn 2013), the mandible is no longer useful for the estimation of chronological age. Nonetheless, the present study included the analysis of ageing and any influence it may have on the hard-tissue chin shape.

5.1 WALKER METHOD

Although the application of the method (Walker 2008) to 3D surfaces was feasible, an observer's personal affinity for assessing bone or 3D and the level of experience should be considered. Some observers might simply be more affine for assessing a tactile sex estimation trait in a 3D modality than others. Possibly due to the lack of tactile sensation during scoring, not all four observers were consistent in their scoring when using the two modalities. In addition, the intricate anatomical structure of the mental eminence (Lewis and Garvin 2016) might have contributed to the difficulties among the observers in consistently scoring the trait. In the Walker (2008) method, although being referred to as 'visual', three of the five described traits on the human skull are scored tactilely, the mental eminence among them. The feasibility of the application of the method to 3D surfaces is justified by the similar outcomes of the scoring when compared to bones. Overall, the observers performed very similarly in both modalities.

The relatively low agreement between observers and modalities was consistent with previous studies. For example, the glabella, mastoid process and nuchal crest were found to be more reliable traits (repeatability of scoring) than the mental eminence (Krüger et al. 2015; Lewis and Garvin 2016; Dereli et al. 2018). Overall, the intra- and interobserver agreement in the study by Krüger and colleagues (2015), ranged between 0.60 and 0.90 (moderate to excellent), except for the mental eminence, where agreement did not exceed 0.40 (fair). Among the three observers in the study by Dereli and colleagues (2018), on average the mental eminence (0.64) ranged slightly higher than the supraorbital margin (0.63). This stood in contrast to the remaining three traits: nuchal crest (0.71), mastoid (0.72) and glabella (0.88). Similarly, an investigation into sexing skulls and pelves from a medieval skeletal sample from the Netherlands (Maat et al. 1997), showed that the results from sexing an individual from the mandible was not reliable. However, a different sex estimation technique of the mandibular aspects was employed: the robustness of the bone, the shape of the mentum, the prominence and shape of the gonial angle and the robustness of the inferior margin were estimated (Maat et al. 1997). In consequence, more than half of the females were sexed as males.

Overall, both modalities were scored similarly. The difference between the observation of the trait in bone versus 3D surfaces could be neglected. The better agreement in the intraobserver error (intraOE) as opposed to the interobserver error (interOE), however, suggested that the observation of the trait in bone or in 3D surfaces might be a matter of personal preference or of motivation, as the intraOE was carried out by the principal investigator who had done the biggest amount of reading into the subject prior to scoring. The observers' level of experience might have slightly influenced the outcome. This corroborated the findings of the study of Byrnes et al. (2017), who found that the level of observers' experience influenced the results both for the morphoscopic and the metric sex estimation on the mandible, if only to a negligible degree. However, the study by Byrnes and colleagues (2017) assessed the chin shape by looking at it from a cranial perspective and scoring the observed chin according to its shape (blunt, pointed, square or bilobate). Thus, different criteria from the Walker (2008) method were involved, rendering direct comparison of results difficult.

Other challenges in scoring the sample included that the complete sample was analysed without any differentiation made between ancestries, the lack of tactile sensation when observing 3D surfaces, the low accuracy of the mental eminence and, potentially, the personal affinity for assessing 3D surfaces. These difficulties might also explain the low agreement among observers; they were reflected in the observers' perception in the qualitative part. Moreover, the low comparability within observers might be explained by the above-mentioned challenges. However, the overall tendency in both modalities pointed to a feasibility to use 3D surfaces, taking into consideration that the mental eminence in isolation is not a reliable sex estimation trait.

The overall average scores of all four observers for the two modalities suggested a tendency to score the expression of the mental eminence slightly lower (more feminine) in 3D surfaces than in bone; this might be due to the lack of tactile sensation when scoring 3D surfaces. The lack of immediate tactile comparison with other mental eminences when scoring the bone, might have contributed to the slight underscoring of 3D surfaces. However, as the interOE of bone versus 3D surfaces did not differ much, the slightly lower average scoring observed in 3D surfaces may not necessarily preclude the use of 3D surfaces in sex estimation for this method. The use of virtual 3D surfaces in a morphoscopic method has the advantage of eliminating the handling of bones, thus limiting any possible damage to the bone tissue. In addition, the ready availability of scans, as opposed to skeletal material, for verification of previously made estimations, is advantageous. A disadvantage of applying a morphoscopic method to 3D surfaces, however, is the lack of tactile sensation of the expression of the feature in question (Dereli et al. 2018), a fact which is also reflected in the qualitative section of this dissertation.

Even though the interOE agreement on the complete sample was low, a tendency could be detected for obtaining the highest percentage in correctly sexing the specimens in bone, but less often in 3D surfaces. Only observer 4 achieved the highest percentage in correctly sexing the complete sample in both modalities. Three of the four observers concurred more often in correctly sexing white South Africans, compared to black South Africans. This could be indicative of a more prominent expression of sexual dimorphism in the mental eminence among South African whites when compared to blacks (L'Abbé et al. 2013; Krüger et al. 2015).

Females were more often correctly sexed than males. This was surprising as the results found by Krüger et al. (2015) suggested the opposite. This might be due to the consideration of all five traits on the skull in the previous study versus the mental eminence in isolation in the present research, a wider shape variation in the mental eminence among black and white females as opposed to males, or the use of (partially) edentulous mandibles. Furthermore, the sex bias in the sample of the present study (42 females, 63 males) could also account for the differences in results noted.

The observers' relative likelihood of sexing black females (BF) and white males (WM) correctly in both modalities could be due to the enhanced gracility of the former and robusticity of the latter (Krüger et al. 2015). Hence, the relative unlikelihood of sexing black males (BM) and white females (WF) correctly was not surprising, as the expression of their mental eminence lies between the two morphological extremes of BF and WM, representing the continuum of the trait expression which is harder to score.

Observers 1, 3 and 4 almost always concurred in the outcome that BF and WM were more often correctly scored, which in turn concurred with the application of the method to the same population groups in the previous study by Krüger and colleagues (2015). Observer 2 performed more ambiguously in the process of scoring the ancestral-sex subsamples. Generally, score frequency in the ancestral-sex groups for BF and BM corroborated the findings of Krüger et al. (2015) that scores 2 and 3 were most often attributed to the two subsamples, respectively, in bone. For WF and WM, however, score frequencies differed between the two studies. While WF were most often scored a 3 in the present study in bone, Krüger and colleagues (2015) most often scored WF a 2. For WM, the score frequencies also differed by one score; the four observers in the present study scored WM most often a 5 in bone and Krüger et al. (2015) a 4. In 3D surfaces, the highest score frequency of the four observers in this study was a 2 for both BF and BM. For WF and WM, the highest score frequency was a 3 in the present study. The score frequency in 3D surfaces thus showed that males were scored too low (more feminine) while females had the same highest score frequency in bone and 3D surfaces.

Although the subsample sizes in the age groups varied, implying a cautious interpretation of the findings, a tendency could be detected confirming the results of the ancestral-sex group analysis: BF and WM were the most likely to be correctly sexed, in contrast to BM and WF, irrespective of age.

5.2 CHIN SHAPE VARIATION IN SOUTH AFRICANS

The chin shape variation part of the present study analysed the possible influence of ancestry, sex, age as well as size (allometry) on the shape of the chin in black and white South Africans. The usability of cone-beam computed tomography (CBCT) scans for 3D as compared to dry bone measurements was established previously, with Pearson correlation coefficients ranging between 0.992 and 1 (Kamburoğlu et al. 2011). The same materials (CBCT scans) and methods, craniometric landmarks and geometric morphometrics (GMM), were applied to black and white South Africans to study the influence of the same parameters (ancestry, sex, age and allometry) to the mid-facial region (Ridel 2019). The present study was complementary to other studies performed on facial features in the FARC group (Oettlé 2014; Krüger et al. 2015; Dorfling et al. 2018; Ridel 2019), aiming at an incorporation of the findings on the hard-tissue so as to enable forensic anthropologists in South Africa to improve biological profiling and create better facial approximations from skeletal remains, by applying the methodology used by Ridel 2019.

As the identification of landmarks for 3D shape analysis in this study was pivotal, reproducibility of the predefined landmarks was considered before detailing the effects of the demographic factors. While the landmarking placement process has pitfalls of its own (Bookstein 1991; Wärmländer et al. 2019), the automatic placement of the craniometric landmarks was favourable over the manual placement, due to the higher accuracy of the former (Ridel et al. 2018; Ridel 2019). As could be expected, some of the landmarks showed higher reproducibility (subspinale, prosthion, infradentale and gnathion) due to the relative precision of their definition, while other landmarks with less precise definitions resulted in a lower reproducibility (supramentale, pogonion, mental tubercle right and gonion left) (Caple and Stephan 2016). Apart from the imprecise definitions of these craniometric landmarks, the orientation of the 3D surfaces in the software during the manual landmarking process might have accounted for the lower reproducibility of the mentioned landmarks. The automatic landmarking process, in contrast, excluded a great degree of imprecision, as was also shown in previous studies (Ridel et al. 2018, Ridel 2019).

The influence of ancestry on the chin shape corroborated the findings of previous research (L'Abbé et al. 2011; Garvin and Ruff 2012; Stull et al. 2014; Byrnes et al. 2017). In Figure 4.4, the broader gonial region in whites, as compared to blacks, as reported in previous studies (Parr 2005; Oettlé et al. 2009b), can be noted. Furthermore, the relative prognathism in blacks compared to whites is visible in Figure 4.4. According to previous studies, the enhanced prognathism in South African blacks could render the pronounced chin redundant, as the required space for the tongue was allotted by prognathism, thus not inhibiting swallowing and breathing in the posterior part of the oral cavity (Coquerelle et al. 2013a; Coquerelle et al. 2013b). Hence, prognathism in South African blacks corroborated the finding of the chin shape in blacks as being less square, more rounded or even pointed, in contrast to South African whites, whose chin is often perceived as 'square' (De Villiers 1968; Parr 2005; Garvin and Ruff 2012; Oettlé 2014). In the hard-tissue shape of the mid-face of black and white South Africans, ancestry was a shape-influencing factor when craniometric landmarks and GMM were employed (Ridel 2019).

The influence of ancestry in the complete sample of the present study as well as within sex groups was detectable. Sexual dimorphism, on the other hand, was non-significant in the complete sample on the eleven craniometric landmarks, and non-significant also within ancestral groups (Figure 4.27). However, sexual dimorphism proved to be significant in the complete sample, when the seven selected landmarks were analysed (Figure 4.28). This indicated that the shape concerning the gonia and the maxillary landmarks did not significantly vary between the sexes, while the bony menton did. Significant results in the analysis of sexual dimorphism were obtained in the mid-facial region, although to a greater extent in black than in white South Africans (Ridel 2019). In white South Africans, sex did not significantly influence some of the analysed shapes on the mid-facial region (the nasal bones and the nasal aperture) (Ridel 2019).

Furthermore, the influence of age on the chin shape in the complete sample was important. However, when ancestral groups were separated, age was no longer influential. In white South Africans, age was influential only on the shape of all eleven craniometric landmarks (Figure 4.27), but not on the seven selected craniometric landmarks (Figure 4.28). This discrepancy might be explained by a difference in tooth loss patterns in white as compared to black South Africans (Oettlé et al. 2009b).

In addition, some other, unknown factor affecting the relative position of the chin in white South Africans might be responsible. Although individuals with severe tooth loss were excluded, those with partial tooth loss (up to Eichner Index B3) were included. The effects of tooth loss on chin shape were not the aim of this study. In an attempt to minimalise the effects of tooth loss, samples with a greater extent of tooth loss were not included. For this reason, samples with tooth loss exceeding dentition group B3 (Ikebe et al. 2010) were not used. Tooth loss beyond B3 is associated with significantly decreased masticatory performance (Ikebe et al. 2010). In addition, individuals up to group B3 have intact incisors and canines, which would render the effect of tooth loss in group B3 unlikely responsible for differences noted between groups in the seven selected landmarks depicting the chin shape. However, a future study could incorporate the chin shape variation in conjunction with the dentition patterns according to the Eichner Index. Furthermore, it should be stressed that when interpreting the outcomes related to age groups in this study, the varying subsample sizes in the age groups need to be considered. When age was combined with ancestry and sex, again no influence on the chin shape was found, indicating that the influence of ancestry and sex was greater than that of ageing. Age was also found to significantly influence the mid-facial hard-tissue region, though to a greater extent in blacks than in whites (Ridel 2019).

As in the present study, allometry was also found to be a significant shape-influencing factor of the mid-facial region in black and white South Africans (Ridel 2019). Allometry resulted in significant outcomes across all parts of the mid-face; thus, allometry was as statistically significant as ancestry across the complete sample (Ridel 2019). The combination of ancestry and sex in the present study to assess allometry did not, however, influence the chin shape. This finding could indicate that sex influenced the allometry reported in the separate ancestral groups, and when sexes were evaluated separately, the effect of allometry was diminished. Another reason for the insignificance of allometry in the ancestral-sex groups could be attributed to the diminution of the subsample sizes.

Previous studies had shown that the expression of sexual dimorphism in South African populations is lower than in their North American counterparts, relating to the cranium as opposed to postcranial traits (McDowell et al. 2012; L’Abbé et al. 2013; Krüger et al. 2015). More precisely, the extent of sexual dimorphism also varies between black and white South Africans, with blacks exhibiting a lower degree than whites (Tobias 1974; L’Abbé et al. 2013). The discrepancy in the extent of sexual dimorphism might be an explanation for the greater significance of the allometric effect in South African whites as opposed to blacks, as shape variation with size may be confounded by a more pronounced sexual variation in size and shape. This difference in sexual dimorphism may in part be due to the comparatively lower socio-economic situation of South African blacks than whites. It is postulated that during the critical pubertal growth period, limited food resources may hinder optimal growth (Tobias 1974), and therefore perhaps influence the allometric effect noticed on the shape of the chin in the black South Africans. However, with the ongoing socio-political changes in South Africa, blacks might be expected to extend the degree of sexual dimorphism in the future (L'Abbé et al. 2013).

Using the seven selected versus the eleven craniometric landmarks had no influence on the significance found between the covarying factors (ancestry, sex, age and allometry), except for the effects of sexual dimorphism in the complete sample, and ageing in white South Africans. The few differences between findings involving only the menton compared to all eleven landmarks could indicate that the bony menton shape is linked to the gonia and the maxillary landmarks.

5.3 GENERAL DISCUSSION

Both parts of this study concurred in their findings regarding the factors influencing the shape of the hard-tissue chin in black and white South Africans. The influence of sexual dimorphism in the selected landmarks on the menton explained why, in the Walker part of this study, estimating sex from the chin was feasible in the complete sample, although not consistently by all four observers. The influence of ancestry and sexual dimorphism explained why correctly scoring BF and WM was feasible in the Walker part of this study. The four ancestral-sex groups could be described as a continuum of the chin shape variation, with BF being the most gracile and smallest, and WM the most robust and largest (Krüger et al. 2015), representing scores 1 and 5, respectively, of the Walker (2008) method. The BM and WF groups were located between these two extreme chin shape expressions, representing scores 2, 3 and 4, which were harder to score. The overall relatively low expression of sexual dimorphism reported in the studied South African populations (McDowell et al. 2012; L'Abbé et al. 2013; Krüger et al. 2015) agreed with the outcomes of the present study, detecting sexual dimorphism in the complete sample, but only on the seven selected landmarks, and not in the ancestral groups.

The fact that ancestry had a greater influence on the chin shape than sexual dimorphism corroborated the findings of a previous study (L'Abbé et al. 2013). The higher likelihood of sexing the white as opposed to the black South Africans correctly, concurred with the finding of a slightly higher degree of sexual dimorphism in South African whites than in blacks. It also confirmed the result in the chin shape analysis part of this study, showing a wider shape variation in whites than in blacks, although non-significant. The question remains, however, why females were generally more often correctly sexed than males, as this outcome did not concur with the findings of a previous study (Krüger et al. 2015); both sexes should have been equally well scored. As mentioned before, other studies have used all five traits of the Walker (2008) method, while the present study concentrated on the mental eminence. Another reason could be the sex bias; the females in the sample were fewer (n=42) than males (n=63), with the WF being the smallest (n=8). Also, personal affinity for assessing one of the modalities could be an explanation.

Age-related shape variation was only partly influential. This was not surprising, as it concurred with previous studies. Even though post-menopausal women were found to present with slight morphological changes in the mandible due to bone resorption, shape changes were not statistically significant (Windhager et al. 2019).

The importance of size (allometry) on the chin shape in the complete sample, and in the ancestral groups separately, was corroborated in the findings of the Walker (2008) method part, such that the distinction between BF and WM could otherwise hardly be obtained; BF representing the smallest and WM the largest expression of the mental eminence.

The overall findings of both parts of this study are thus corroborative of each other, as well as of most related previous studies. The human chin could develop in order to allot enough space for the tongue in the oral cavity so as not to obstruct the posterior space for breathing and swallowing. Thus, enhanced prognathism might make a prominent chin superfluous by allotting the necessary space for the tongue. The generally greater gonial eversion in whites, compared to blacks, described in earlier studies (Oettlé et al. 2009a) was also detected in this study, represented in the minimum and maximum shapes in the analysis of all eleven craniometric landmarks. The importance of ancestry on the human chin shape corroborated previous studies (De Villiers 1968; Tobias 1974; Loth and Henneberg 2000;

Parr 2005; Oettlé et al. 2009a; Oettlé et al. 2009b; L'Abbé et al. 2011; Garvin and Ruff 2012; Hefner and Ousley 2014; Oettlé et al. 2017), while the detection and quantification of sexual dimorphism were previously found to be more challenging (Loth and Henneberg 1996; 2000; Franklin et al. 2007; Oettlé et al. 2009b; Garvin and Ruff 2012; Byrnes et al. 2017).

In this sense, the expression of sexual dimorphism on the bony menton of the complete sample pointed to a wide shape variation, which was largely due to having both ancestries in the sample. Within each ancestral group, sexual dimorphism was not detectable. Likewise, the importance of age in the complete sample was relativised by the influence of ancestry and sex, thus supporting the fact that mandibles beyond the eruption of the third molar are not usually indicative of age.

The apparent advantage of including micro-XCT scans into the Walker study was to have high-resolution 3D images of bones from a skeletal collection. With the advancing availability of such scans through projects like Bakeng se Afrika (https://www.up.ac.za/bakeng-se-afrika), scans are being made accessible to researchers around the globe, and a sex estimation methods (Walker 2008) can be validated for a variety of population groups. The use of CBCT scans for the chin shape variation study was justified by the inclusion of partially dentate, living patients being scanned for medical reasons, with a low-radiation scanning device. The use of software in this study was made dependent on availability. Using a different software should not influence the outcome unless the high-resolution depiction of the scans cannot be guaranteed. A comparison of software programs could, however, be interesting, depending on whether, for instance, the source of light is moveable.

CHAPTER 6 CONCLUSION

In recent years, three-dimensional (3D) imaging techniques, originally used in medical diagnostics, have inspired researchers in forensic anthropology to test existing, and to develop new methods dedicated to biological profiling. The present research took these contexts into consideration, focussing on the analysis of chin shape variation in black and white South Africans, involving craniometric landmarks and geometric morphometrics (GMM).

The four observers in the morphoscopic part of this study performed very similarly in bone and in micro-focus X-ray computed tomography (micro-XCT) scans. The slight difference in performance among the four observers could have been due to the observers' level of experience and a possible personal affinity for assessing 3D surfaces. The application of the Walker method (2008) to the mental eminence implied that sexual dimorphism was detectable in the human chin. Indeed, sexual dimorphism was shown to influence the sample (on the selected landmarks) of 291 cone beam computed tomography (CBCT) scans, using craniometric landmarks and GMM. Ageing, like sexual dimorphism, proved to influence the chin shape in the complete sample, but not in the ancestral-sex groups. Moreover, ancestry and size (allometry) influenced the chin shape, not only in the complete sample but also in the analysed subsamples. Ancestry and size were thus more relevant than sexual dimorphism and ageing in the studied sample.

The use of craniometric landmarks, the automatic landmarking process and GMM on the chin in black and white South Africans were reliable methods for this study.

6.1 FUTURE RESEARCH NEEDS

Regarding the applicability of the morphometric sex estimation technique (Walker 2008) to 3D surfaces, a study could be carried out in bones and the respective micro-XCT scans for all five traits. This would allow the comparison of the results to those obtained in this study as well as in previous studies (Krüger et al. 2015; Lewis and Garvin 2016; Dereli et al. 2018) and to test the applicability of 3D surfaces to the broader context of this method for South African populations. The analysis of all five traits would also allow testing for the possible personal affinity for assessing 3D surfaces. This would result in deeper knowledge on whether observers should evaluate their personal affinity before applying the method to scans of unknown parameters.

As ancestry, sexual dimorphism, ageing and size were shape-influencing factors in the bony chin, the correlation between the hard- and soft-tissue shapes of the chin could be studied. If the soft-tissue chin shape was also influenced by ancestry, sex, age and size, an automated 3D approximation of the chin could be attempted, similar to that of the nasal shape (Ridel et al. 2018). This could enable forensic anthropologists in South Africa to reliably estimate the lower part of the face for the purpose of victim identification. In the wider sense, the shape of the lower part of the face (chin and mouth) could be analysed; this would also include the quantification of prognathism shown in Figure 4.4. Furthermore, other South African population groups could be investigated in connection with chin shape variation.

As is true for any study, the validity of the results could possibly be limited by the sample composition. Only persons presenting for medical reasons at the Oral and Dental Hospital, University of Pretoria, were included, making this a random study sample of patients with a medical condition. However, patients with distorting conditions were excluded. The outcomes of this study might be applicable only in a local geographical context but are not inhibited by anatomically distorting features. In order to apply the findings to a broader population, further studies might be needed.

CHAPTER 7 REFERENCES

Acsádi, G. and Nemeskéri, J. 1970. *History of human life span and mortality.* Budapest: Akadémiai Kiadó.

Adams, D., Collyer, M. and Sherratt, E. 2018. A Geometric Morphometric Analysis of 2D/3D Landmark Data. R package 'geomorph'. Viewed 28 October 2019: https://www.semanticscholar.org/paper/Title-Geometric-Morphometric-Analyses-of-2d%2F3d-Data-Adams-Collyer/42956016973181d2d3dabdbacc82c418f6dc2a95.

Allam, E., Mpofu, P., Ghoneima, A., Tuceryan, M. and Kula, K. 2018. The Relationship Between Hard Tissue and Soft Tissue Dimensions of the Nose in Children: A 3D Cone Beam Computed Tomography Study. *Journal of Forensic Sciences* 63(6), pp. 1652–1660. doi: 10.1111/1556-4029.13801.

Barreto, F.S. and Avise, J.C. 2011. The genetic mating system of a sea spider with male-biased sexual size dimorphism: evidence for paternity skew despite random mating success. *Behavioral Ecology and Sociobiology* 65(8), pp. 1595–1604. doi: 10.1007/s00265-011-1170-x.

Becker, M.J. 1986. Mandibular symphysis (medial suture) closure in modernHomo sapiens: Preliminary evidence from archaeological populations. *American Journal of Physical Anthropology* 69(4), pp. 499–501. doi: 10.1002/ajpa.1330690409.

Bejdová, Š., Krajíček, V., Velemínská, J., Horák, M. and Velemínský, P. 2013. Changes in the sexual dimorphism of the human mandible during the last 1200 years in Central Europe. *HOMO* 64(6), pp. 437–453. doi: 10.1016/j.jchb.2013.05.003.

Berkelaar, M. et al. 2019. *Package 'lpSolve', version 5.6.13.3*. Available at: https://CRAN.R-project.org/package=lpSolve [Accessed: 4 October 2019].

Bermejo-Fenoll, A., Panchón-Ruíz, A. and Sánchez del Campo, F. 2019. Homo sapiens, Chimpanzees and the Enigma of Language. *Frontiers in Neuroscience* 13, pp. 558. doi: 10.3389/fnins.2019.00558.

Bertl, M.H., Bertl, K., Wagner, M., Gahleitner, A., Stavropoulos, A., Ulm, C. and Mitteroecker, P. 2016. Second premolar agenesis is associated with mandibular form: a geometric morphometric analysis of mandibular cross-sections. *International Journal of Oral Science* 8(4), pp. 254–260. doi: 10.1038/ijos.2016.41.

Blasi, D.E., Moran, S., Moisik, S.R., Widmer, P., Dediu, D. and Bickel, B. 2019. Human sound systems are shaped by post-Neolithic changes in bite configuration. *Science* 363(6432), pp. eaav3218. doi: 10.1126/science.aav3218.

Bloom, J. 2015. *1272 Unidentified Bodies in Gauteng Mortuaries in 2014/2015*. Available at: http://www.politicsweb.co.za/politics/1272-unidentified-bodies-in-gauteng-mortuaries-in-. [Accessed: 8 February 2019].

Bloom, J. 2019. *1117 Unidentified Bodies in Gauteng Mortuaries.* Available at: https://www.politicsweb.co.za/news-and-analysis/1117-unidentified-bodies-in-gauteng-mortuaries--ja. [Accessed: 7 February 2020].

Borelli, C. and Berneburg, M. 2009. "Beauty lies in the eye of the beholder"? Aspects of beauty and attractiveness. *Journal der Deutschen Dermatologischen Gesellschaft* 8(5), pp. 326–330. doi: 10.1111/j.1610-0387.2009.07318.x.

Bookstein, F.L. 1991. *Morphometric tools for landmark data: geometry and biology*. Cambridge: Cambridge University Press.

Braun, S., Thackeray, J.F. and Loots, M. 2004. A morphometric technique to assess probabilities of conspecificity in extant primates and Plio-Pleistocene hominids. *Annals of the Transvaal Museum* 41, pp. 93-95.

Bruzek, J. 2002. A method for visual determination of sex, using the human hip bone. *American Journal of Physical Anthropology* 117(2), pp. 157–168. doi: 10.1002/ajpa.10012.

Bucca, C., Cicolin, A., Brussino, L., Arienti, A., Graziano, A., Erovigni, F., Pera, P., Gai, V., Mutani, R., Preti, G., Rolla, G. and Carossa, S. 2006. Tooth loss and obstructive sleep apnoea. *Respiratory Research* 7(1), pp. 8. doi: 10.1186/1465-9921-7-8.

Buikstra, J. and Ubelaker, D. 1994. Standards for Data Collection from Human Skeletal Remains: Proceedings of a Seminar at the Field Museum of Natural History. *Arkansas Archaeology Research Series* 44. Fayetteville, Arkansas Archaeological Survey.

Byrnes, J.F., Kenyhercz, M.W. and Berg, G.E. 2017. Examining Interobserver Reliability of Metric and Morphoscopic Characteristics of the Mandible. *Journal of Forensic Sciences* 62(4), pp. 981–985. doi: 10.1111/1556-4029.13349.

Caple, J. and Stephan, C.N. 2016. A standardized nomenclature for craniofacial and facial anthropometry. *International Journal of Legal Medicine* 130(3), pp. 863–879. doi: 10.1007/s00414-015-1292-1.

Chou, H.-Y., Satpute, D., Müftü, A., Mukundan, S. and Müftü, S. 2015. Influence of mastication and edentulism on mandibular bone density. *Computer Methods in Biomechanics and Biomedical Engineering* 18(3), pp. 269–281. doi: 10.1080/10255842.2013.792916.

Ciochon, R.L., Nisbett, R.A. and Corruccini, R.S. 1997. Dietary consistency and craniofacial development related to masticatory function in minipigs. *Journal of Craniofacial Genetics and Developmental Biology* 17(2), pp. 96–102.

Church, M.S. 1995. Determination of Race from the Skeleton through Forensic Anthropological Methods. *Forensic Science Review* 7(1), pp. 1-39.

Claes, P. 2007. *A robust statistical surface registration framework using implicit function representations. Application in craniofacial reconstruction.* PhD Thesis, Katholieke Universiteit Leuven.

Claes, P., Walters, M., Shriver, M.D., Puts, D., Gibson, G., Clement, J., Baynam, G., Verbeke, G., Vandermeulen, D. and Suetens, P. 2012. Sexual dimorphism in multiple aspects of 3D facial symmetry and asymmetry defined by spatially dense geometric morphometrics: Spatially dense sexual dimorphism in 3D facial shape. *Journal of Anatomy* 221(2), pp. 97–114. doi: 10.1111/j.1469-7580.2012.01528.x.

Coquerelle, M., Bookstein, F.L., Braga, J., Halazonetis, D.J., Weber, G.W. and Mitteroecker, P. 2011. Sexual dimorphism of the human mandible and its association with dental development. *American Journal of Physical Anthropology* 145(2), pp. 192–202. doi: 10.1002/ajpa.21485.

Coquerelle, M., Prados-Frutos, J.C., Benazzi, S., Bookstein, F.L., Senck, S., Mitteroecker, P. and Weber, G.W. 2013a. Infant growth patterns of the mandible in modern humans: a closer exploration of the developmental interactions between the symphyseal bone, the teeth, and the suprahyoid and tongue muscle insertion sites. *Journal of Anatomy* 222(2), pp. 178–192. doi: 10.1111/joa.12008.

Coquerelle, M., Prados-Frutos, J.C., Rojo, R., Mitteroecker, P. and Bastir, M. 2013b. Short Faces, Big Tongues: Developmental Origin of the Human Chin. Frayer, D. ed. *PLoS ONE* 8(11), pp. e81287. doi: 10.1371/journal.pone.0081287.

Coquerelle, M., Prados-Frutos, J.C., Rojo, R., Drake, A.G., Murillo-Gonzalez, J.A. and Mitteroecker, P. 2017. The Fetal Origin of the Human Chin. *Evolutionary Biology* 44(3), pp. 295–311. doi: 10.1007/s11692-017-9408-9.

von Cramon-Taubadel, N. 2011. Global human mandibular variation reflects differences in agricultural and hunter-gatherer subsistence strategies. *Proceedings of the National Academy of Sciences* 108(49), pp. 19546–19551. doi: 10.1073/pnas.1113050108.

Cummaudo, M., Guerzoni, M., Marasciuolo, L., Gibelli, D., Cigada, A., Obertovà, Z., Ratnayake, M., Poppa, P., Gabriel, P., Ritz-Timme, S. and Cattaneo, C. 2013. Pitfalls at the root of facial assessment on photographs: a quantitative study of accuracy in positioning facial landmarks. *International Journal of Legal Medicine* 127(3), pp. 699–706. doi: 10.1007/s00414-013-0850-7.

Darwin, C. 1871. *The Descent of Man and Selection in Relation to Sex.* New York: D. Appleton.

De Villiers, H. 1968. *The Skull of the South African Negro: a biometrical and morphometrical study*. Johannesburg: Witwatersrand University Press.

De Vos, W., Casselman, J. and Swennen, G.R.J. 2009. Cone-beam computerized tomography (CBCT) imaging of the oral and maxillofacial region: A systematic review of the literature. *International Journal of Oral and Maxillofacial Surgery* 38(6), pp. 609–625. doi: 10.1016/j.ijom.2009.02.028.

Dereli, A.K., Zeybek, V., Sagtas, E., Senol, H., Ozgul, H.A. and Acar, K. 2018. Sex determination with morphological characteristics of the skull by using 3D modeling techniques in computerized tomography. *Forensic Science, Medicine and Pathology* 14(4), pp. 450–459. doi: 10.1007/s12024-018-0029-0.

Dorfling, H.F., Lockhat, Z., Pretorius, S., Steyn, M. and Oettlé, A.C. 2018. Facial approximations: Characteristics of the eye in a South African sample. *Forensic Science International* 286, pp. 46–53. doi: 10.1016/j.forsciint.2018.02.029.

Dryden, I.L. and Mardia, K.V. 2016. *Statistical shape analysis: with applications in R*. John Wiley & Sons.

DuBrul, L.E. and Sicher, H. 1954. *The Adaptive Chin*. Springfield: Charles.

Eichner, K. 1955. Über eine Gruppeneinteilung des Lückengebisses für die Prothetik. *Deutsche Zahnärztliche Zeitschrift* 10, pp. 1831-1834.

Ekizoglu, O., Inci, E., Hocaoglu, E., Sayin, I., Kayhan, F. and Can, I. 2014. The Use of Maxillary Sinus Dimensions in Gender Determination: A Thin-Slice Multidetector Computed Tomography Assisted Morphometric Study. *Journal of Craniofacial Surgery* 25(3), pp. 957–960. doi: 10.1097/SCS.0000000000000734.

Enlow, D.H., Biano, H.J. and Eklund, S. 1976. The remodeling of the edentulous mandible. *The Journal of Prosthetic Dentistry* 36, pp. 685-693.

Enlow, D.H. 1990. *Facial Growth, 3rd ed*. Philadelphia: Saunders.

Fazekas, I.G. and Kósa, F. 1978. *Forensic Fetal Osteology*. Budapest: Akadémiai Kiadó.

Fleiss, J.L. 1971. Measuring nominal scale agreement among many raters. *Psychological Bulletin* 76(5), pp. 378–382. doi: 10.1037/h0031619.

Franklin, D., Oxnard, C.E., O'Higgins, P. and Dadour, I. 2007. Sexual Dimorphism in the Subadult Mandible: Quantification Using Geometric Morphometrics. *Journal of Forensic Sciences* 52(1), pp. 6–10. doi: 10.1111/j.1556-4029.2006.00311.x.

Franklin, D., Cardini, A., Flavel, A. and Kuliukas, A. 2013. Estimation of sex from cranial measurements in a Western Australian population. *Forensic Science International* 229(1–3), pp. 158.e1-158.e8. doi: 10.1016/j.forsciint.2013.03.005.

Fukase, H. and Suwa, G. 2008. Growth-related changes in prehistoric Jomon and modern Japanese mandibles with emphasis on cortical bone distribution. *American Journal of Physical Anthropology* 136(4), pp. 441–454. doi: 10.1002/ajpa.20828.

Fully, G. 1956. Une nouvelle méthode de détermination de la taille. *Annales de Médecine Légale* 36, pp. 266-273.

Gamer, M., Lemon, J., Fellows, I. and Singh, P. 2019. *Package 'irr', version 0.84.1*. Available at: https://CRAN.R-project.org/package=irr [Accessed: 4 October 2019].

Garvin, H.M. and Ruff, C.B. 2012. Sexual dimorphism in skeletal browridge and chin morphologies determined using a new quantitative method. *American Journal of Physical Anthropology* 147(4), pp. 661–670. doi: 10.1002/ajpa.22036.

Garvin, H.M. and Stock, M.K. 2016. The Utility of Advanced Imaging in Forensic Anthropology. *Academic Forensic Pathology* 6(3), pp. 499–516. doi: 10.23907/2016.050.

George, R. 1993. Anatomical and artistic guidelines for forensic facial reconstruction. In: İşcan, M.Y. and Helmer, R. (eds.) *Forensic Analysis of the Skull.* New York: Wiley-Liss, Inc.

Gerasimov, M.M. 1971. *Face Finder*. New York: CRC Press.

Gilbert, S.F. 2000. Chromosomal Sex Determination. In: Gilbert, S.F. (ed.) *Developmental Biology, 6th ed*. Sunderland: Sinauer Associates.

Goodall, C. 1991. Procrustes Methods in the Statistical Analysis of Shape. J*ournal of the Royal Statistical Society, B Series* 53(2), pp. 285-339.

Gould, S.J. 1977. *Ontogeny and Phylogeny*. Cambridge, MA: The Belknap Press of Harvard University Press.

Grabherr, S., Cooper, C., Ulrich-Bochsler, S., Uldin, T., Ross, S., Oesterhelweg, L., Bolliger, S., Christe, A., Schnyder, P., Mangin, P. and Thali, M.J. 2009. Estimation of sex and age of "virtual skeletons"–a feasibility study. *European Radiology* 19(2), pp. 419–429. doi: 10.1007/s00330-008-1155-y.

Grammer, K., Fink, B., Møller, A.P. and Thornhill, R. 2003. Darwinian aesthetics: sexual selection and the biology of beauty. *Biological Reviews* 78(3), pp. 385–407. doi: 10.1017/S1464793102006085.

Grammer, K. and Thornhill, R. 1994. Human (Homo sapiens) facial attractiveness and sexual selection: The role of symmetry and averageness. *Journal of Comparative Psychology* 108(3), pp. 233–242. doi: 10.1037/0735-7036.108.3.233.

Guo, Y., Yan, C., Lin, X., Zhou, H., Pan, F., Wei, L., Tang, Z., Liang, F. and Chen, T. 2014. Studies of the chronological course of third molars eruption in a northern Chinese population. *Archives of Oral Biology* 59(9), pp. 906–911. doi: 10.1016/j.archoralbio.2014.05.018.

Guyomarc'h, P., Dutailly, B., Charton, J., Santos, F., Desbarats, P. and Coqueugniot, H. 2014. Anthropological Facial Approximation in Three Dimensions (AFA3D): Computer-Assisted Estimation of the Facial Morphology Using Geometric Morphometrics. *Journal of Forensic Sciences* 59(6), pp. 1502–1516. doi: 10.1111/1556-4029.12547.

Hefner, J.T. and Ousley, S.D. 2014. Statistical Classification Methods for Estimating Ancestry Using Morphoscopic Traits. *Journal of Forensic Sciences* 59(4), pp. 883–890. doi: 10.1111/1556-4029.12421.

Hennessy, R.J., Kinsella, A. and Waddington, J.L. 2002. 3D laser surface scanning and geometric morphometric analysis of craniofacial shape as an index of cerebro-craniofacial morphogenesis: initial application to sexual dimorphism. *Biological Psychiatry* 51(6), pp. 507–514. doi: 10.1016/S0006-3223(01)01327-0.

Hennessy, R.J. and Stringer, C.B. 2002. Geometric morphometric study of the regional variation of modern human craniofacial form. *American Journal of Physical Anthropology* 117(1), pp. 37–48. doi: 10.1002/ajpa.10005.

Hershkovitz, P. 1970. The decorative chin. *Bulletin of the Field Museum of Natural History* 41, pp. 6–10.

Hiiemae, K.M. and Palmer, J.B. 2003. Tongue movements in feeding and speech. *Critical Reviews in Oral Biology & Medicine* 14(6), pp. 413–429. doi: 10.1177/154411130301400604.

Hoffman, J.W. and De Beer, F. 2012. *Characteristics of the Micro-Focus X-Ray Tomography Facility (MIXRAD) at Necsa in South Africa*. Paper presented at the 18th World Conference on Nondestructive Testing, 16-20 April 2012 in Durban, South Africa. Available at: https://www.ndt.net/article/wcndt2012/papers/37_wcndtfinal00037.pdf [Accessed: 27 August 2019].

Holmes, M.A. and Ruff, C.B. 2011. Dietary effects on development of the human mandibular corpus. *American Journal of Physical Anthropology* 145(4), pp. 615–628. doi: 10.1002/ajpa.21554.

Holton, N.E., Bonner, L.L., Scott, J.E., Marshall, S.D., Franciscus, R.G. and Southard, T.E. 2015. The ontogeny of the chin: an analysis of allometric and biomechanical scaling. *Journal of Anatomy* 226(6), pp. 549–559. doi: 10.1111/joa.12307.

Howells, W.W. 1937. The designation of the principle anthrometric landmarks on the head and skull. *American Journal of Physical Anthropology* 22, pp. 477–494.

Howells, W.W. 1973. *Cranial variation in man: a study by multivariate analysis of patterns of difference among recent human populations.* Cambridge: Harvard University Press.

Hrdlička, A. 1911. Human dentition and teeth from the evolutionary and racial standpoint. *Dominion Dental Journal*, 1-15.

Hutchinson, E.F. 2011. *An Assessment of Growth and Sex from Mandibles of Cadaver Foetuses and Newborns*. MSc dissertation, University of Pretoria.

Hutchinson, E.F., L'Abbé, E.N. and Oettlé, A.C. 2012. An assessment of early mandibular growth. *Forensic Science International* 217(1–3), pp. 233.e1-233.e6. doi: 10.1016/j.forsciint.2011.11.014.

Hutchinson, E.F., Farella, M. and Kramer, B. 2015. Importance of teeth in maintaining the morphology of the adult mandible in humans. *European Journal of Oral Sciences* 123(5), pp. 341–349. doi: 10.1111/eos.12203.

Hylander, W.L. 1985. Mandibular Function and Biomechanical Stress and Scaling. *American Zoologist* 25, pp. 315-330.

Ichim, I., Kieser, J. and Swain M. 2007. Tongue contractions during speech may have led to the development of the bony geometry of the chin following the evolution of human language: A mechanobiological hypothesis for the development of the human chin. *Medical Hypotheses* 69(1), pp. 20–24. doi: 10.1016/j.mehy.2006.11.048.

Ikebe, K., Matsuda, K., Murai, S., Maeda, Y. and Nokubi, T. 2010. Validation of the Eichner index in relation to occlusal force and masticatory performance. *The International Journal of Prosthodontics* 23(6), pp. 521–524.

Irish, J.D. and Scott, G.R. eds. 2016. *A companion to dental anthropology*. Chichester, UK ; Malden, MA: John Wiley & Sons.

İşcan, M.Y., Loth, S.R. and Wright, R.K. 1984. Metamorphosis at the sternal rib end: A new method to estimate age at death in white males. *American Journal of Physical Anthropology* 65(2), pp. 147–156. doi: 10.1002/ajpa.1330650206.

İşcan, M.Y. and Steyn, M. 1999. Craniometric determination of population affinity in South Africans. *International Journal of Legal Medicine* 112(2), pp. 91-97.

İşcan, M.Y. and Steyn, M. 2013. *The human skeleton in forensic medicine*. Third edition. Springfield, Illinois, U.S.A: Charles C Thomas Publisher, LTD.

Jantz, R.L. and Ousley, S. 2005. *FORDISC 3.1 Personal Computer Forensic Discriminant Functions*. Available at: https://fac.utk.edu/fordisc-3-1-personal-computer-forensic-discriminant-functions/ [Accessed: 31 October 2019].

Jensen, E. and Palling, M. 1954. The gonial angle: A Survey. *American Journal of Orthodontics* 40, pp 120-133.

Jindal, G. 2015. Rare Enlargement of Genial Tubercles and its Management: A Case Report. *Journal of Clinical and Diagnostic Research*. Available at: http://jcdr.net/article_fulltext.asp?issn=0973-709x&year=2015&volume=9&issue=11&page=ZD23&issn=0973-709x&id=6827 [Accessed: 26 February 2020].

Kamburoğlu, K., Kolsuz, E., Kurt, H., Kılıç, C., Özen, T. and Paksoy, C.S. 2011. Accuracy of CBCT Measurements of a Human Skull. *Journal of Digital Imaging* 24(5), pp. 787–793. doi: 10.1007/s10278-010-9339-9.

Kendall, D.G. 1977. The diffusion of shape. *Advances in Applied Probability* 9, pp. 428-430.

Kendall, D.G. 1984. Shape Manifolds, Procrustean Metrics, and Complex Projective Spaces. *Bulletin of the London Mathematical Society* 16(2), pp. 81–121. doi: 10.1112/blms/16.2.81.

Kingsmill, V.J. 1999. Post-Extraction Remodeling of the Adult Mandible. *Critical Reviews in Oral Biology & Medicine* 10(3), pp. 384–404. doi: 10.1177/10454411990100030801.

Klales, A.R., Ousley, S.D. and Vollner, J.M. 2012. A revised method of sexing the human innominate using Phenice's nonmetric traits and statistical methods. *American Journal of Physical Anthropology* 149(1), pp. 104–114. doi: 10.1002/ajpa.22102.

Klingenberg, C.P. and McIntyre, G.S. 1998. Geometric morphometrics of developmental instability: analyzing patterns of fluctuating asymmetry with Procrustes methods. *Evolution* 52(5), pp. 1363-1375.

Klingenberg, C.P., Barluenga, M. and Meyer, A. 2002. Shape analysis of symmetric structures: quantifying variation among individuals and asymmetry. *Evolution* 56(10), pp. 1909–1920. doi: 10.1111/j.0014-3820.2002.tb00117.x.

Klingenberg, C.P. 2016. Size, shape, and form: concepts of allometry in geometric morphometrics. *Development Genes and Evolution* 226(3), pp. 113–137. doi: 10.1007/s00427-016-0539-2.

Krogman, W. and Sassouni, V. 1957. *A syllabus in roentgenographic cephalometry*. Philadelphia: Center for Research in Child Growth.

Krogstad, O. and Dahl, B.L. 1985. Dento-facial morphology in patients with advanced attrition. *The European Journal of Orthodontics* 7(1), pp. 57–62. doi: 10.1093/ejo/7.1.57.

Krüger, G.C., L'Abbé, E.N., Stull, K.E. and Kenyhercz, M.W. 2015. Sexual dimorphism in cranial morphology among modern South Africans. *International Journal of Legal Medicine* 129(4), pp. 869–875. doi: 10.1007/s00414-014-1111-0.

Krüger, G.C., Liebenberg, L., Myburgh, J., Meyer, A., Oettlé, A.C., Botha, D., Brits, D.M., Kenyhercz, M.W., Stull, K.E., Sutherland, C. and L'Abbé, E.N. 2018. Forensic Anthropology and the Biological Profile in South Africa. In: *New Perspectives in Forensic Human Skeletal Identification*. Elsevier, pp. 313–321. Available at: https://linkinghub.elsevier.com/retrieve/pii/B9780128054291000272 [Accessed: 19 June 2019].

Kuć, J., Sierpinska, T. and Golebiewska, M. 2015. The relationship between facial morphology and the structure of the alveolar part of the mandible in edentulous complete denture wearers. A preliminary study. *Acta Odontologica Scandinavica* 73(1), pp. 57–66. doi: 10.3109/00016357.2014.950181.

L'Abbé, E.N., Loots, M. and Meiring, J.H. 2005. The Pretoria Bone Collection: A modern South African skeletal sample. *HOMO* 56(2), pp. 197–205. doi: 10.1016/j.jchb.2004.10.004.

L'Abbé, E.N., Van Rooyen, C., Nawrocki, S.P. and Becker, P.J. 2011. An evaluation of non-metric cranial traits used to estimate ancestry in a South African sample. *Forensic Science International* 209(1–3), pp. 195.e1-195.e7. doi: 10.1016/j.forsciint.2011.04.002.

L'Abbé, E.N., Kenyhercz, M., Stull, K.E., Keough, N. and Nawrocki, S. 2013. Application of Fordisc 3.0 to Explore Differences Among Crania of North American and South African Blacks and Whites. *Journal of Forensic Sciences* 58(6), pp. 1579–1583. doi: 10.1111/1556-4029.12198.

Lagravère, M.O., Low, C., Flores-Mir, C., Chung, R., Carey, J.P., Heo, G. and Major, P.W. 2010. Intraexaminer and interexaminer reliabilities of landmark identification on digitized lateral cephalograms and formatted 3-dimensional cone-beam computerized tomography images. *American Journal of Orthodontics and Dentofacial Orthopedics* 137(5), pp. 598–604. doi: 10.1016/j.ajodo.2008.07.018.

Landis, J.R. and Koch, G.G. 1977. The measurement of observer agreement for categorical data. *Biometrics* 33(1), pp. 159–174.

Langsrud, O. 2002. 50-50 multivariate analysis of variance for collinear responses. *Journal of the Royal Statistical Society: Series D (The Statistician)* 51(3), pp. 305–317. doi: 10.1111/1467-9884.00320.

Langsrud, Ø., Jørgensen, K., Ofstad, R. and Næs, T. 2007. Analyzing Designed Experiments with Multiple Responses. *Journal of Applied Statistics* 34(10), pp. 1275–1296. doi: 10.1080/02664760701594246.

Langsrud, Ø. and Mevik, B.H. 2012. *ffmanova: Fifty-Fifty MANOVA*. Available at: http://CRAN. Rproject. org/package= ffmanova [Accessed: 2 May 2019].

Larsen, C.S. 2003. Equality for the sexes in human evolution? Early hominid sexual dimorphism and implications for mating systems and social behavior. *Proceedings of the National Academy of Sciences* 100(16), pp. 9103–9104. doi: 10.1073/pnas.1633678100.

Lewis, C.J. and Garvin, H.M. 2016. Reliability of the Walker Cranial Nonmetric Method and Implications for Sex Estimation. *Journal of Forensic Sciences* 61(3), pp. 743–751. doi: 10.1111/1556-4029.13013.

Liddell, T. and Kruschke, J.K. 2017. *Analyzing ordinal data with metric models: What could possibly go wrong?* Open Science Framework. Available at: https://osf.io/9h3et [Accessed: 14 November 2019].

Lieberman, D.E., McCarthy, R.C., Hiiemae, K.M. and Palmer, J.B. 2001. Ontogeny of postnatal hyoid and larynx descent in humans. *Archives of Oral Biology* 46(2), pp. 117–128. doi: 10.1016/S0003-9969(00)00108-4.

Liversidge, H.M. 2016. Tooth Eruption and Timing. In: Irish, J.D. and Scott, G.R. eds. *A Companion to Dental Anthropology*. Chichester: John Wiley & Sons, pp. 159-171.

Loth, S.R. and Henneberg, M. 1996. Mandibular Ramus Flexure: A new morphologic indicator of sexual dimorphism in the human skeleton. *American Journal of Physical Anthropology* 99, pp. 473-485.

Loth, S.R. and Henneberg, M. 2000. Gonial eversion: facial architecture, not sex. *HOMO* 51, pp. 81-89.

Loth, S.R. and Henneberg, M. 2001. Sexually dimorphic mandibular morphology in the first few years of life. *American Journal of Physical Anthropology* 115(2), pp. 179–186. doi: 10.1002/ajpa.1067.

Luther, F. 1993. A cephalometric comparison of medieval skulls with a modern population. *The European Journal of Orthodontics* 15(4), pp. 315–325. doi: 10.1093/ejo/15.4.315.

Maat, G.J.R., Mastwijk, R.W. and Van Der Velde, E.A. 1997. On the Reliability of Non-metrical Morphological Sex Determination of the Skull Compared with that of the Pelvis in The Low Countries. *International Journal of Osteoarchaeology* 7, pp. 575-580.

MacCurdy, G.G. 1912. International congress of prehistoric anthropology and archaeology. *Science* 36, pp. 603-608.

Marklein, K.E., Torres, Rouff, C., King, L.M. and Hubbe, M. 2019. The Precarious State of Subsistence: Reevaluating Dental Pathological Lesions Associated with Agricultural and Hunter-Gatherer Lifeways. *Current Anthropology* 60(3), pp. 341–368. doi: 10.1086/703376.

Martin, R. 1928. *Lehrbuch der Anthropologie in systematischer Darstellung: mit besonderer Berücksichtigung der anthropologischen Methoden für Studierende, Ärzte und Forschungsreisende.* Stuttgart: Gustav Fischer.

Martin, R. and Knussmann, R. 1988. *Anthropologie: Handbuch der vergleichenden Biologie des Menschen.* Stuttgart: Gustav Fischer.

Martinez-Maza, C., Rosas, A. and Nieto-Díaz, M. 2013. Postnatal changes in the growth dynamics of the human face revealed from bone modelling patterns. *Journal of Anatomy* 223(3), pp. 228–241. doi: 10.1111/joa.12075.

McDowell, J.L., L'Abbé, E.N. and Kenyhercz, M.W. 2012. Nasal aperture shape evaluation between black and white South Africans. *Forensic Science International* 222(1–3), pp. 397.e1-397.e6. doi: 10.1016/j.forsciint.2012.06.007.

Miloro, M., Borba, A.M., Ribeiro-Junior, O., Naclério-Homem, M.G. and Jungner, M. 2014. Is there consistency in cephalometric landmark identification amongst oral and maxillofacial surgeons? *International Journal of Oral and Maxillofacial Surgery* 43(4), pp. 445–453. doi: 10.1016/j.ijom.2013.08.007.

Mitteroecker, P. and Gunz, P. 2009. Advances in Geometric Morphometrics. *Evolutionary Biology* 36(2), pp. 235–247. doi: 10.1007/s11692-009-9055-x.

Morelli, D.L., Jackson, N., Gislason, T., Arnardottir, E.S., Benediktsdottir, B., Juliusson, S., Thorarinsson, G.H., Maislin, G., Kim, C. and Schwab, R. 2011. The Effects of Edentulism on Ahi, Odi, and Tongue Morphology in Iceland Sleep Apnea Cohort (isac). *American Journal of Respiratory and Critical Care Medicine*, 183:A3676.

Munn, L. and Stephan, C.N. 2018. Changes in face topography from supine-to-upright position—And soft tissue correction values for craniofacial identification. *Forensic Science International* 289, pp. 40–50. doi: 10.1016/j.forsciint.2018.05.016.

Nagasaka, S. 2003. Development of a non-radiographic cephalometric system. *The European Journal of Orthodontics* 25(1), pp. 77–85. doi: 10.1093/ejo/25.1.77.

Nakhaeizadeh, S., Dror, I.E. and Morgan, R.M. 2014. Cognitive bias in forensic anthropology: Visual assessment of skeletal remains is susceptible to confirmation bias. *Science & Justice* 54(3), pp. 208–214. doi: 10.1016/j.scijus.2013.11.003.

Netter, F.H. 2014. *Atlas of human anatomy*. Sixth edition. Philadelphia, PA: Saunders/Elsevier.

Noback, M.L. and Harvati, K. 2015. The contribution of subsistence to global human cranial variation. *Journal of Human Evolution* 80, pp. 34–50. doi: 10.1016/j.jhevol.2014.11.005.

Noble, J., Cardini, A., Flavel, A. and Franklin, D. 2019. Geometric morphometrics on juvenile crania: Exploring age and sex variation in an Australian population. *Forensic Science International* 294, pp. 57–68. doi: 10.1016/j.forsciint.2018.10.022.

Nuzzolese, E., Randolph-Quinney, P., Randolph-Quinney, J. and Di Vella, G. 2019. Geometric morphometric analysis of sexual dimorphism in the mandible from panoramic X-ray images. *The Journal of Forensic Odonto-Stomatology* 2(37), pp. 35–44.

Oettlé, A.C., Pretorius, E. and Steyn, M. 2005. Geometric morphometric analysis of mandibular ramus flexure. *American Journal of Physical Anthropology* 128(3), pp. 623–629. doi: 10.1002/ajpa.20207.

Oettlé, A.C., Pretorius, E. and Steyn, M. 2009a. Geometric morphometric analysis of the use of mandibular gonial eversion in sex determination. *HOMO* 60(1), pp. 29–43. doi: 10.1016/j.jchb.2007.01.003.

Oettlé, A.C., Becker, P.J., de Villiers, E. and Steyn, M. 2009b. The influence of age, sex, population group, and dentition on the mandibular angle as measured on a South African sample. *American Journal of Physical Anthropology* 139(4), pp. 505–511. doi: 10.1002/ajpa.21009.

Oettlé, A.C. 2014. *Effects of dental loss and senescence on aspects of adult mandibular morphology in South Africans*. PhD Thesis, University of Pretoria.

Oettlé, A.C., Demeter, F.P. and L'Abbé, E.N. 2017. Ancestral Variations in the Shape and Size of the Zygoma. *The Anatomical Record* 300(1), pp. 196–208. doi: 10.1002/ar.23469.

Otieno, G., Marinda, E., Bärnighausen, T. and Tanser, F. 2015. High rates of homicide in a rural South African population (2000–2008): findings from a population-based cohort study. *Population Health Metrics* 13(1), pp. 20. doi: 10.1186/s12963-015-0054-0.

Ousley, S. and Jantz, R.L. 1996. *FORDISC 2.0 personal computer forensic discriminant functions*. Knoxville: Forensic Anthropology Centre, University of Tennessee.

Ousley, S., Jantz, R., and Freid, D. 2009. Understanding race and human variation: why forensic anthropologists are good at identifying race. *American Journal of Physical Anthropology* 139, pp. 68-76.

Papillault, G. 1906. Entente internationale pour l'unification des mesures craniométriques et céphalométriques. *L'Anthropologie* 17, pp. 559-572.

Papillault, G. 1919. The international agreement for the unification of craniometric and cephalometric measurements. *American Journal of Physical Anthropology* 2, pp. 46-60.

Parr, N.M. 2005. *Determination of Ancestry from Discrete Traits of the Mandible*. MSc Dissertation, University of Indianapolis.

Parr, N.M., Passalacqua, N.V. and Skorpinski, K. 2017. Investigations Into Age-related Changes in the Human Mandible. *Journal of Forensic Sciences* 62(6), pp. 1586–1591. doi: 10.1111/1556-4029.13475.

Patriquin, M.L. 2013. *The relationship between masticatory stress and prognathism: a finite element and morphometric study*. PhD Thesis, University of Pretoria.

Pernter, P., Gostner, P., Egarter Vigl, E. and Rühli, F.J. 2007. Radiologic proof for the Iceman's cause of death (ca. 5'300BP). *Journal of Archaeological Science* 34(11), pp. 1784–1786. doi: 10.1016/j.jas.2006.12.019.

Phulari, B. 2013. *An atlas on cephalometric landmarks.* New Delhi: Jaypee Brothers Medical Publishers.

Potgieter, P.J., Monteith, B.D. and Kemp, P.L. 1983. The determination of free-way space in edentulous patients: a cephalometric approach. *Journal of Oral Rehabilitation* 10, pp. 283-293.

Pretorius, E., Steyn, M. and Scholtz, Y. 2006. Investigation into the usability of geometric morphometric analysis in assessment of sexual dimorphism. *American Journal of Physical Anthropology* 129(1), pp. 64–70. doi: 10.1002/ajpa.20251.

R Core Team. 2012. *R: a language and environment for statistical computing*. Vienna: Foundation for Statistical Computing. Available at: http://www.R-project.org [Accessed: 2 May 2019].

Ramsthaler, F., Kettner, M., Gehl, A. and Verhoff, M.A. 2010. Digital forensic osteology: Morphological sexing of skeletal remains using volume-rendered cranial CT scans. *Forensic Science International* 195(1–3), pp. 148–152. doi: 10.1016/j.forsciint.2009.12.010.

Reichs, K.J. 1986. *Forensic Osteology, Advances in the Identification of Human Remains*. Springfield: Charles C. Thomas.

Revelle, W. 2019. *Package 'psych', version 1.8.12*. Available at: https://cran.r-project.org/web/packages/psych/psych.pdf [Accessed: 4 October 2019].

Ridel, A.F., Demeter, F., Liebenberg, J., L'Abbé, E.N., Vandermeulen, D. and Oettlé, A.C. 2018. Skeletal dimensions as predictors for the shape of the nose in a South African sample: A cone-beam computed tomography (CBCT) study. *Forensic Science International* 289, pp. 18–26. doi: 10.1016/j.forsciint.2018.05.011.

Ridel, A.F. 2019. *An automated computer-assisted approximation of the nose in South Africans from CBCT (Cone Beam Computed Tomography)*. PhD Thesis, University of Pretoria.

Ridel, A.F., Demeter, F., Galland, M., L'Abbé, E.N., Vandermeulen, D. and Oettlé, A.C. 2020. Automatic landmarking as a convenient prerequisite for geometric morphometrics. Validation on cone beam computed tomography (CBCT)- based shape analysis of the nasal complex. *Forensic Science International* 306, pp. 1-10. doi: 10.1016/j.forsciint.2019.110095.

Rohlf, F.J. and Slice, D. 1990. Extensions of the Procrustes Method for the Optimal Superimposition of Landmarks. *Systematic Zoology* 39(1), pp. 40. doi: 10.2307/2992207.

Ronay, V., Miner, R.M., Will, L.A. and Arai, K. 2008. Mandibular arch form: The relationship between dental and basal anatomy. *American Journal of Orthodontics and Dentofacial Orthopedics* 134(3), pp. 430–438. doi: 10.1016/j.ajodo.2006.10.040.

Roosenboom, J., Indencleef, K., Lee, M.K., Hoskens, H., White, J.D., Liu, D., Hecht, J.T., Wehby, G.L., Moreno, L.M., Hodges-Simeon, C., Feingold, E., Marazita, M.L., Richmond, S., Shriver, M.D., Claes, P., Shaffer, J.R. and Weinberg, S.M. 2018. SNPs Associated With Testosterone Levels Influence Human Facial Morphology. *Frontiers in Genetics* 9, pp. 497. doi: 10.3389/fgene.2018.00497.

Scarfe, W.C., Farman, A.G. and Sukovic, P. 2006. Clinical applications of cone-beam computed tomography in dental practice. *Journal of the Canadian Dental Association* 72(1), pp. 75–80.

Scarfe, W.C., Azevedo, B., Toghyani, S. and Farman, A.G. 2017. Cone Beam Computed Tomographic imaging in orthodontics. *Australian Dental Journal* 62, pp. 33–50. doi: 10.1111/adj.12479.

Schaefer, M., Black, S. and Scheuer, L. 2009. *Juvenile osteology: a laboratory and field manual*. Amsterdam; Burlington, MA: Elsevier/Academic Press.

Schlager, S. 2013. *Morpho: Calculations and Visualisations Related to Geometric Morphometrics*. R package version 0.23, 3.

Schlager, S. and Rüdell, A. 2015. Analysis of the human osseous nasal shape-population differences and sexual dimorphism: Human Osseous Nasal Shape. *American Journal of Physical Anthropology* 157(4), pp. 571–581. doi: 10.1002/ajpa.22749.

Schwartz, J.H. and Tattersall, I. 2000. The human chin revisited: what is it and who has it? *Journal of Human Evolution* 38(3), pp. 367–409. doi: 10.1006/jhev.1999.0339.

Scrucca, L. 2000. Assessing Multivariate Normality through Interactive Dynamic Graphics. *Quaderni di Statistica* 2, pp. 221-240.

Seedat, M., Van Niekerk, A., Jewkes, R., Suffla, S. and Ratele, K. 2009. Violence and injuries in South Africa: prioritising an agenda for prevention. *The Lancet* 374(9694), pp. 1011–1022. doi: 10.1016/S0140-6736(09)60948-X.

Seiler, R., Öhrström, L.M., Eppenberger, P., Gascho, D., Rühli, F.J. and Galassi, F.M. 2019. The earliest known case of frontal sinus osteoma in man: The Earliest Case of Frontal Sinus Osteoma. *Clinical Anatomy* 32(1), pp. 105–109. doi: 10.1002/ca.23301.

Sella-Tunis, T., Pokhojaev, A., Sarig, R., O'Higgins, P. and May, H. 2018. Human mandibular shape is associated with masticatory muscle force. *Scientific Reports* 8(1), pp. 6042. doi: 10.1038/s41598-018-24293-3.

Shannon, J.L. 1972. The mentalis muscle in relation to edentulous mandibles. *The Journal of Prosthetic Dentistry* 27(5), pp. 477–484. doi: 10.1016/0022-3913(72)90259-4.

Sharma, K.S., Gong, H., Ghasemalizadeh, O., Yu, H., Wang, G. and Cao, G. 2014. Interior micro-CT with an offset detector: Interior micro-CT with an offset detector. *Medical Physics* 41(6Part1), pp. 061915. doi: 10.1118/1.4876724.

Sholts, S.B., Walker, P.L., Kuzimsky, S.C., Miller, K.W.P. and Wärmländer, S.K.T.S. 2011. Identification of Group Affinity from Cross-sectional Contours of the Human Midfacial Skeleton Using Digital Morphometrics and 3D Laser Scanning Technology. *Journal of Forensic Sciences* 56(2), pp. 333-338.

Short, L.J., Khambay, B., Ayoub, A., Erolin, C., Rynn, C. and Wilkinson, C. 2014. Validation of a computer modelled forensic facial reconstruction technique using CT data from live subjects: A pilot study. *Forensic Science International* 237, pp. 147.e1-147.e8. doi: 10.1016/j.forsciint.2013.12.042.

Slice, D.E. 2001. Landmark Coordinates Aligned by Procrustes Analysis Do Not Lie in Kendall's Shape Space. Olmstead, R. ed. *Systematic Biology* 50(1), pp. 141–149. doi: 10.1080/10635150119110.

Slice, D.E. 2007. Geometric Morphometrics. *Annual Review of Anthropology* 36(1), pp. 261–281. doi: 10.1146/annurev.anthro.34.081804.120613.

Snow, C.C., Gatliff, B.P. and McWilliams, K.R. 1970. Reconstruction of facial features from the skull: An evaluation of its usefulness in forensic anthropology. *American Journal of Physical Anthropology* 33(2), pp. 221–227. doi: 10.1002/ajpa.1330330207.

Snyders, J., Claes, P., Vandermeulen, D. and Suetens, P. 2014. *Development and comparison of non-rigid surface registration algorithms and extensions.* Technical report KUL/ESAT/PSI/1401, KU Leuven, ESAT, January 2014, Leuven, Belgium.

Spiros, M.C. and Hefner, J.T. 2019. Ancestry Estimation Using Cranial and Postcranial Macromorphoscopic Traits. *Journal of Forensic Sciences* 65(3), pp. 921-929. doi.org/10.1111/1556-4029.14231.

Spoor, C.F., Zonnefeld, F.W. and Macho, G.A. 1993. Linear measurements of cortical bone and dental enamel by computed tomography: Applications and problems. *American Journal of Physical Anthropology* 91(4), pp. 469–484. doi: 10.1002/ajpa.1330910405.

Spradley, M.K. 2016. Metric Methods for the Biological Profile in Forensic Anthropology: Sex, Ancestry, and Stature. *Academic Forensic Pathology* 6(3), pp. 391–399. doi: 10.23907/2016.040.

Standring, S. 2008. *Gray's Anatomy 40th ed*. Spain: Churchill Livingstone Elsevier.

Statistics South Africa, 2018/2019. *Statistical Release P0341 Victims of Crime. Governance, Public Safety and Justice Survey, GPSJS 2018/2019*. Available at: http://www.statssa.gov.za/publications/P0341/P03412018.pdf [Accessed: 30 October 2019].

Stephan, C.N., Henneberg, M. and Sampson, W. 2003. Predicting nose projection and pronasale position in facial approximation: A test of published methods and proposal of new guidelines. *American Journal of Physical Anthropology* 122(3), pp. 240–250. doi: 10.1002/ajpa.10300.

Stephan, C.N. and Davidson, P.L. 2008. The Placement of the Human Eyeball and Canthi in Craniofacial Identification. *Journal of Forensic Sciences* 53(3), pp. 612–619. doi: 10.1111/j.1556-4029.2008.00718.x.

Stock, M.K. 2018. A Preliminary Analysis of the Age of Full Expression of Sexually Dimorphic Cranial Traits. *Journal of Forensic Sciences* 63(6), pp. 1802–1808. doi: 10.1111/1556-4029.13780.

Stull, K.E., Kenyhercz, M.W. and L'Abbé, E.N. 2014. Ancestry estimation in South Africa using craniometrics and geometric morphometrics. *Forensic Science International* 245, pp. 206.e1-206.e7. doi: 10.1016/j.forsciint.2014.10.021.

Tallgren, A. and Tryde, G. 1992. Swallowing activity of lip muscles in patients with a complete upper and partial lower denture. *Journal of Oral Rehabilitation* 19, pp. 329-341.

Tallgren, A. 2003. The continuing reduction of the residual alveolar ridges in complete denture wearers: a mixed-longitudinal study covering 25 years. *The Journal of Prosthetic Dentistry* 89(5), pp. 427–435. doi: 10.1016/S0022-3913(03)00158-6.

Taylor, K.T. 2000. *Forensic Art and Illustration*. 0 ed. CRC Press. Available at: https://www.taylorfrancis.com/books/9781420036954 [Accessed: 2 April 2020].

Thackeray, J.F. and Dykes, S. 2016. Morphometric analyses of hominoid crania, probabilities of conspecificity and an approximation of a biological species constant. *HOMO* 67(1), pp. 1–10. doi: 10.1016/j.jchb.2015.09.003.

Thayer, Z.M. and Dobson, S.D. 2010. Sexual dimorphism in chin shape: Implications for adaptive hypotheses. *American Journal of Physical Anthropology* 143(3), pp. 417–425. doi: 10.1002/ajpa.21330.

Thornhill, R. and Gangestad, S.W. 1999. Facial attractiveness. *Trends in Cognitive Sciences* 3(12), pp. 452–460. doi: 10.1016/S1364-6613(99)01403-5.

Tobias, P.V. 1974. *The Biology of the South African Negro.* London and Boston: Routledge and Kegan Paul.

Todd, T.W. 1920. Age changes in the pubic bone: I. The male White pubis. *American Journal of Physical Anthropology* 3, pp. 285-334.

Toro-Ibacache, V., Ugarte, F., Morales, C., Eyquem, A., Aguilera, J. and Astudillo, W. 2019. Dental malocclusions are not just about small and weak bones: assessing the morphology of the mandible with cross-section analysis and geometric morphometrics. *Clinical Oral Investigations* 23(9), pp. 3479–3490. doi: 10.1007/s00784-018-2766-6.

Ubelaker, D.H. 1984. *Human Skeletal Remains.* Washington DC: Taraxacum.

Vanezis, P., Blowes, R.W., Linney, A.D., Tan, A.C., Richards, R. and Neave, R. 1989. Application of 3-D computer graphics for facial reconstruction and comparison with sculpting techniques. *Forensic Science International* 42(1–2), pp. 69–84. doi: 10.1016/0379-0738(89)90200-4.

Varrela, J. 1990. Effects of attritive diet on craniofacial morphology: a cephalometric analysis of a Finnish skull sample. *The European Journal of Orthodontics* 12(2), pp. 219–223. doi: 10.1093/ejo/12.2.219.

Villa, C. 2017. Forensic 3D documentation of skin injuries. *International Journal of Legal Medicine* 131(3), pp. 751–759. doi: 10.1007/s00414-016-1499-9.

Walker, P.L. 2008. Sexing skulls using discriminant function analysis of visually assessed traits. *American Journal of Physical Anthropology* 136(1), pp. 39–50. doi: 10.1002/ajpa.20776.

Wärmländer, S.K.T.S., Garvin, H., Guyomarc'h, P., Petaros, A. and Sholts, S.B. 2019. Landmark Typology in Applied Morphometrics Studies: What's the Point? *The Anatomical Record* 302(7), pp. 1144–1153. doi: 10.1002/ar.24005.

Weber, G.W. and Bookstein, F.L. 2011. *Virtual anthropology: a guide to a new interdisciplinary field*. New York: Springer.

White, T.D. and Folkens, P.A. 2005. *The human bone manual*. Amsterdam ; Boston: Elsevier Academic.

Wilkinson, C. 2004. *Forensic Facial Reconstruction*. Cambridge: Cambridge University Press.

Windhager, S., Mitteroecker, P., Rupić, I., Lauc, T., Polašek, O. and Schaefer, K. 2019. Facial aging trajectories: A common shape pattern in male and female faces is disrupted after menopause. *American Journal of Physical Anthropology*, pp. ajpa.23878. doi: 10.1002/ajpa.23878.

Wolff, J. 1986. The Law of Bone Remodeling. In: Maquet, P. and Furlong, R. (eds.) *Bone Remodeling*. Berlin: Springer Verlag.

Xie, Q.-F. and Ainamo, A. 2004. Correlation of gonial angle size with cortical thickness, height of the mandibular residual body, and duration of edentulism. *The Journal of Prosthetic Dentistry* 91(5), pp. 477–482. doi: 10.1016/j.prosdent.2004.02.020.

Zetkin, M. and Schaldach, H. 1980. *Wörterbuch der Medizin*. München: dtv.

Zysk, A.M., Garson III, A.B., Xu, Q., Brey, E.M., Zhou, W., Brankov, J.G., Wernick, M.N., Kuszak, J.R. and Anastasio, M.A. 2012. Nondestructive volumetric imaging of tissue microstructure with benchtop x-ray phase-contrast tomography and critical point drying. *Biomedical Optics Express* 3(8), pp. 1924. doi: 10.1364/BOE.3.001924.

CHAPTER 8 APPENDIX

Appendix A

Table 1 List of 105 specimens of the Walker method study, from the Pretoria Bone Collection (PBC), University of Pretoria.

Number	Ancestry	Sex	Age
4256	Black South African	F	42
4384	Black South African	F	80
4417	Black South African	F	60
4448	Black South African	F	38
4537	White South African	M	59
4540	Black South African	F	49
4565	Black South African	F	47
4578	Black South African	F	40
4636	Black South African	F	53
4956	Black South African	F	40
5056	White South African	F	45
5150	Black South African	F	31
5203	Black South African	F	75
5248	Black South African	M	80
5259	Black South African	F	35
5347	White South African	M	64
5407	White South African	M	73
5462	Black South African	M	87
5483	Black South African	M	80
5684	White South African	M	80
5688	White South African	M	52
5692	Black South African	F	44
5735	Black South African	M	50
5752	Black South African	M	52
5754	White South African	M	74
5760	Black South African	M	66
5785	Black South African	F	56

5796	Black South African	M	30
5797	Black South African	F	28
5837	Black South African	F	48
5845	Black South African	F	44
5848	White South African	M	61
5865	White South African	M	76
5875	White South African	M	64
5886	Black South African	M	71
5892	Black South African	F	26
5895	White South African	F	57
5903	Black South African	M	30
5905	Black South African	M	40
5912	Black South African	M	37
5925	White South African	M	68
5942	Black South African	M	41
5951	Black South African	M	60
5953	Black South African	M	27
5954	Black South African	M	36
5957	Black South African	F	29
5958	Black South African	M	34
5966	Black South African	M	77
5981	Black South African	M	45
5991	Black South African	M	71
6002	Black South African	M	36
6010	Black South African	F	70
6011	Black South African	M	60
6023	Black South African	M	50
6024	Black South African	F	65
6028	Black South African	F	45
6030	Black South African	M	26
6031	White South African	M	58
6034	Black South African	M	35
6035	Black South African	M	39
6145	Black South African	F	46
6172	Black South African	F	53
6217	Black South African	M	35
6228	White South African	M	55
6231	Black South African	M	32
6234	Black South African	F	25
6237	Black South African	F	56
6242	Black South African	M	65
6247	Black South African	M	54
6248	White South African	M	49
6296	Black South African	M	58
6305	Black South African	M	50
6309	Black South African	M	70
6315	Black South African	F	64
6318	Black South African	M	36
6322	White South African	F	81
6334	Black South African	M	35
6335	Black South African	M	54
6338	White South African	F	21

6339	White South African	F	65
6358	Black South African	F	37
6370	Black South African	F	60
6374	White South African	M	51
6388	Black South African	F	47
6390	Black South African	F	24
6407	White South African	M	71
6416	Black South African	M	30
6426	Black South African	M	98
6430	Black South African	M	50
6432	White South African	F	48
6437	White South African	M	78
6440	Black South African	M	50
6444	White South African	M	68
6449	White South African	F	59
6458	Black South African	M	50
6459	Black South African	M	57
6461	White South African	F	55
6463	Black South African	F	35
6470	Black South African	F	60
6482	Black South African	F	53
6504	White South African	M	31
6526	Black South African	M	44
7018	White South African	M	80
7019	Black South African	M	86
7053	White South African	M	65

Table 2 List of the 25 specimens of the Walker method study used for the intraOE, from the Pretoria Bone Collection (PBC), University of Pretoria.

Number	Ancestry	Sex	Age
6339	White South African	F	65
6358	Black South African	F	37
6370	Black South African	F	60
6374	White South African	M	51
6388	Black South African	F	47
6390	Black South African	F	24
6407	White South African	M	71
6416	Black South African	M	30
6426	Black South African	M	98
6430	Black South African	M	50
6432	White South African	F	48
6437	White South African	M	78
6440	Black South African	M	50
6444	White South African	M	68
6449	White South African	F	59
6458	Black South African	M	50

6459	Black South African	M	57
6461	White South African	F	55
6463	Black South African	F	35
6470	Black South African	F	60
6482	Black South African	F	53
6504	White South African	M	31
6526	Black South African	M	44
7018	White South African	M	80
7019	Black South African	M	86

Table 3 List of 291 specimens of the chin shape analysis study, scanned at the Oral and Dental Hospital, University of Pretoria.

Number	Ancestry	Sex	Age
1	Black South African	F	38
5	Black South African	F	57
7	Black South African	F	72
11	Black South African	F	40
13	Black South African	F	33
15	Black South African	F	33
20	Black South African	F	28
24	Black South African	F	38
28	Black South African	F	27
29	Black South African	F	37
30	Black South African	F	67
33	Black South African	F	58
38	Black South African	F	53
52	Black South African	F	43
53	Black South African	F	46
54	Black South African	F	55
69	Black South African	F	32
70	Black South African	F	56
74	Black South African	F	54
75	Black South African	F	34
78	Black South African	F	27
86	Black South African	F	27
88	Black South African	F	49
90	Black South African	F	23
91	Black South African	F	50
93	Black South African	F	20
99	Black South African	F	34
102	Black South African	F	68
111	Black South African	F	35
112	Black South African	F	35
114	Black South African	F	25
116	Black South African	F	32
134	Black South African	F	37
136	Black South African	F	20

138	Black South African	F	34
156	Black South African	F	30
163	Black South African	F	29
175	Black South African	F	30
183	Black South African	F	55
184	Black South African	F	43
187	Black South African	F	29
206	Black South African	F	53
212	Black South African	F	37
216	Black South African	F	40
217	Black South African	F	19
235	Black South African	F	31
238	Black South African	F	27
4	Black South African	M	23
8	Black South African	M	53
12	Black South African	M	28
22	Black South African	M	30
25	Black South African	M	19
26	Black South African	M	26
31	Black South African	M	33
32	Black South African	M	26
37	Black South African	M	29
39	Black South African	M	40
41	Black South African	M	27
42	Black South African	M	32
43	Black South African	M	39
44	Black South African	M	33
46	Black South African	M	31
47	Black South African	M	39
49	Black South African	M	43
50	Black South African	M	44
59	Black South African	M	39
60	Black South African	M	26
62	Black South African	M	30
65	Black South African	M	42
68	Black South African	M	33
71	Black South African	M	50
79	Black South African	M	20
84	Black South African	M	45
85	Black South African	M	21
87	Black South African	M	22
92	Black South African	M	57
94	Black South African	M	50
98	Black South African	M	41
101	Black South African	M	21
104	Black South African	M	33
105	Black South African	M	46
106	Black South African	M	21
110	Black South African	M	24
113	Black South African	M	28
115	Black South African	M	29
117	Black South African	M	43

118	Black South African	M	21
119	Black South African	M	32
120	Black South African	M	32
126	Black South African	M	25
130	Black South African	M	51
139	Black South African	M	31
171	Black South African	M	20
172	Black South African	M	29
173	Black South African	M	65
177	Black South African	M	29
179	Black South African	M	27
188	Black South African	M	57
192	Black South African	M	31
199	Black South African	M	32
211	Black South African	M	26
214	Black South African	M	38
222	Black South African	M	37
223	Black South African	M	44
224	Black South African	M	33
225	Black South African	M	59
226	Black South African	M	31
228	Black South African	M	25
229	Black South African	M	57
233	Black South African	M	21
236	Black South African	M	48
237	Black South African	M	51
239	Black South African	M	41
240	Black South African	M	29
241	Black South African	M	23
242	Black South African	M	33
243	Black South African	M	32
3	White South African	F	31
6	White South African	F	21
9	White South African	F	67
17	White South African	F	24
19	White South African	F	54
27	White South African	F	48
34	White South African	F	27
35	White South African	F	34
36	White South African	F	54
40	White South African	F	33
45	White South African	F	46
48	White South African	F	56
51	White South African	F	62
55	White South African	F	22
56	White South African	F	54
57	White South African	F	33
58	White South African	F	30
61	White South African	F	67
63	White South African	F	20
64	White South African	F	54
72	White South African	F	41

80	White South African	F	63
81	White South African	F	49
83	White South African	F	66
103	White South African	F	51
107	White South African	F	74
108	White South African	F	20
109	White South African	F	52
123	White South African	F	48
127	White South African	F	57
128	White South African	F	64
129	White South African	F	62
132	White South African	F	57
133	White South African	F	21
135	White South African	F	61
137	White South African	F	38
140	White South African	F	20
141	White South African	F	60
142	White South African	F	55
143	White South African	F	57
144	White South African	F	49
145	White South African	F	18
147	White South African	F	52
148	White South African	F	55
149	White South African	F	38
150	White South African	F	41
151	White South African	F	20
152	White South African	F	47
153	White South African	F	57
154	White South African	F	25
157	White South African	F	57
158	White South African	F	62
159	White South African	F	57
160	White South African	F	51
161	White South African	F	24
164	White South African	F	25
165	White South African	F	51
167	White South African	F	25
168	White South African	F	65
169	White South African	F	19
170	White South African	F	45
174	White South African	F	45
176	White South African	F	36
178	White South African	F	34
181	White South African	F	75
185	White South African	F	39
186	White South African	F	61
190	White South African	F	69
191	White South African	F	57
193	White South African	F	34
195	White South African	F	33
196	White South African	F	54
197	White South African	F	74

198	White South African	F	21
200	White South African	F	59
201	White South African	F	35
204	White South African	F	75
205	White South African	F	27
207	White South African	F	63
218	White South African	F	26
220	White South African	F	72
227	White South African	F	49
231	White South African	F	57
232	White South African	F	55
234	White South African	F	22
244	White South African	F	23
245	White South African	F	24
246	White South African	F	29
247	White South African	F	19
248	White South African	F	23
253	White South African	F	37
254	White South African	F	38
255	White South African	F	32
256	White South African	F	37
257	White South African	F	34
263	White South African	F	56
264	White South African	F	56
265	White South African	F	47
266	White South African	F	57
267	White South African	F	47
268	White South African	F	55
269	White South African	F	58
270	White South African	F	50
276	White South African	F	76
277	White South African	F	68
278	White South African	F	62
279	White South African	F	66
280	White South African	F	65
281	White South African	F	66
282	White South African	F	54
283	White South African	F	61
284	White South African	F	77
285	White South African	F	69
290	White South African	F	43
291	White South African	F	44
2	White South African	M	21
10	White South African	M	43
14	White South African	M	54
16	White South African	M	25
18	White South African	M	46
21	White South African	M	20
23	White South African	M	53
66	White South African	M	24
67	White South African	M	23
73	White South African	M	65

76	White South African	M	55
77	White South African	M	67
82	White South African	M	31
89	White South African	M	52
95	White South African	M	53
96	White South African	M	50
97	White South African	M	45
100	White South African	M	27
121	White South African	M	84
122	White South African	M	62
124	White South African	M	62
125	White South African	M	51
131	White South African	M	74
146	White South African	M	32
155	White South African	M	26
162	White South African	M	49
166	White South African	M	26
180	White South African	M	52
182	White South African	M	47
189	White South African	M	55
194	White South African	M	59
202	White South African	M	71
203	White South African	M	58
208	White South African	M	39
209	White South African	M	25
210	White South African	M	38
213	White South African	M	37
215	White South African	M	74
219	White South African	M	24
221	White South African	M	61
230	White South African	M	69
249	White South African	M	24
250	White South African	M	29
251	White South African	M	18
252	White South African	M	30
258	White South African	M	37
259	White South African	M	34
260	White South African	M	31
261	White South African	M	41
262	White South African	M	43
271	White South African	M	49
272	White South African	M	48
273	White South African	M	48
274	White South African	M	47
275	White South African	M	45
286	White South African	M	61
287	White South African	M	72
288	White South African	M	60
289	White South African	M	21

Table 4 List of 10 specimens used for the intra- and interOD, scanned at the Oral and Dental Hospital, University of Pretoria and at the Life Groenkloof Hospital (*), Pretoria.

Number	Ancestry	Sex	Age
1	Black South African	F	29
15	Black South African	M	21
21	Black South African	F	41
31	Black South African	M	33
38	Black South African	M	32
43	Black South African	F	56
47	Black South African	M	52
55	Black South African	M	35
63*	Black South African	F	27
91	Black South African	M	23

Appendix B

Qualitative analysis

1 – Which modality took you longer to score, bone or 3D surfaces?

Obs. 1: Bone.

Obs. 2: 3D surfaces.

Obs. 3: 3D surfaces (due to loading time in software).

Obs. 4: 3D surfaces (loading time in software and impossibility to compare mandibles with one another).

2 – Which modality did you find harder to score, bone or 3D surfaces?

Obs. 1: Bone.

Obs. 2: 3D surfaces.

Obs. 3: No difference.

Obs. 4: 3D surfaces (lack of immediate comparison with other mandibles and lack of tactile experience).

3 – Which score(s) (1, 2, 3, 4 and/or 5) did you find the hardest to do, both, in bone and 3D surfaces?

Obs. 1: 3 most difficult but also 2 and 4.

Obs. 2: I found scores 2 and 3 the hardest to do, both, in mandibles and 3D surfaces.

Obs. 3: 1 and 5 were fairly distinct. The hardest was between 1 and 2, and 2 and 3.

Obs. 4: Mostly 2 and 3; 1 and 5 are rather clear; 4 is also not too difficult to discern.

4 – How did you score the mandibles (comparing the mental eminence to other mandibles, etc.)?

Obs. 1: I evaluated each mandible whether it has no eminence (1) or very pronounced (5) and then if I could not decide whether it was very pronounced gave it a score 4; score 3 was indecisive and 2 had the slightest eminence. When evaluating the 3D images, however, my impression was that it was almost always possible to discern some eminence, which might have been missed when evaluating the dried bone.

Obs. 2: On bone: first evaluation of all mandibles in order to have some template for each score, and then I compared all the mandibles to the templates chosen. On surface: one by one without comparing the mental eminence to other mandibles.

Obs. 3: I compared the shape of the mental eminence to the definitions and the line drawings on pp. 41 (Walker 2008).

Obs. 4: I touched and looked at a number of mandibles to discern the degree of variation in the mental eminence and comparing it to the figure in the Walker paper (Walker 2008, pp. 41) before scoring them. I had the figure next to me in order to compare.

5 – How did you score the 3D surfaces (zoom, rotation, etc.)?

Obs. 1: No zooming, only rotating.

Obs. 2: Zooming and rotating; changing the exposition to the light.

Obs. 3: I rotated the mandible around the screen and looked at it from all angles. I did not use the zoom.

Obs. 4: Rotation to see the light throw shadows of the mental eminence from different angles; I also zoomed in and out to try and discern the eminence better